



NASA CR-134491

FINAL REPORT  
DESIGN AND DEVELOPMENT  
OF  
SPACE STORABLE, EXPLOSIVELY ACTUATED VALVE

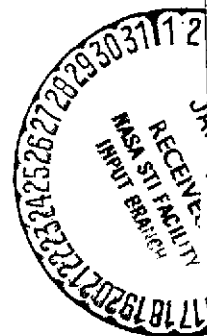
by  
G. P. Meyer

PYRONETICS  
A CORDON INTERNATIONAL COMPANY  
SANTA FE SPRINGS, CALIFORNIA

Prepared for  
NATIONAL AERONAUTICS AND SPACE ADMINISTRATION

NASA Lewis Research Center  
Contract NAS3-14340

Larry H. Gordon, Project Manager



(NASA-CR-134491) DESIGN AND DEVELOPMENT  
OF SPACE STORABLE, EXPLOSIVELY ACTUATED  
VALVE Final Report, Jun. 1970 - Dec.  
1971 (Pyronetics, Inc.) 192 p HC \$11.25

CSCL 131 G3/15

Unclass  
24853

N74-13200

1. Report No. NASA CR-134491		2. Government Accession No.		3. Recipient's Catalog No.	
4. Title and Subtitle Design and Development of Space Storable, Explosively Actuated Valve				5. Report Date December 1973	
				6. Performing Organization Code	
7. Author(s) Gerhard P.F. Meyer				8. Performing Organization Report No.	
				10. Work Unit No.	
9. Performing Organization Name and Address Pyronetics A Cordon International Company 10025 Shoemaker Avenue Santa Fe Springs, California 90670				11. Contract or Grant No. NAS3-14340	
				13. Type of Report and Period Covered Final Report June 1970 - December 1971	
12. Sponsoring Agency Name and Address National Aeronautics and Space Administration Lewis Research Center Cleveland, Ohio 44135				14. Sponsoring Agency Code	
15. Supplementary Notes					
16. Abstract  An experimental program was conducted to design, fabricate, and test a lightweight, explosively actuated valve, specifically for use with cryogenic fuels and fluorinated oxidizers. Flow tests were made on a normally open valve, 2-1/2 inch (6.35 cm) line size, in H <sub>2</sub> O, LH <sub>2</sub> , LF <sub>2</sub> and CCl <sub>4</sub> to evaluate flow characteristics, leakage rates, material compatibility, primer and main charge burn rates, and system dynamics. The program resulted in demonstrating valve compatibility with LF <sub>2</sub> and sealing ability in H <sub>2</sub> O and LH <sub>2</sub> . The valve failed to close securely with fluids whose density was similar to LF <sub>2</sub> regardless of the valve temperature. Concurrently, an analytical model describing the valve actuation and the associated energy dissipation was developed. This model indicated that the valve design will be capable of functioning in high density fluids by increasing the input actuation energy. Proposed modifications to the existing valve were noted and a subsequent valve design was made but was not fabricated or tested.					
17. Key Words (Suggested by Author(s)) Explosively Actuated Valves Cartridge Initiator			18. Distribution Statement Distribution of this document is unlimited.		
19. Security Classif. (of this report) Unclassified		20. Security Classif. (of this page) Unclassified		21. No. of Pages	
				22. Price*	

\* For sale by the National Technical Information Service, Springfield, Virginia 22151

## FOREWORD

The work described in this report was conducted for the NASA-Lewis Research Center, Cleveland, Ohio by Pyronetics, a Cordon International Company, Santa Fe Springs, California. The work was conducted in accordance with the provisions of Contract NAS3-14340.

Mr. L. H. Gordon of the NASA-Lewis Research Center was the NASA Technical Project Manager. The Pyronetics Program Manager was Mr. G. P. Meyer.

PRECEDING PAGE BLANK NOT FILMED

# TABLE OF CONTENTS

	Page
FOREWORD . . . . .	iii
CONTENTS . . . . .	v
ABSTRACT . . . . .	xi
1.0 SUMMARY . . . . .	1
2.0 INTRODUCTION . . . . .	3
3.0 TASK I: DESIGN AND ANALYSIS . . . . .	7
3.1 Concept Selection . . . . .	7
3.2 Fluorine Related Problem Areas . . . . .	10
3.3 Design Description . . . . .	11
3.4 Development Tests . . . . .	13
3.5 Design Evolution . . . . .	25
3.6 Discussion of Results . . . . .	28
4.0 TASK II: CARTRIDGE VERIFICATION TESTING . . . . .	29
4.1 Margin Valve Tests . . . . .	31
4.2 Orifice Effects . . . . .	41
4.3 Cartridge Verification Testing . . . . .	45
4.4 Discussion of Results . . . . .	73
5.0 MANUFACTURING . . . . .	79
5.1 Contamination Control . . . . .	79
5.2 Special Manufacturing Techniques . . . . .	81
6.0 TASK IV: VALVE FUNCTIONAL ACCEPTANCE TESTING . . . . .	83
6.1 Zero Flow Fluorine Test . . . . .	84
6.2 Failure Mode Verification Test . . . . .	86
6.3 Discussion of Results . . . . .	90
7.0 ANALYSIS . . . . .	95
7.1 Cartridge Energy . . . . .	96
7.2 Energy Losses During Deceleration . . . . .	105
7.3 Summary and Application . . . . .	110
7.4 Discussion of Results . . . . .	117
8.0 DUAL CARTRIDGE VALVE DESIGN . . . . .	119
8.1 Analysis . . . . .	119
8.2 Design Description . . . . .	121
8.3 Development Tests . . . . .	121
9.0 CONCLUSIONS . . . . .	125
REFERENCES . . . . .	127
BIBLIOGRAPHY . . . . .	129

APPENDIX A POPPET/SEAT ANALYSIS . . . . .	A-1
APPENDIX B VIRTUAL MASS ANALYSIS . . . . .	B-1
APPENDIX C COMPUTER PROGRAM . . . . .	C-1
APPENDIX D DISTRIBUTION LIST . . . . .	D-1

# FIGURES

NO.	TITLE	PAGE
1	Fluorine Valve Design Evaluation. . . . .	9
2	2-1/2 Inch Explosively Actuated Valve . . . . . (Initial Design)	12
3	Fluorine Valve Test Program . . . . .	14
4	External Leak Test Schematic . . . . .	20
5	Actuation Test Schematic . . . . .	21
6	Flow Test Schematic . . . . .	24
7	2-1/2 Inch Explosively Actuated Valve . . . . . (Final Design)	27
8	Disassembled Margin Valve . . . . .	30
9	Explosive Actuator . . . . .	31
10	Margin Firing Test Installation . . . . .	33
11	Modified Margin Valve Setup . . . . .	35
12	Hinged Poppet, Margin Valve . . . . .	37
13	Hinged Poppet After Actuation (Water) . . . . .	39
14	Hinged Poppet After Actuation (Liquid Hydrogen)	40
15	Orifice Effect Test Schematic . . . . .	42
16	Orifice Effects, Graphical Representation . . . . .	44
17	Cartridge External Envelope . . . . .	47
18	Cartridge Firing Data Nomenclature . . . . .	49
19	Cartridge Firing Bomb . . . . .	50
20	Cartridge Firing Trace . . . . .	51
21	Cartridge Firing Trace . . . . .	53
22	Liquid Hydrogen Cartridge Firing Test Setup . . . . .	55
23	Cartridge Firing Trace . . . . .	56
24	Cartridge Firing Trace . . . . .	57
25	Firing Installation, Thermal Shock Test . . . . .	58
26	LH <sub>2</sub> Thermal Shock Test Setup. . . . .	59
27	Thermal Shock Temperature Plot . . . . .	60
28	Cartridge Firing Trace . . . . .	61
29	Cartridge Firing Trace . . . . .	62
30	Cartridge Leak Test Installation . . . . .	63
31	Cartridge Firing Trace . . . . .	64
32	Cartridge Firing Trace . . . . .	66
33	Cartridge Firing Trace . . . . .	67
34	Vibration Setup . . . . .	68
35	Cartridge Firing Trace . . . . .	70
36	Cartridge Firing Trace . . . . .	71
37	Cartridge Firing Trace . . . . .	72
38	Cartridge Firing Test Summary . . . . .	74
39	Equipment List . . . . .	77
40	Hinged Poppet, Pre-Machined . . . . .	81
41	Zero Flow Fluorine Test Setup . . . . .	84
42	Underactuation of Piston . . . . .	85
43	Density Effects on Valve Closure . . . . .	93
44	Kinetic Energy Vs. Displacement . . . . .	95
45	Theoretical Cartridge Pressure Curve . . . . .	98
46	Poppet/Actuator Schematic . . . . .	100
47	Flow Model Schematic . . . . .	106

## FIGURES (Continued)

NO.	TITLE	PAGE
48	Theoretical Effect of Fluid Density . . . . .	112
49	Theoretical Effect of Poppet Weight . . . . .	114
50	Theoretical Effect of Line Restriction . . . . .	116
51	Dual Cartridge Energy Distribution . . . . .	122
52	Dual Cartridge Valve Design . . . . .	123

# TABLES

NO.	TITLE	PAGE
1	Cartridge Verification Testing . . . . .	29
2	Margin Valve Test Results . . . . .	36
3	Orifice Effects Test Results . . . . .	43
4	Cartridge Performance Specification . . . . .	46
5	Cartridge Firing Data . . . . .	52
6	Cartridge Firing Data . . . . .	52
7	Cartridge Firing Data . . . . .	54
8	Cartridge Firing Data . . . . .	60
9	Cartridge Firing Data . . . . .	65
10	Cartridge Firing Data . . . . .	68
11	Cartridge Firing Data . . . . .	69
12	Task IV Test Schedule . . . . .	83
13	Summary Test Matrix . . . . .	92
14	Summary of Hydrodynamic Mass Calculations .	104
15	Effect of Fluid Density . . . . .	113
16	Effect of Poppet Weight . . . . .	115
17	Effect of Line Restriction . . . . .	117
18	Comparison of Input Data . . . . .	120



## ABSTRACT

An experimental program was conducted to design, fabricate, and test a flightweight, explosively actuated valve, specifically for use with cryogenic fuels and fluorinated oxidizers. Flow tests were made on a normally open valve, 2-1/2 inch (6.35 cm) line size, in  $H_2O$ ,  $LH_2$ ,  $LF_2$ , and  $CCl_4$  to evaluate flow characteristics, leakage rates, material compatibility, primer and main charge burn rates, and system dynamics. The program resulted in demonstrating valve compatibility with  $LF_2$  and sealing ability in  $H_2O$  and  $LH_2$ . The valve failed to close securely with fluids whose density was similar to  $LF_2$  regardless of the valve temperature. Concurrently, an analytical model describing the valve actuation and the associated energy dissipation was developed. This model indicated that the valve design will be capable of functioning in high density fluids by increasing the input actuation energy. Proposed modifications to the existing valve were noted and a subsequent valve design was made but was not fabricated or tested.

PRECEDING PAGE BLANK NOT FILMED

## 1.0 SUMMARY

The primary objective of this program was to design, fabricate, and test a flightweight, explosively actuated valve specifically for use with fluorinated oxidizers and cryogenic fuels. To accomplish this objective, flow tests were made on a normally open valve, 2-1/2 inch (6.35 cm) line size, in  $\text{LH}_2$ ,  $\text{LF}_2$ ,  $\text{H}_2\text{O}$ , and  $\text{CCL}_4$  to evaluate flow characteristics, leakage rates, material compatibility, primer and main charge burn rates, and system dynamics. A secondary objective was to generate an analytical method which would enable the designer to scale the valve design for either larger or smaller line sizes without having to resort to lengthy trial and error development tests.

Several major problem areas had been identified at the start of the program. The highly reactive nature of liquid fluorine made it necessary to completely isolate the products of combustion of the electro-explosive cartridge from the liquid flowing through the valve. A second problem area was the uncertainty which existed with respect to the low temperature effects on the cartridge. The possibility existed that the low temperature of liquid hydrogen ( $-423^\circ\text{F}$ ,  $-253^\circ\text{C}$ ) would either shrink or crack the explosive in the cartridge and thereby prevent reliable cartridge performance. A third area of concern was the compatibility of the valve with liquid fluorine. Here the uncertainty existed not only with the materials of construction but also the amount of localized heat produced by the unique hinged poppet mechanism.

The development effort described in this report was structured such that each area of concern could be fully investigated and the results incorporated into the valve design. The program was divided into six tasks. During Task I, "Design and Analysis", a valve actuator was developed which completely isolated the products of combustion from the fluid flowing through the valve. The valve poppet and seat geometry was optimized for maximum retention and sealing capability. In addition, a preliminary analytical model was developed which described the dynamic behavior of the valve. Task II, "Cartridge Verification Testing" was designed to verify the effects of temperature, vibration, and shock on the cartridge explosive charge. Also during Task II the effect of varying the cartridge energy output was investigated. Thus Tasks I and II provided answers to two of the major problem areas which had been defined at the beginning of the program. Namely, that positive isolation of the products of combustion of the cartridge was possible and that the effects of low temperature on the cartridge explosive charge were negligible.

During Task III, "Valve Manufacture" two lots of valves were manufactured which were to be allotted for Task IV, "Valve Functional Acceptance Testing" and Task V, "Valve Fluorine Compatibility Testing". During "Valve Functional Acceptance Testing" several new problem areas were discovered. It was found that the valve was affected by restrictions in the downstream line connections, and that fluid density had a much greater impact on valve closure than was originally predicted. However, the exact quantitative influence of both factors could not be determined. For this reason, the valves allotted for Task V, "Fluorine Compatibility Testing" were used to investigate more fully the effects of fluid density, line restriction and cartridge energy transfer.

In summary, the design and development effort described in this report resulted in a valve which was capable of sealing off flow of cryogenic propellants with a density of less than  $62.4 \text{ lb/ft}^3$  ( $1 \text{ gm/cm}^3$ ). The leak rates at these conditions were less than  $1 \times 10^{-7}$  scc/sec of helium at a pressure of 250 psig ( $172.41 \text{ N/cm}^2$ ) provided that no restrictions exist in the line.

The electro-explosive cartridge used was capable of functioning consistently over a temperature spectrum of  $-423^\circ\text{F}$  to  $+120^\circ\text{F}$  ( $-253^\circ\text{C}$  to  $+49^\circ\text{C}$ ). The basic valve design is compatible with liquid fluorine. In addition, the design effort resulted in a formalized method of analysis which will allow the designer to scale the valve for use with high density fluids as well as with larger or smaller line sizes.

## 2.0 INTRODUCTION

The heavier payloads, longer durations and greater operational flexibility projected for future space explorations led to the investigation and the development of large scale, high performance propulsion systems. The high efficiency oxidizers, such as liquid fluorine as well as liquid fluorine/liquid oxygen mixtures appear to be particularly attractive for this application. Fluorine has long been recognized as offering the highest performance of all stable chemical rocket oxidizers. However, the handling of fluorine in a physical system requires that certain precautionary criteria be observed. These criteria have been established as a result of several previous investigative efforts and they apply to all phases of fluorine use.

Among the areas which have previously been investigated are material compatibility, facility design, flight system design, fluorine production, fluorine transportation, personnel safety, and, finally, component design.

The development of criteria for liquid fluorine feed system components has been the subject of some recent investigative reports. Conceptual design studies and performance evaluations of shut-off valves, vent relief valves, quick disconnect couplings and other fluid control devices have been conducted and are documented in the literature on the subject. However, one class of devices, the explosively actuated valves, have up to this point, never been fully investigated. During an investigation conducted by the McDonnell Douglas Astronautics Company (Ref. 1) several types of explosively actuated valves have been evaluated in a fluorine test system. However, the valves tested were not specifically designed for fluorine environments and as a consequence valve failures occurred during operation. The need for further investigation in this area was recognized by the NASA and resulted in the program described in this report.

Explosively actuated valves are available from manufacturers in two functionally different configurations. The normally closed configuration contains the fluid which is to be controlled by the valve until a signal is received to open the flow passage. Conversely, the normally open configuration allows fluid flow to occur until a signal is received to close the flow passage. As a class, these single function valves owe their unique characteristics to the fact that a small explosive charge contains a very high level of energy which can be released by a very low level trigger signal. The actuation energy is contained within an explosive cartridge in the form of an explosive charge. Valve operation occurs when the energy contained in the explosive charge is released upon receipt of an electrical signal of extremely low amplitude. This characteristic has several advantages.

Because their sole function is to provide a low amplitude triggering current, electrical power supplies and storage systems can be kept small. Auxiliary power supplies which are necessary for such conventional valve actuators as pneumatic or hydraulic cylinders, electro-mechanical power trains, or solenoid coils, can be avoided. The energy contained in the explosive charge is released very rapidly and transferred directly to the valve actuation mechanism. For this reason valve response times are extremely short. Furthermore, in the normally closed configuration, the flow passage is designed to provide hermetic sealing during the fluid storage period. The high energy density of the explosive charge makes it possible to shear off the hermetic sealing section of the flow passage. The normally open configuration takes advantage of the high energy density by providing an extremely high degree of plastic deformation between poppet and seat (commonly referred to as cold welding). Therefore post actuation leak rates of less than  $1 \times 10^{-8}$  scc/sec of helium are obtained even with large scale valves.

All of the positive attributes possessed by explosively actuated valves have long been recognized and have made them very attractive for use in long duration space flight missions, however, directly related to them are several negative characteristics which are particularly suspect for use in fluorine propulsion systems. Fluorine will react spontaneously when in contact with the combustion gases of the explosive cartridge. A method had to be devised by which the products of combustion could be contained within a hermetic container thereby preventing direct contact with the fluorine. The low temperature environments associated with space flight made it necessary to investigate the effect of temperature, vibration, and shock on the explosive charge since it was expected that cracking or intermolecular degradation might affect reliable valve operation. The high response times possible with explosive actuators also presented the possibility of the introduction of high but localized energy inputs which could result in a fluorine reaction. And finally the prior state of the art of explosively actuated valve development was restricted to line sizes of less than one inch (2.54 cm) in diameter. Consequently, this program effort was governed by two major parameters, increased flow capacity and wider environmental spectrums.

The investigative and developmental effort described in this report was divided into a logical sequence of separate tasks. The structure of the program was such that the above major problem areas could be investigated during the early phases of the program in order to incorporate necessary design changes into the final valve configuration.

The total program was divided into six distinct tasks:

- I. Design and Analysis
- II. Cartridge Verification Testing
- III. Manufacturing
- IV. Valve Functional Acceptance Testing
- V. Valve Fluorine Compatibility Testing
- VI. Data Analysis and Reporting

Task I "Design and Analysis" was devoted to optimization of the basic valve design as conceived during the proposal stage. Guidelines for the basic valve design were established with respect to its use in a fluorine environment. Also during this stage a valve actuator was developed which was capable of completely isolating the products of combustion of the explosive cartridge. The valve poppet and seat geometry was optimized for maximum sealing capability.

Task II "Cartridge Verification Testing" was aimed at establishing that the selected cartridge could indeed be used to actuate the valve under all environmental conditions. The verification of the cartridge was particularly important since prior to this program cartridges had not been systematically tested under  $-423^{\circ}\text{F}$  ( $-253^{\circ}\text{C}$ ) liquid hydrogen conditions. Furthermore, prior experience with cartridges fired under cryogenic conditions had shown that some variation in pressure output could be expected; and it was not known what form the variation of pressure would take. Also during Task II the effect of varying the input energy of the cartridge to the actuator was investigated.

During Task III "Valve Manufacture" two lots of valves were manufactured. One lot of seven valves was to be consumed during Task IV "Functional Acceptance Testing". The second lot of six valves was to be used for Task V "Fluorine Compatibility Testing". During the manufacture of the first lot of valves several critical manufacturing processes and assembly procedures were developed in order to eliminate possible contamination of the component parts.

Task IV "Valve Functional Acceptance Testing" was originally conceived to verify that the valves would function in a full flow cryogenic environment. In addition one valve was to be actuated in a zero flow fluorine test system. This was deemed necessary in view of the developmental nature of the valves as well as the hazards associated with fluorine testing. The zero flow, low volume liquid fluorine test system was completely isolated from the existing full flow fluorine facility. The

zero flow fluorine valve failed to lock in the closed position when the cartridge was fired. As a consequence of this failure, which was attributed to the higher density of the liquid fluorine, a series of tests was conducted with the remaining valves in order to investigate in detail why the valve was so susceptible to density effects.

Since the basic valve design had proved capable of achieving the low leakage rate requirements in fluids having a density of less than  $62.4 \text{ lb/ft}^3$  ( $1 \text{ gm/cm}^3$ ) such as water and liquid hydrogen the program effort was redirected towards refining the analytical model.

Based on the revised analytical model several modifications were made to the existing valve design. The remaining program effort consolidated the information gained into a formalized method of analysis which would permit a designer to forego costly and time consuming trial and error approaches.

### 3.0 TASK I: DESIGN AND ANALYSIS

The purpose of the program described in this report, briefly stated, was to design and develop a normally open valve, capable of functioning in fluorine, fluorine oxygen mixtures, nitrogen and liquid hydrogen. The first phase of this development effort, a phase which was initiated during the proposal stage, was the selection of the basic valve concept. There are six basic valve types which were under investigation for ultimate development and adaptation to fluorine use. These basic valve types are:

Butterfly Valves

Poppet or Globe Valves

Gate Valves

Ball Valves

Blade Valves

Swing Check Valves

The selection of the basic valve type which was to be ultimately developed was made after an evaluation of the inherent advantages and disadvantages present in the six valve types listed above. In addition to the inherent advantages and disadvantages which a specific valve type might possess, a prime consideration during the selection process was the feasibility of mating the basic valve type to the explosive actuator. This latter selection criterium was strongly influenced by existing state-of-art technology.

#### 3.1 Concept Selection

In general, the inherent characteristics of any potentially promising valve concept must be evaluated with respect to the ultimate use of the valve. In this instance the evaluation was based on how well the concept would work in a flight weight, fluorine propulsion system. The functional characteristics of the various valve types which were under investigation were cleanability, pressure drop, flow protuberance, weight, envelope, leak rate, actuator adaptation, internal friction, and prior state-of-art.

Experience in handling fluorine and fluorine/oxygen mixtures has shown that most system failures that resulted in burn-out could be traced to some form of contamination. Thus, strict cleanliness is required during all assembly and maintenance operations. A valve concept must therefore be evaluated with respect to its ability to be cleaned during and after assembly and also after installation into the propulsion system.



Flow capacity of the valve, specifically its resistance to flow, is of prime importance when the valve is used in a flight system. If a valve concept exhibits high resistance to flow its impact on the size of the transfer pressurization system will obviously be detrimental.

The inner flow surfaces which form the fluorine boundary should be free from unnecessary protrusions or cavities. This requirement is closely related to cleanability and flow capacity of the valve.

The impact of valve weight and external valve envelope on the overall system design is obviously of importance. Some valve concepts lend themselves much more readily to the optimization of weight and envelope than others.

Leakage, both prior to valve actuation and after valve actuation, must be listed as one of the most important characteristics to be considered. A valve concept which exhibits the least number of external leak paths is obviously more desirable for fluorine end use. Leakage after actuation is important since it impacts the long term storage capability of the system.

Explosive actuators are linear actuators which deliver high actuation forces over short distances. A potential valve concept must be evaluated with respect to ease of adaptation to the explosive actuator. If a valve type requires a long actuation stroke or a rotational actuation mode it becomes less attractive for use with an explosive actuator.

High internal friction of the valve mechanism must be considered both in terms of energy demands on the explosive actuator and in terms of possible high localized heat inputs which could result in a fluorine reaction. Therefore, a valve concept which requires the least amount of sliding friction would be more attractive than one which exhibits high internal friction.

A final consideration during the selection of the basic valve concept was the prior state-of-art of explosive valve technology. Although explosive valve technology was restricted to valves having line sizes of less than 1.0 inches (2.54 cm) in diameter, a concept which showed promise to be easily adapted to larger line sizes would have the advantage over a valve concept which had never been used in conjunction with an explosive actuator.

The six basic valve concepts were evaluated on the basis of the inherent valve characteristics discussed above. A summary of this evaluation is shown in Figure 1. The swing-check concept was finally selected on the basis of its total score in relationship with the other basic valve types. Its high score was due to the fact that the concept had been used before, it was adaptable to an explosive actuator, the expected leakage was low enough to meet design requirements, and its internal configuration minimized contaminant entrapment.

FUNCTIONAL CHARACTERISTICS	RANGE	V A L V E   T Y P E					
		BUTTERFLY	POPPET	GATE	BALL	BLADE	SWING CHECK
CLEANABILITY	0-10	8	8	6	6	4	8
PRESSURE DROP	0-05	3	2	4	5	4	4
FLOW PROTUBERANCE	0-05	2	2	4	5	4	4
WEIGHT	0-05	5	2	2	3	4	3
ENVELOPE	0-05	5	2	2	2	4	3
LEAK RATE	0-07	3	7	6	4	3	7
ADAPTATION	0-07	4	6	6	4	4	6
INTERNAL FRICTION	0-05	3	4	2	2	2	4
STATE-OF-ART	0-05	2	5	5	2	2	5
TOTAL SCORE	54	35	38	37	37	31	44

Figure 1. Fluorine Valve Design Evaluation

### 3.2 Fluorine Related Problem Areas

The mechanism design and the overall configuration of the valve evolved through a logical consideration of the problem areas associated with a fluorine environment. The highly reactive nature of fluorine when in contact with contamination influenced the design in several key areas.

In study programs conducted by the McDonnell Douglas Astronautics Company (Ref. 1) and Germantown Laboratories (Ref. 2) valve failures occurred which apparently could be traced to contamination caused by the products of combustion entering into the fluorine fluid stream. The valves tested in these programs utilized a variety of sealing techniques, none of which were capable of containing the products of combustion of the explosive cartridge within a chamber separate from the flow passage. Recognizing the necessity of containing the products of combustion an effort was made to develop a valve actuator which contains the products of combustion within a metallic bellows. Metallic bellows had been used successfully to isolate explosive cartridge gases. For this particular application the question arose whether or not a bellows actuator was capable of containing the combustion products while being exposed to liquid hydrogen temperatures.

When an explosively actuated valve is functioned, shock inputs of considerable magnitude are introduced into the feed system installation. This can have the effect of loosening fittings and connections with resultant fluorine leakage. It should be pointed out that leaks can occur without ignition or catastrophic failure; however, loosened connections or points of leakage are particularly susceptible to contamination and subsequent ignition. For this reason it is important that shock inputs into the feed system installation are minimized. The swing-check concept minimizes the effect of shock input into the feed system installation by virtue of the fact that the shock associated with valve closure is taken out parallel to the feed line axis and not perpendicularly to it as would be the case with a gate or poppet valve.

It was initially known that certain explosive cartridges are highly susceptible to the influence of cryogenic temperatures. For instance, some types of cartridges failed to ignite when conditioned and fired at  $-327^{\circ}\text{F}$  ( $-199^{\circ}\text{C}$ ). Although the exact failure mechanism was not known, it was suspected that the failure to ignite was due to separation of the ignition mix from the bridgewire. Since the program effort described in this report did not include the development of a reliable cryogenic cartridge, it was imperative that the most promising cartridge be selected and subsequently subjected to a systematic test program. This effort was undertaken early in the program so that in the event of failure the program could be concluded without undue expenditures of cost.

### 3.3 Design Description

The basic valve design is shown in Figure 2. It consisted of the explosive actuator, the valve housing, and the outlet assembly. This basic design underwent a series of design changes during the initial development effort. These design changes were of a detailed nature rather than of a conceptual nature and they will be discussed more fully later in this report.

The explosive actuator consisted of the actuator assembly which was housed in the actuator housing. The actuator assembly was made up of the explosive cartridge, a piston assembly, the cartridge adaptor which was welded to a single ply, metallic bellows made of 321 corrosion resistant steel. The actuator assembly contacted the separation piston which in turn was located within a separation screw. The separation screw was held in position by a retaining nut. In this position the metallic bellows were in the compressed stage. When the electro-explosive cartridge was ignited, the piston within the cartridge adaptor was forced against the separation piston which in turn contacted the separation screw. Separation then occurred along a stress riser groove. This action forced the lower portion of the separation screw to accelerate the hinged poppet of the outlet assembly. The upper portion of the separation screw was provided with a tapered hole. The separation piston was provided with a tapered section which was designed to wedge itself into the tapered hole thereby providing a metal to metal seal between the fluorine fluid passage and the explosive actuator. During the acceleration stroke a small amount of fluorine would be expected to enter the volume between separation screw and cartridge adaptor, however, this portion of the fluorine would be hermetically isolated from the products of combustion contained within the cartridge adaptor.

In this design all external and internal leak paths were protected by metallic, gold plated seals. The arrangements of the seals was such that threaded sections did not come in contact with the liquid fluorine, a feature which was deemed necessary in light of possible contamination entrapment within the threaded sections.

The outlet assembly consisted of the outlet and the hinged poppet. The poppet was held in the open position by two aluminum shear pins. The shear pins were press fitted into both the poppet and the outlet in order to minimize possible contamination entrapment. The hinged poppet rotated around two hinge pins which were also press fitted into the outlet but which provided clearance between the pins and the hinged poppet. In this design the poppet featured a spherical surface which was designed to wedge itself into a tapered section

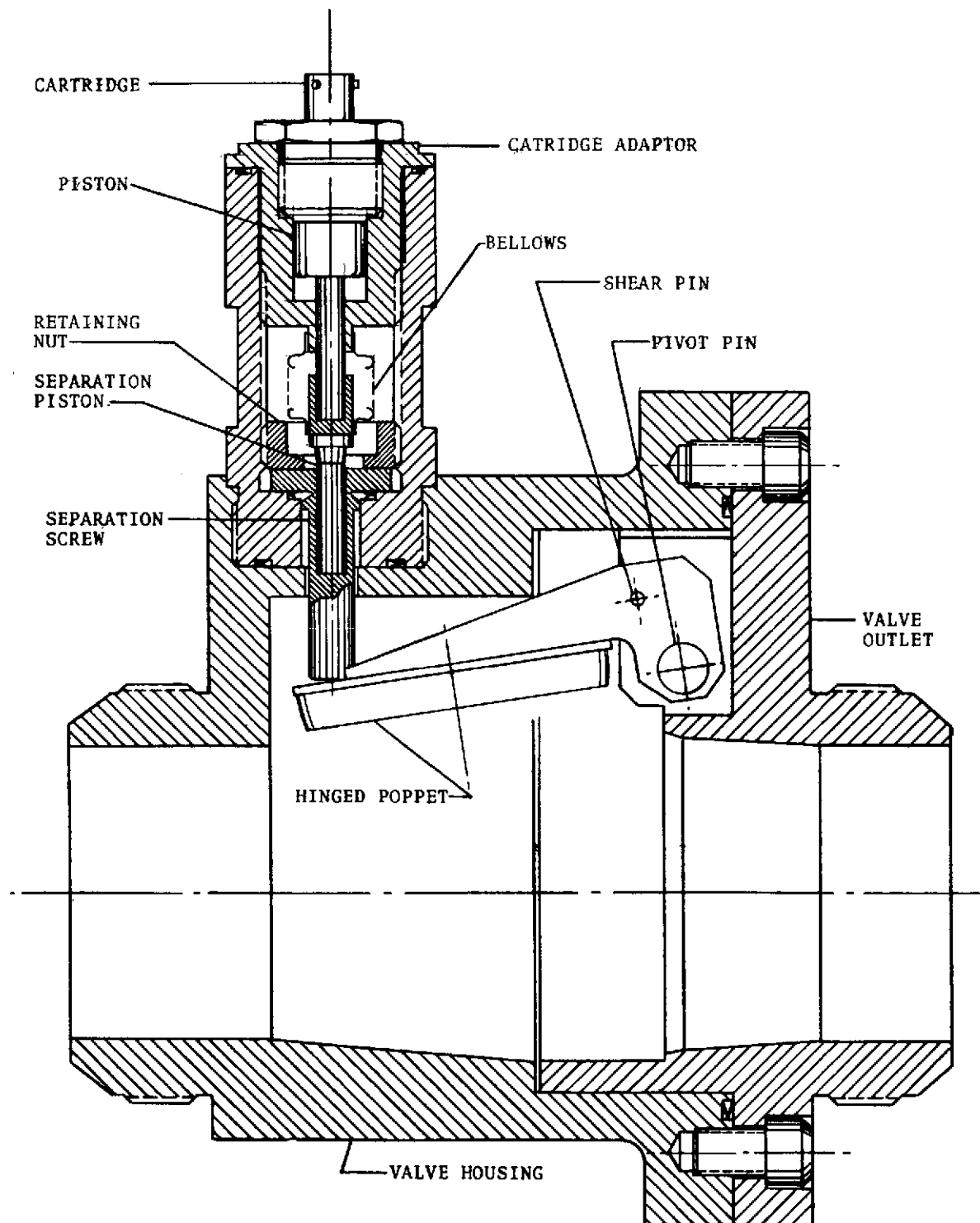


FIGURE 2. 2-1/2 INCH, EXPLOSIVELY ACTUATED VALVE  
(INITIAL DESIGN)

in the outlet. The hinged poppet was contained within the outlet so that there were no external leak paths around the hinge pins. There were only two external leak paths and these were protected by gold plated, metallic seals.

In general, the valve was designed to minimize external leak paths, to provide as much streamlining of the flow passage as practical, to protect all threaded connections from contact with fluorine, and to minimize cavities within the flow passage which could entrap contaminants. In the event that cracks or narrow interfaces could not be avoided, these interfaces were made intentionally larger in order to facilitate final cleaning and flushing of the valve assembly.

The hinged poppet had three stages in its rotational displacement. First, it was accelerated to a high rotational velocity during the actuation stroke of the explosive actuator. Then during the non-powered stage of its rotational displacement it decelerated due to drag losses. Finally the hinged poppet wedged itself into the tapered section of the outlet and formed an intimate metal-to-metal seal with the outlet.

It should be pointed out that this design concept had been used previously in a tandem design, where a normally open and a normally closed valve were coupled together within one body to reduce total system envelope. This previous valve had only a one inch (2.54 cm) diameter line size but it did function successfully in water.

### 3.4 Development Tests

The overall test program to which the valve design was to be subjected is shown in Figure 3. The program was designed to investigate in a logical fashion the influences of various environments on valve functioning. There were six major test activities scheduled:

1. Valve Development Tests
2. Valve Margin Tests
3. Cartridge Temperature Verification Tests
4. Cartridge Vibration Verification Tests
5. Valve Functional Acceptance Tests
6. Valve Fluorine Compatibility Tests

Although the basic valve concept had been used previously, the substantial increase in line size from 1.00 inch (2.54 cm)

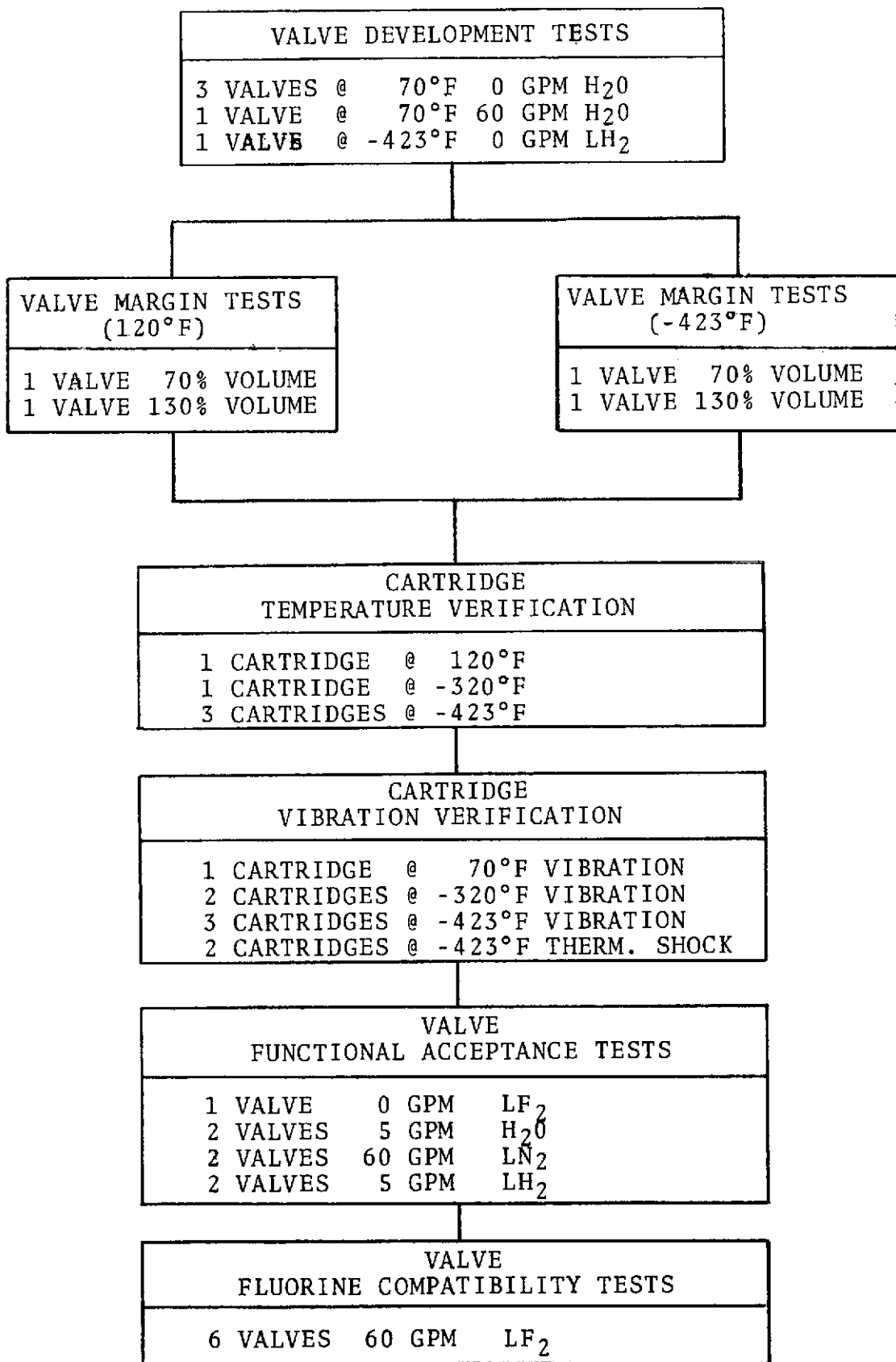


FIGURE 3. FLUORINE VALVE TEST PROGRAM

to 2.50 inches (6.35 cm) necessitated a number of development tests. There were several key areas of concern which needed to be investigated. First in importance was the verification of the structural integrity of the explosive actuator and the poppet hinge mechanism. Also under investigation during this initial development effort was the stroke length required to impart sufficient kinetic energy to the hinged poppet to enable it to form a positive seal. A second area of concern was the thermal effects on the hinge mechanism and on the metallic bellows. Then finally, the third area of concern was the effect of drag forces under flow conditions on the hinge mechanism. In order to investigate these areas, the development test program was divided into three groups of tests:

1. Actuator Development Tests in H<sub>2</sub>O
2. Cryogenic Development Tests in LH<sub>2</sub>
3. Flow Test in H<sub>2</sub>O at 60 gpm (3.78 l/sec)

#### Actuator Development Tests

The purpose of the actuator development tests was to verify the structural integrity of the various valve components, particularly the poppet hinge mechanism and the explosive actuator. A great deal of uncertainty also existed with regard to actuator stroke length.

The first actuator development test was conducted on 18 September 1970. A completely assembled valve was submerged in water and actuated by the explosive cartridge. Both the inlet and the outlet were completely open in order to provide unobstructed flow downstream of the valve seat. Valve actuation occurred as anticipated, however, post fire examination revealed the following deficiencies:

1. The hinged poppet was wedged into the outlet in a partially open position.
2. The hinge struts of the poppet were slightly bent and showed very light stress marks.
3. A force of approximately 10 pounds (44.48N) applied perpendicularly to the poppet face was required to dislodge the hinged poppet from the seat.

Conclusions drawn from the results of this first development test were as follows:



1. The deformation of the hinge struts occurred during the acceleration phase of poppet travel, i.e., during contact with the actuator piston.
2. This deformation prevented the poppet from contacting the valve seat perpendicularly and resulted in the observed partially open but wedged position.
3. The kinetic energy imparted to the hinged poppet during the acceleration phase was insufficient to lock the hinged poppet in the outlet.

On the basis of the results obtained during the first development test the following changes were made to the valve design:

1. The preactuation volume between piston and cartridge was increased to provide for a lower initial pressure. It was anticipated that this would result in reduced acceleration of the hinged poppet and thereby prevent deformation of the poppet hinge struts.
2. The actuator piston stroke was increased from a nominal distance of .200 inch (.508 cm) to a nominal distance of .400 inch (1.016 cm). It was expected that this change would allow for an increase in energy transfer from the actuator piston to the hinged poppet.
3. A study was made of various poppet and outlet seat geometries with the purpose of obtaining optimum poppet retention or locking. It was found that optimum retention was obtainable with a 3 degree taper in the outlet. (See Appendix A for an analytical discussion of this effort.)

On 24 September 1970 the second development firing was conducted. The test valve incorporated all the changes discussed above. The complete valve assembly was again submerged in water with the inlet and outlet open. Valve actuation occurred as anticipated. Post test examination revealed that the valve was completely closed. A force of 15 pounds (66.75 N) was applied perpendicularly to the poppet backside, i.e., the outlet side. It was found that this force, which is equivalent to 3 psig (2.06 N/cm<sup>2</sup>) hydrostatic pressure, dislodged the seat. The conclusions drawn from this second development test were as follows:

1. The increase in preactuation volume resulted in a lower initial pressure and prevented the previously noted deformation of the poppet hinge struts. This allowed the poppet to contact the outlet seat perpendicularly and form a seal sufficiently strong to withstand a back pressure of 3 psig (2.06 N/cm<sup>2</sup>).

2. Since the design requirements demanded that the poppet/seat interface must withstand a back pressure of at least 250 psig ( $172.41 \text{ N/cm}^2$ ) this test revealed that insufficient energy was transmitted to the hinged poppet to meet design requirements.

An analysis of the pressure decay within the cartridge adaptor was then conducted. The analysis revealed that the hinged poppet had indeed retained only marginal kinetic energy at the end of the non-powered rotational displacement.

As a result of the analytical findings described above the development hardware was then modified. The modifications consisted of weighting the hinged poppet and increasing the power stroke of the actuator to .500 inch (1.27 cm). On 26 October 1970 the third actuator development firing was conducted. The complete valve assembly was again submerged in water with inlet and outlet unrestricted.

Valve actuation occurred as anticipated, however, post fire examination revealed the following deficiencies:

1. The valve poppet did not lock in the outlet.
2. The separation piston was severely deformed.
3. The separation screw was split radially at the sealing shoulder.

The conclusions drawn from the results of this third development test were as follows:

1. The deformation of the separation piston occurred because this part had not been properly heat treated.
2. The deformation prevented the actuator from fully stroking.

On the basis of the results obtained the decision was made to repeat the test but to use properly heat treated components.

On 30 October 1970 the fourth actuator development test was conducted. The valve was again submerged in water with inlet and outlet unrestricted. The cartridge was fired and valve actuation occurred as anticipated. Visual observation of the valve showed that the poppet was wedged securely in the valve seat. The valve was then hydrostatically pressurized with freon in order to determine at what pressure the poppet would lift from the seat. No effort was made at this point to determine actual leakage. The maximum pressure

reached at which the poppet lifted from the seat was 380 psig (262.06 N/cm<sup>2</sup>). Since this pressure was well above the design requirement of 250 psig (172.41 N/cm<sup>2</sup>) it was concluded that this last actuator development test was finally successful.

In summary, the four actuator development tests described above established the following facts:

1. The hinge mechanism of the poppet was structurally sound.
2. The explosive actuator, specifically the metallic bellows weldment, was structurally sound.
3. The stroke length of the explosive actuator was sufficient to lock the hinged poppet in the seat.
4. The quality of the seal formed between the poppet and the seat was directly related to the weight of the poppet.

The modifications made to the basic valve design during the four actuator development tests were considered to be sufficient to warrant cryogenic development testing.

#### Cryogenic Development Test

The purpose of the cryogenic development test was to investigate the effect of liquid hydrogen temperature [-423°F (-253°C)] on the explosive cartridge, the metallic bellows and the hinge mechanism. With regard to the cartridge the uncertainty existed whether sufficient pressure could be generated to lock the poppet in the seat. The metallic bellows were suspected of cracking under cryogenic conditions combined with the high acceleration rates produced by the explosive actuator. And finally the effect of metal shrinkage within the hinge mechanism needed to be verified. Also during the course of this cryogenic test an effort was made to gather quantitative data of leak rates at the poppet/seat interface and at all other component interfaces.

A fifth development valve was therefore assembled and prepared for cryogenic testing.

Each valve component was visually and dimensionally examined for conformance to the latest configuration as identified on the appropriate detail drawings and the parts list. No anomalies were noted on the valve.

The actuator weldment was then subjected to an internal leak test at 100 psig (68.96 N/cm<sup>2</sup>). The actuator weldment was internally pressurized with helium and leak tested in a vacuum

bell jar. The leak rate measured was  $4.5 \times 10^{-9}$  scc/sec, well within the design requirements.

Valve external leakage between actuator housing and separation screw, between actuator housing and valve housing, and between valve housing and outlet assembly was measured with the valve internally pressurized to 100 psig (68.95 N/cm<sup>2</sup>) helium. Gross leakage was noted and the valve was submerged in water while pressurized with helium to detect the leak path. Bubbles could be observed at the flange, at the socket head cap screws and tube connections (B-Nuts). Further tightening of the connections did not improve the leak rate. At this point, after consultation with Parker Seal Company, the manufacturer of the metallic seals used in the valve, it was decided to close all flange leak paths by electron beam welding.

The valve was again placed in the test setup and pressurized with helium. Leak rates in excess of  $1 \times 10^{-4}$  scc/sec could be detected. The flanged tube connections were then modified to accept a teflon o-ring. The valve was retested and the leak rates dropped to  $3 \times 10^{-6}$  scc/sec. The teflon o-ring was then coated with Halocarbon 25-58 and the leak rates dropped to  $5 \times 10^{-10}$  scc/sec. At this point it was concluded that the valve passed the ambient external leak test.

The valve was then subjected to an internal pressure of 800 psig (551.72 N/cm<sup>2</sup>) for five minutes. No evidence of rupture or permanent deformation was noted.

The valve was installed in the test setup shown in Figure 4. After stabilizing the valve temperature at -423°F (-253°C) the liquid hydrogen supply was shut off and the valve internally pressurized with helium. Gross leakage could be observed at the flared tubing connections. Since the valve material was 2219 aluminum alloy and the flared tubing connections were stainless steel it was decided to retest the valve with aluminum connections in order to eliminate the difference in thermal expansion. The valve was again stabilized at -423°F (-253°C), then pressurized with helium at 100 psig (68.96 N/cm<sup>2</sup>). After two minutes the observed leak rate was  $1.4 \times 10^{-7}$  scc/sec of helium with valve temperature at -404°F (-242°C). It should be noted that repeated tightening of the flared tubing connections was required at cryogenic temperatures.

The valve was then installed in the test setup shown in Figure 5 with inlet and outlet unrestricted. After submerging and stabilizing the valve in liquid hydrogen for fifteen minutes the cartridge was actuated.

Post actuation inspection revealed that the valve had closed

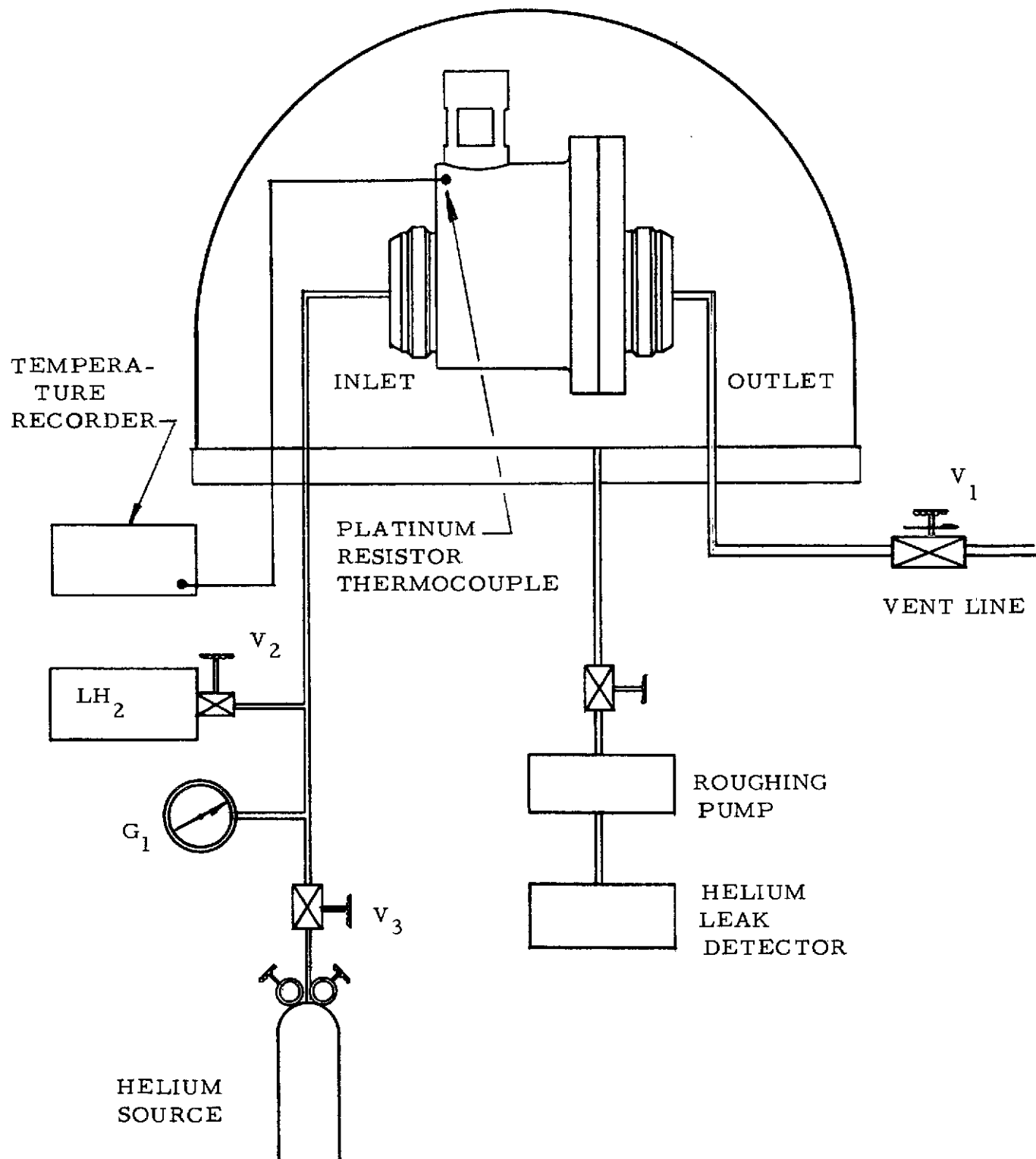


FIGURE 4. EXTERNAL LEAK TEST SCHEMATIC  
(LIQUID HYDROGEN)

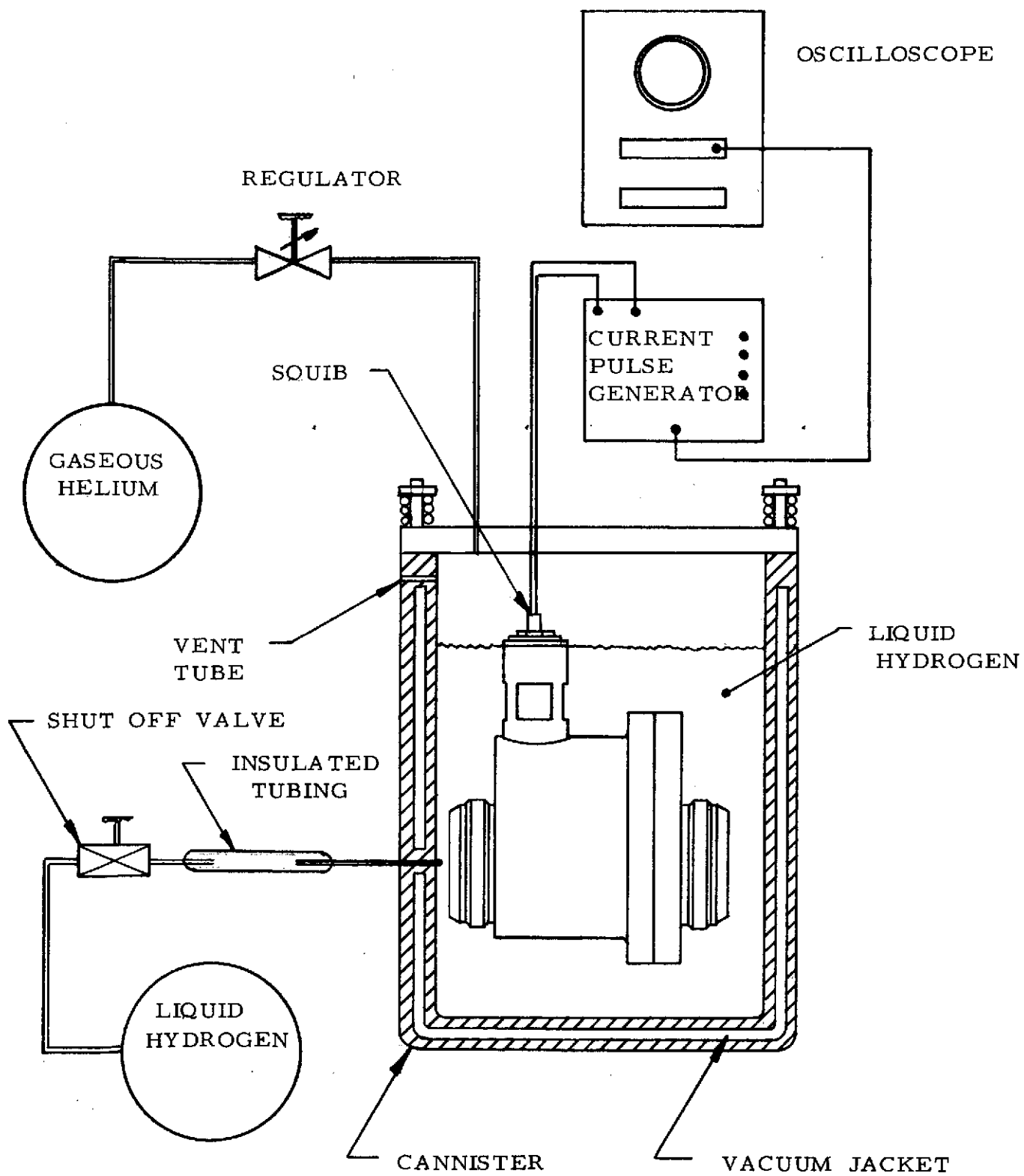


FIGURE 5. ACTUATION TEST SCHEMATIC  
(LIQUID HYDROGEN)

and no external rupture had occurred. However, a portion of the shear bolt was found in the closed-off flow cavity upstream of the poppet.

The valve assembly was installed in the vacuum leak chamber and pressurized from the outlet side with 100 psig (68.96 N/cm<sup>2</sup>) helium. The noted leak rate was  $4.2 \times 10^{-6}$  scc/sec.

The valve outlet was pressurized hydrostatically until the poppet dislodged. Back pressure required to dislodge the poppet was 700 psig (482.75 N/cm<sup>2</sup>).

The bellows actuator was pressurized internally to 100 psig (68.96 N/cm<sup>2</sup>) after actuation at -423°F (-253°C). The recorded leak rate was  $1.2 \times 10^{-8}$  scc/sec of helium.

In summary the cryogenic development test described above established the following facts:

1. The output pressure produced by the cartridge while stabilized at -423°F (-253°C) was sufficient to lock the hinged poppet in the outlet seat.
2. The metallic bellows maintained structural integrity under cryogenic conditions.
3. Metal shrinkage due to cryogenic conditions did not affect the hinge mechanism.
4. The gold plated metallic seal of the outlet assembly was incapable of providing the required sealing. Therefore it was recommended that the outlet assembly be permanently welded to the valve housing.
5. The flared tubing connections (B-Nuts) were incapable of providing the required sealing. Therefore it was recommended that they be placed with Marmon Conoseal Connectors or an equivalent design.
6. The shear screw and shear piston failed to produce the desired secondary seal.
7. The metal-to-metal seal formed by the poppet and outlet seat was sufficient to proceed with the remaining test schedule.

## Flow Development Test

The purpose of the flow test was to verify the structural integrity of the hinge mechanism under flow conditions. It should be remembered that the hinged poppet was held in the open position by two aluminum shear pins of .125 inch (.318 cm) in diameter. The drag forces imparted to the poppet were transmitted directly to these two shear pins and the effect of these forces needed to be investigated. Also during the course of this flow test quantitative data were to be collected with regard to pressure/drop across the valve, water hammer effects, and the pressure required to lift the poppet from the seat after valve closure.

A sixth development valve was assembled and prepared for testing in a 60 gpm (3.78 l/sec) ambient water flow system. The valve was installed in the test set-up shown schematically in Figure 6. The pressure drop between the inlet and outlet was determined while flowing 60 gpm (3.78 l/sec); flow was maintained for 15 minutes. The pressure drop across the valve was measured to be .75 inch of water (1.90 cm) at 60 gpm (3.78 l/sec) and 9.5 psig (6.55 N/cm<sup>2</sup>) inlet pressure. After maintaining flow for 15 minutes, the valve was removed from the test system and disassembled for visual examination of possible damage to the shear pins. No evidence of damage could be observed. The valve was then reinstalled in the test system and flow reestablished at 60 gpm (3.78 l/sec) after which the valve was actuated.

The results of this test are summarized below:

### DEVELOPMENT TEST NO. 6: VALVE FLOW TEST

Bridgewire Burnout Time	2 msec
Poppet Closing Time	11 msec
Water Hammer (upstream)	50 psig (34.48 N/cm <sup>2</sup> )
Water Hammer (downstream)	24 psig (16.55 N/cm <sup>2</sup> )
Back Pressure to Unseat	20 psig (13.79 N/cm <sup>2</sup> )

The flow development test described above revealed the following facts:

1. Drag forces due to flow have no effect on the poppet hinge mechanism.
2. The pressure spike associated with water hammer as a result of valve closure is negligible.



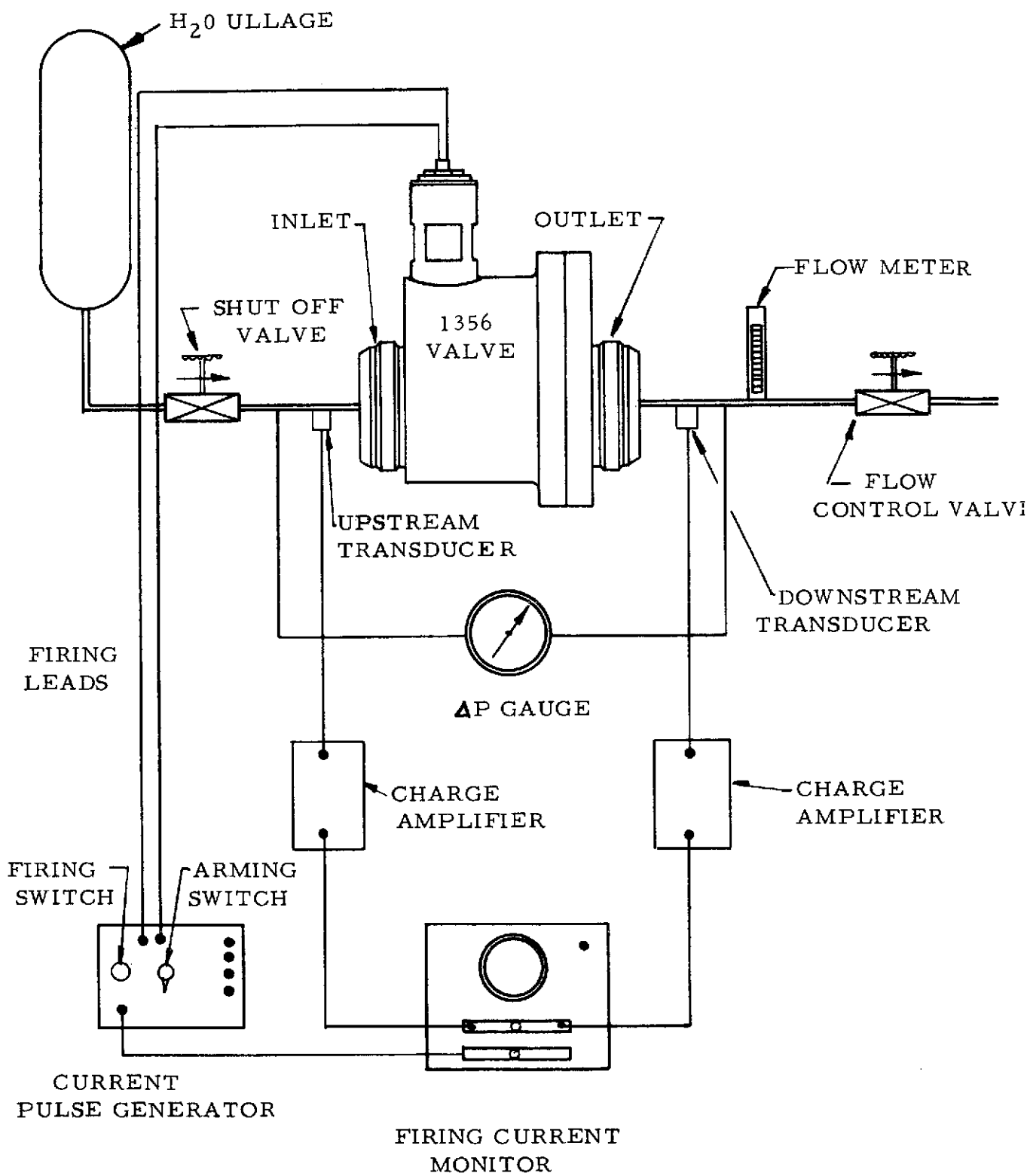


FIGURE 6. FLOW TEST SCHEMATIC

3. System resistance to flow, such as line restrictions, line friction, and static pressure head have a profound effect on the metal-to-metal seal formed between poppet and outlet seat.

Scheduled concurrently with the flow test were the valve margin tests which are described in Section 4.0 of this report. The test results obtained during the valve margin tests also indicated that line restrictions downstream of the valve severely affected valve closure. A quantitative analysis was conducted as a result of these findings which are described in Section 4.2 entitled "Orifice Effects".

### 3.5 Design Evolution

The evolution of the valve design from the beginning of the development program can be seen by comparing Figure 2 and Figure 7. Figure 2 represents the configuration at the start of the development program and Figure 7 represents the final configuration. Basically there were six areas which underwent a change during the development effort:

1. The seat design
2. The poppet design
3. The explosive actuator stroke
4. The piston design
5. The flanged tube connections
6. Valve external sealing methods

#### Seat Design

The original seat design featured a 10 degree tapered seat. The initial design analysis indicated that a 10 degree taper in the outlet seat would provide sufficient retention of the poppet in the seat to withstand a back pressure of at least 250 psig (172.41 N/cm<sup>2</sup>). However, during the initial development stages, it was discovered that a 3 degree taper was necessary to meet the required retentive force. An analysis of the optimum geometry of poppet and seat is presented in Appendix A entitled "Poppet/Seat Analysis".

#### Poppet Design

The original poppet design featured an aluminum poppet. During the course of the actuator development tests it was

discovered that the weight of the poppet had a profound effect on the quality of sealing between poppet and seat. It was necessary to increase the weight by attaching stainless steel coupons to the poppet. The final design featured a heavier stainless steel poppet. An analysis of the effect of the mass moment of inertia on valve sealing is presented in Section 7.0 entitled "Analysis".

### Actuator Stroke

During the course of the four actuator development tests the stroke of the actuator was increased from .200 inch (.508 cm) to .500 inch (1.270 cm). This change was necessitated by the need for a high initial kinetic energy of the poppet.

### Piston Design

The original piston design did not provide for sealing of the products of combustion in the plenum behind the piston. During the actuator development tests it was discovered that a substantial amount of propellant gases entered the bellows cavity. Although the bellows did not rupture during valve actuation and safely contained the products of combustion of the cartridge, the addition of a metallic cup seal on the piston provided added assurance that the cartridge combustion gases would not come in contact with the valve flow media.

### Flanged Tube Connections

The original valve design featured threaded inlet and outlet connections as described by Military Standard MS33656, "Fitting, End, Standard Dimensions for Flared Tube Connections and Gasket Seal". Although this type of connection is used frequently in the industry, they proved to be completely inadequate during cryogenic testing. The design of the inlet and outlet was therefore changed to accept the Marmon Conoseal Connectors. This is a patented design which relies on clamping forces rather than on torque and has proven to be reliable under cryogenic conditions for large line sizes.

### Valve External Sealing

The original valve design featured a number of Metallic V-Seals made of Inconel-X750 and gold plated. Manufacturers specifications indicated that this material is especially suited for its cryogenic and high temperature strength. Although the smaller diameter seals used in the valve proved

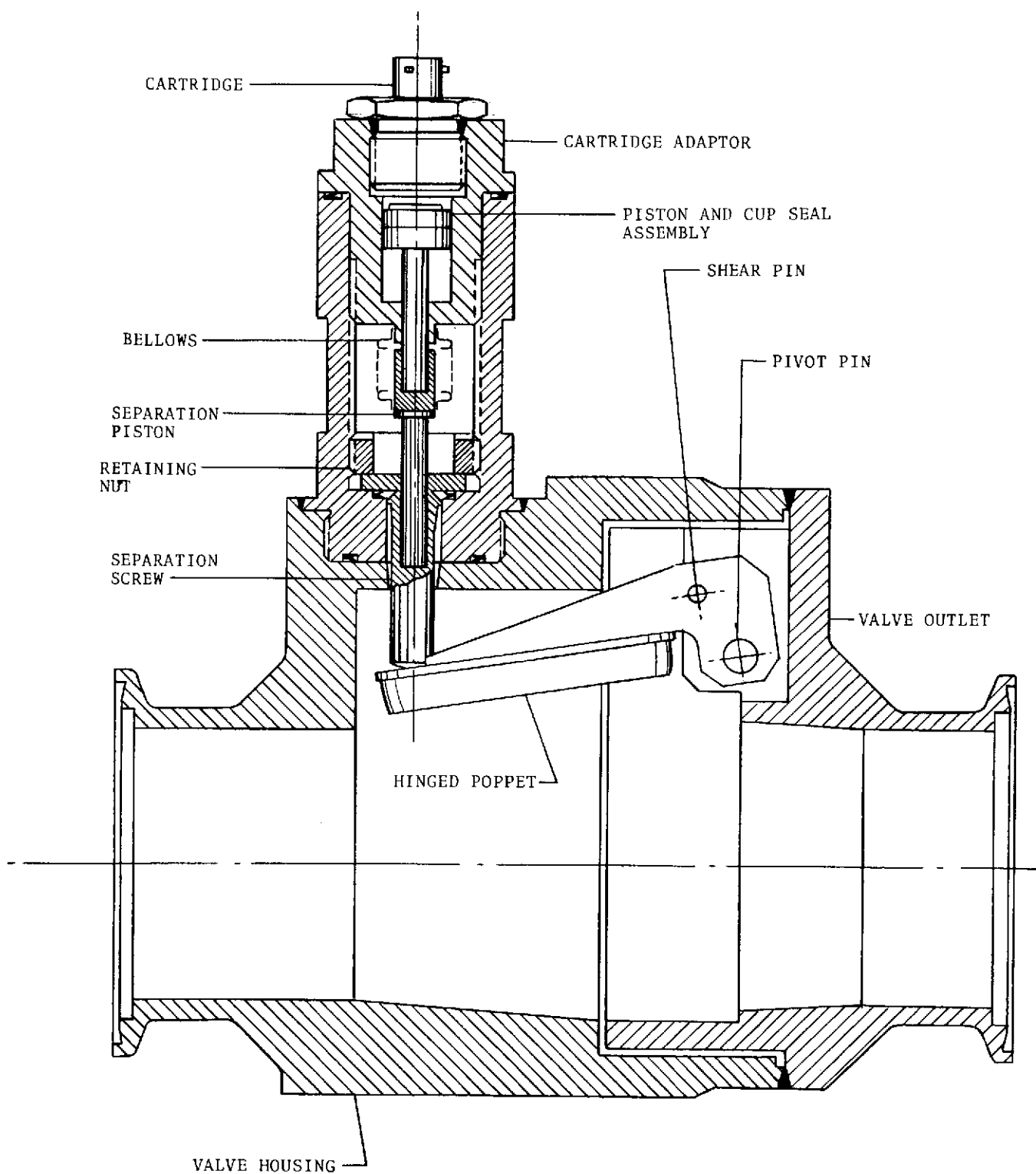


FIGURE 7. 2-1/2 INCH EXPLOSIVELY ACTUATED VALVE  
(FINAL DESIGN)

to be satisfactory it was found during the cryogenic development test that the large 3.125 inch (7.938 cm) diameter flange seal which was installed between valve housing and outlet assembly allowed gross leakage. It was therefore decided to eliminate this seal altogether and rely on electron beam welding to prevent external leakage.

### 3.6 Discussion of Results

The development test program conducted proved that the basic hinged poppet valve design was sound. The actuator development tests verified that the poppet could be locked in the outlet seal with sufficient force to withstand a back pressure of 380 psig (262.06 N/cm<sup>2</sup>). The cryogenic development tests verified that the valve was immune to temperature environments of -423°F (-253°C); specifically that the metallic bellows were capable of sealing the cartridge combustion gases under cryogenic conditions. The flow development test verified that the drag forces imparted to the hinge mechanism were negligible and that the water hammer effects associated with valve closure were minimal. This last development test also showed that the valve was sensitive to line resistance. Although it was realized that this characteristic was not altogether desirable it was also recognized that future valve usage could be limited to those applications where line restrictions were absent.

#### 4.0 TASK II: CARTRIDGE VERIFICATION TESTING

The objective of this phase of the program was twofold. First, since it was known that explosive cartridges are sensitive to environmental influences, it was necessary to determine that the cartridge selected was capable of functioning reliably after exposure to cryogenic temperatures, vibration, and thermal shock. This was accomplished by installing cartridges in a firing chamber of fixed volume and measuring the pressure output after exposure to the various environments.

Second, since explosively actuated devices are inherently sensitive to cartridge output pressure, it was necessary to establish that the valve would function over a broad range of output pressures. This was accomplished by testing four margin valves.

The test schedule of Task II is summarized in the table below.

TABLE 1. CARTRIDGE VERIFICATION TESTING

QUANTITY OF TEST SPECIMEN	TEST TEMPERATURE (°F)	TEST TYPE
1	120	Margin Valve (Overcharge)
1	120	Margin Valve (Undercharge)
1	-423	Margin Valve (Overcharge)
1	-423	Margin Valve (Undercharge)
1	120	Cartridge Firing
1	-320	Cartridge Firing
3	-423	Cartridge Firing
1	Ambient	Cartridge Sine Vibration
2	-320	Cartridge Sine Vibration
3	-423	Cartridge Sine Vibration
2	-423	Cartridge Thermal Shock



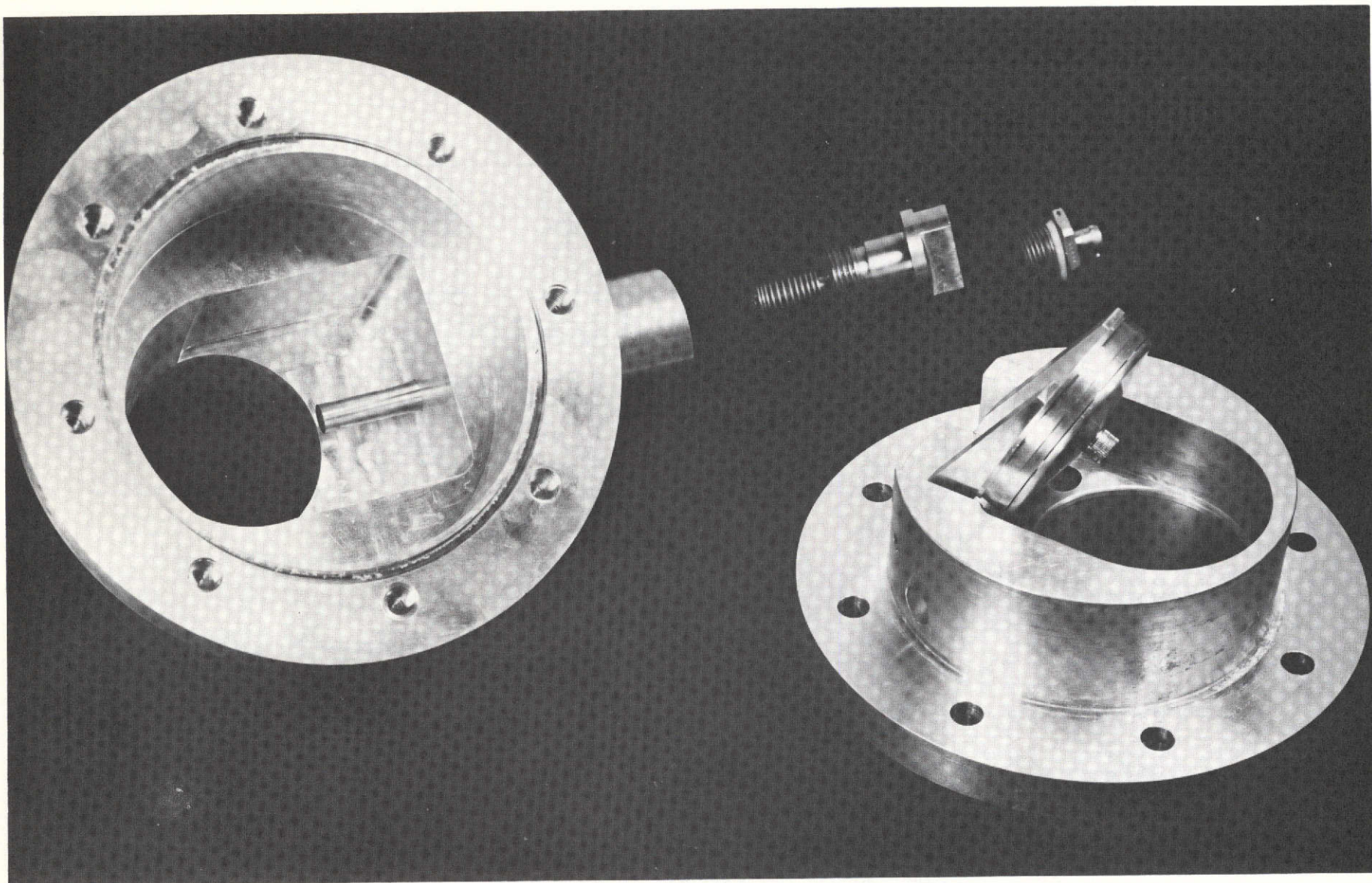


FIGURE 8. DISASSEMBLED MARGIN VALVE

#### 4.1 Margin Valve Tests

Functional margin tests are conducted with explosively actuated devices in order to ascertain that low cartridge pressure output combined with low temperature will still function the device, and that high cartridge pressure output combined with high temperature will have no detrimental effects on the structural soundness of the device. A disassembled margin valve is shown in Figure 8.

The pressure generated by the explosive cartridge was contained within a plenum in the explosive actuator (See Figure 9). The plenum was bounded by the top of the actuator piston and the cartridge closure disc. This volume is called the "Valve Pre-Actuation Volume" and its size determined the pressure generated within the plenum. By intentionally varying the pre-actuation volume it was possible to determine how sensitive the device was to cartridge pressure output. The criterium

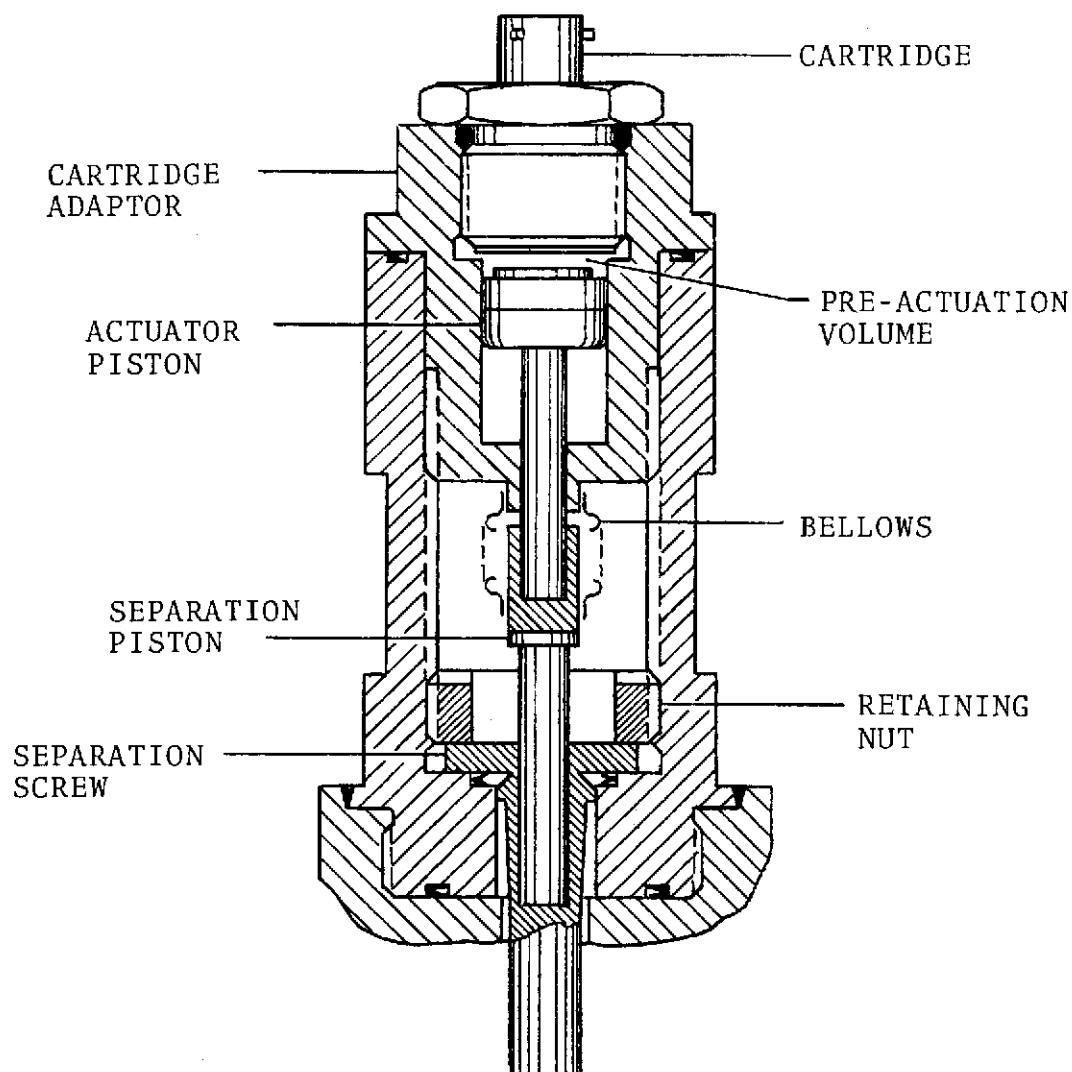


FIGURE 9. EXPLOSIVE ACTUATOR



for valve sensitivity to cartridge pressure output was the force required to lift the poppet from the seat after valve actuation. It was expected that a larger than nominal pre-actuation volume would result in a lower than nominal unlocking force. Conversely, a smaller than nominal pre-actuation volume would result in a higher unlocking force.

A min-max tolerance study was conducted which indicated that a  $\pm 27\%$  variation in the pre-actuation volume was possible due to normal tolerance stack up. For this reason four margin valves were manufactured, two of which had a pre-actuation volume 30% larger than nominal, and two had a pre-actuation volume 30% smaller than nominal. One valve of each type was tested at  $+120^{\circ}\text{F}$  ( $+49^{\circ}\text{C}$ ) in  $\text{H}_2\text{O}$ , and one valve of each type was tested at  $-423^{\circ}\text{F}$  ( $-253^{\circ}\text{C}$ ) in  $\text{LH}_2$ .

#### Margin Test at $120^{\circ}\text{F}$

Margin Valve, S/N 002, with 70% pre-actuation volume, was installed in the test setup shown in Figure 10. The test system utilized a 1.00 inch (2.54 cm) line size, fast acting valve downstream of the valve outlet. The system was filled with water and the valve conditioned to  $120^{\circ}\text{F}$  ( $+49^{\circ}\text{C}$ ). The explosive valve was actuated 100 msec after opening the fast acting valve downstream of the explosive valve. When the explosive valve was removed from the setup for leak test the hinged poppet opened with a force of approximately 2 pounds (8.9 N). Since the design requirements specified a poppet unlocking pressure or back pressure of 250 psig (172.41 N/cm<sup>2</sup>) this test was considered a failure.

After it had been determined that the 1.00 inch (2.54 cm) line size, fast acting valve had indeed opened 100 msec prior to margin valve closure, the most probable cause of failure was investigated.

Two reasons for the failure of the poppet to lock in the outlet seat were advanced:

1. Cartridge Failure
2. Downstream Line Restriction

The cartridges used in this test program were furnished by the Jet Propulsion Laboratory, Pasadena, California. The cartridges were manufactured for the Jet Propulsion Laboratory under strict quality control procedures and they had preliminary qualification status. Up to this point in the program a total of seven (7) valve firings had been conducted in which no cartridge failure had been observed. Subsequent visual inspection of the cartridge revealed complete consumption of the explosive main charge and of the primer charge.

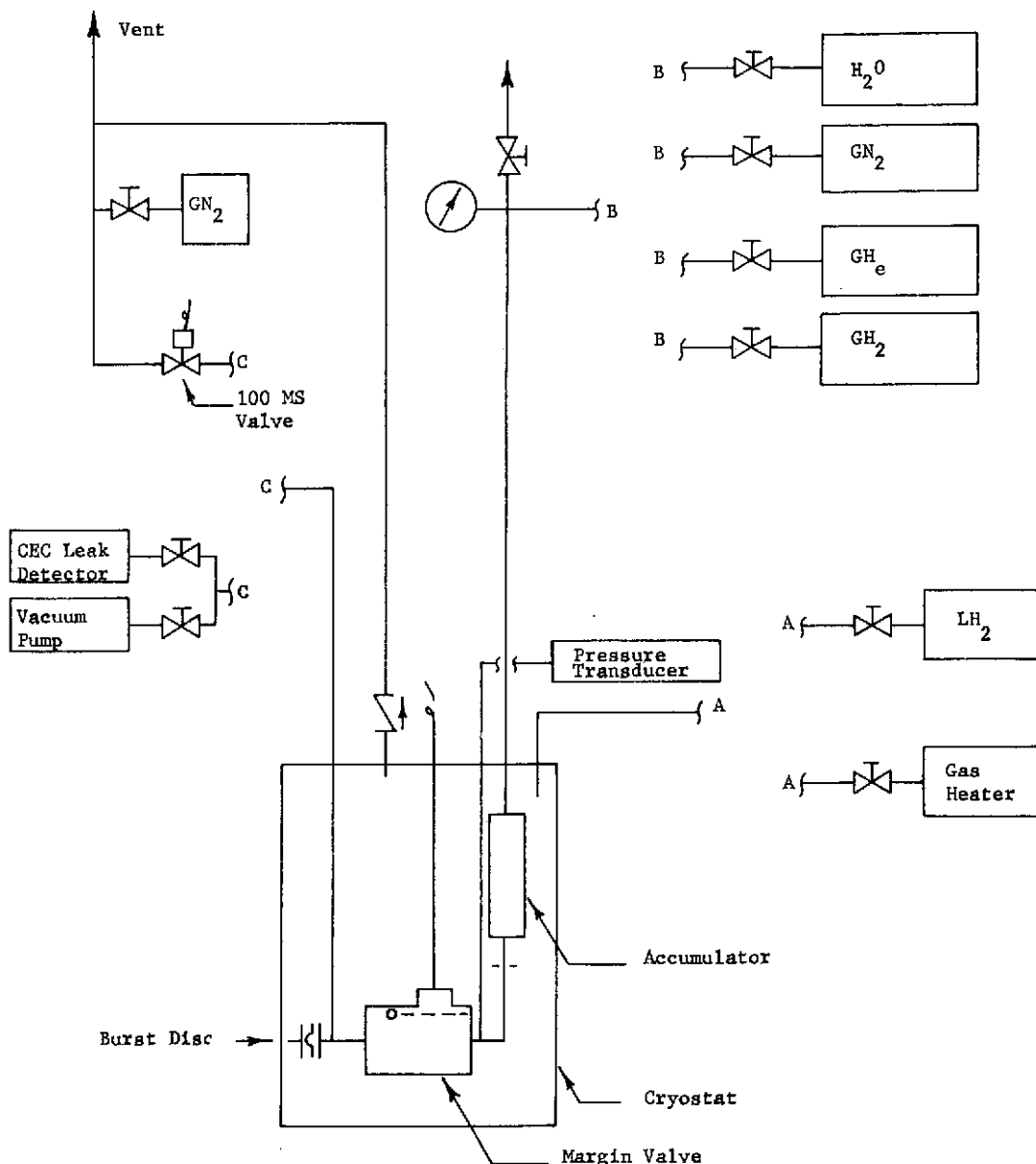


FIGURE 10. MARGIN FIRING TEST INSTALLATION

The first valve margin test was conducted at 120°F (+49°C) a temperature level which was considered to be well within the reliable ignition range. In view of these considerations and in view of the fact that a previous valve failure had occurred under similar circumstances, i.e., with a line restriction present in the test setup, it was concluded that the most probable cause of failure was the downstream restriction posed by the 1.00 inch (2.54 cm) fast acting valve.

In order to verify the failure mode, the second margin test at 120°F (+49°C) was conducted with the valve submerged in water without either inlet or outlet connections. This test setup was in fact identical to the actuator development test

setup. Margin Valve S/N 003 had a pre-actuation volume of 130%. The valve was actuated and subsequent visual inspection revealed that the poppet was firmly locked in the outlet seat. The valve was then removed from the test setup and pressurized from the inlet side to 15 psig (10.34 N/cm<sup>2</sup>) with helium. The internal leakage of the valve was then determined by mass spectrometer leak detector. The leak test did not indicate any leakage at a leak detector sensitivity of  $1.9 \times 10^{-10}$  scc/sec of helium. The valve was then reinstalled in the test setup and hydrostatically pressurized from the outlet side in order to determine the pressure at which the poppet would lift from the seat. Unseating pressure was 350 psig (241.38 N/cm<sup>2</sup>). This unseating pressure compares well with the unseating pressure experienced during the fourth development test which was established at 380 psig (262.06 N/cm<sup>2</sup>).

The lower unseating pressure measured during the margin valve test was attributed to the larger pre-actuation volume of the margin valve. This result had been anticipated. A further observation was made with regard to the unseating pressure of the development valve and that of the margin valve.

The increase in pre-actuation volume resulted in a reduction of unseat pressure of 30 psig (20.68 N/cm<sup>2</sup>) when compared with the unseat pressure of the development valve. It was reasonable to assume that an increase of unseat pressure of approximately 30 psig (20.68 N/cm<sup>2</sup>) would have been the result of the margin test conducted with Valve S/N 002. More specifically, had Valve S/N 002 been tested without a line restriction present in the test setup, the assumption can be made that the unseat pressure would have been approximately 410 psig (282.74 N/cm<sup>2</sup>).

Post-actuation visual examination of both margin valves which had been conditioned at 120°F (+49°C) revealed that the valve was not affected by the combination of high temperature and high pressure as produced by the explosive cartridge. The margin valve test program was therefore continued.

#### Margin Test at -423°F (-253°C)

Margin Valve S/N 004, with a 70% pre-actuation volume, was installed in the test setup shown in Figure 11. A 4.00 inch (10.16 cm) long tube with an inside diameter of 2.00 inches (5.08 cm) was welded to a standard pipe elbow. This assembly was connected to the outlet. No connections were made to the valve inlet.

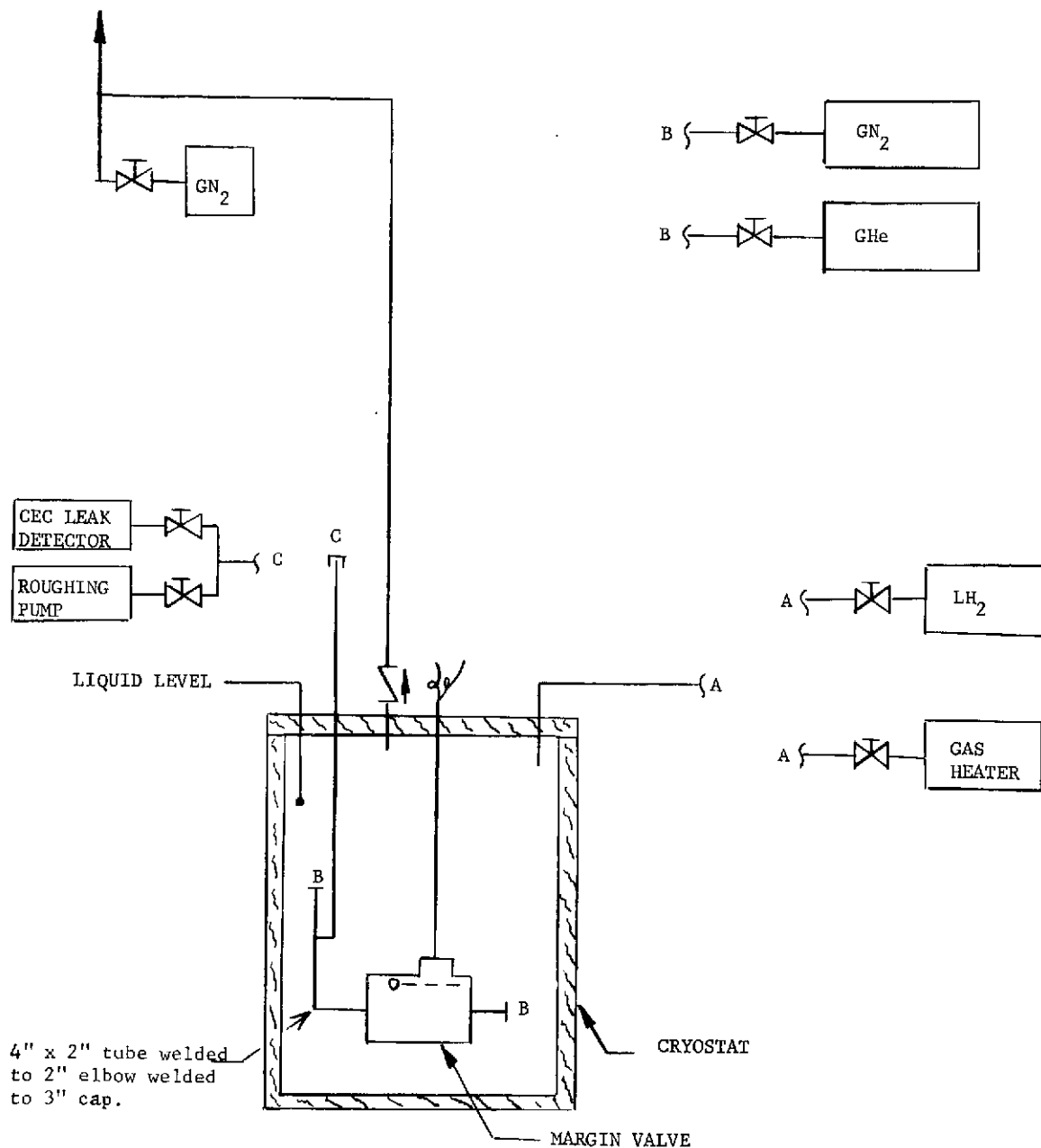


FIGURE 11. MODIFIED MARGIN VALVE SETUP

The valve was then submerged in  $\text{LH}_2$  and stabilized at  $-423^\circ\text{F}$  ( $-253^\circ\text{C}$ ) and the cartridge actuated. Subsequent to cartridge actuation the valve was removed from the test setup and allowed to reach ambient temperature. The valve was then pressurized from the inlet side with helium to a pressure of 15 psig ( $10.34 \text{ N/cm}^2$ ). The leak test indicated no leakage at a leak detector sensitivity of  $1.6 \times 10^{-9} \text{ scc/sec}$ . After

leak testing the valve was hydrostatically pressurized from the outlet side in order to determine the pressure at which the poppet would lift from the seat. The recorded unseating pressure for Valve S/N 004 was 840 psig (579.31 N/cm<sup>2</sup>).

Margin Valve S/N 006, with a 130% pre-actuation volume, was then tested under identical conditions as Valve S/N 004. The recorded leak rate and unseat pressure was  $1.6 \times 10^{-9}$  scc/sec and 740 psig (510.31 N/cm<sup>2</sup>) respectively. A comparison of the two recorded unseat pressures showed that the larger pre-actuation volume resulted in a lower unseat pressure and the smaller pre-actuation volume resulted in a higher unseat pressure. However, a comparison with the results obtained during the valve development tests showed that the nominal pre-actuation volume resulted in an unseat pressure of 700 psig (482.76 N/cm<sup>2</sup>). Several reasons for this discrepancy in unseat pressures could be advanced. It appeared that other factors besides cartridge output pressure determined the force with which the poppet was locked in the seat. These factors could be related to differences in valve hardware such as finishes, tolerances, and component surface treatment. Since this variation was inherent in the design and could be expected to occur, any future valve usage must take this characteristic into account. This could be accomplished by specifying unseat pressures which are higher than maximum expected system pressure. A direct comparison of the test results obtained during the margin tests is shown in the table below.

TABLE 2. MARGIN VALVE TEST RESULTS

VALVE S/N	PRE-ACTUATION VOLUME (% OF NOMINAL)	TEST MEDIUM	TEST TEMPERATURE		BACK PRESSURE TO UNSEAT POPPET		LEAKAGE
			°F	°C	PSI	N/CM <sup>2</sup>	SCC/SEC
002	70	H <sub>2</sub> O	120	49	---	-----	-----
003	130	H <sub>2</sub> O	120	49	350	241	$1.9 \times 10^{-10}$
004	70	LH <sub>2</sub>	-423	-253	840	579	$1.6 \times 10^{-9}$
006	130	LH <sub>2</sub>	-423	-253	740	510	$1.6 \times 10^{-9}$

As can be seen from the table, the difference in unseat pressure between the valves tested in  $H_2O$  and  $LH_2$  was quite pronounced. The reason for this difference is directly related to the densities of the test fluids. The hinged poppet of the valve was subjected to drag forces and the magnitude of these forces was determined by the density of the fluid. It could therefore be expected that for a given valve design with a fixed energy input from the explosive cartridge higher unseating pressures are possible in fluids such as  $LH_2$ .

Visual evidence of the influence of fluid density on valve closure forces could be seen by comparing the hinged poppets of the margin valves. The four margin valves had been equipped with poppets machined from aluminum alloy. During the development tests it was discovered that the weight of the poppet had to be increased by installing steel coupons in order to minimize the effect of drag. A cross section of the weighted poppet is shown in Figure 12.

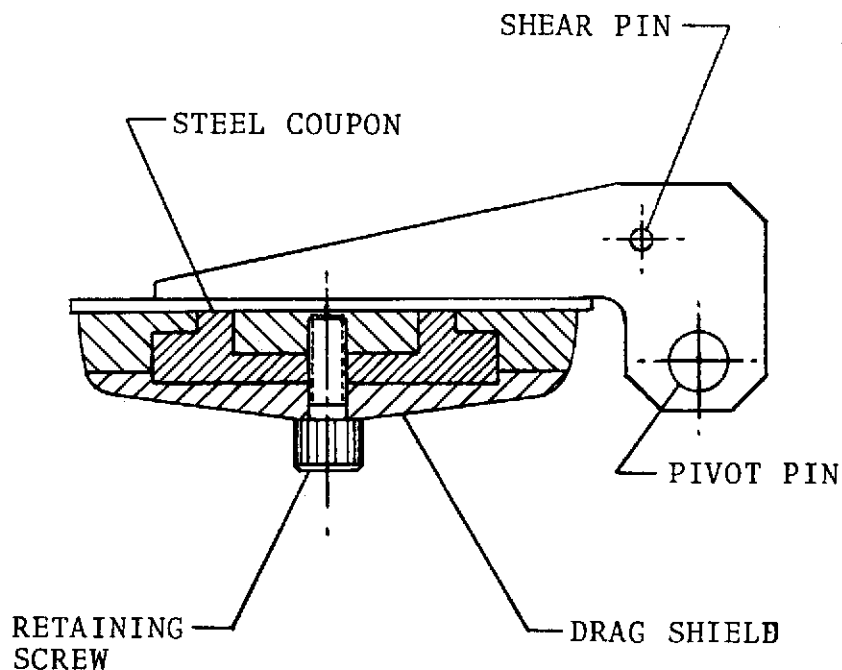
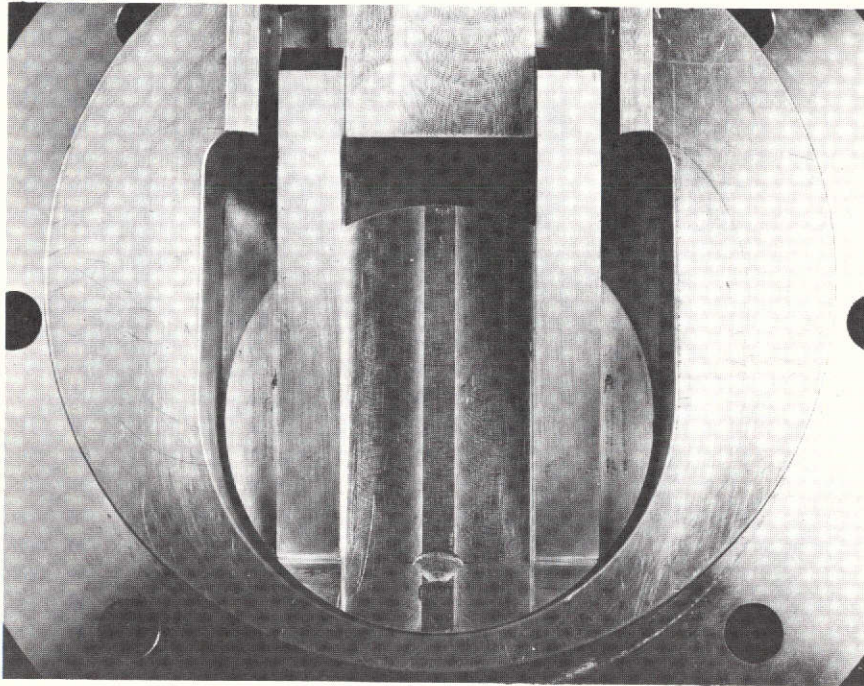


FIGURE 12. HINGED POPPET, MARGIN VALVE

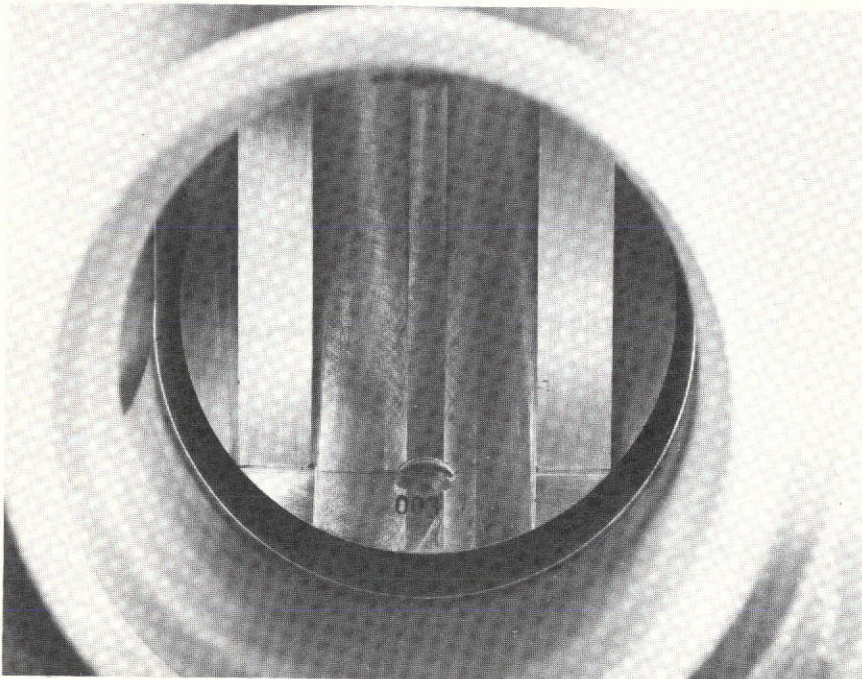
A cavity was machined into the poppet in order to accommodate the steel coupon. The thickness of the cross section was reduced in an annular area around the center of the poppet. The thickness of the remaining material was .060 inch (.152 cm). A comparison of the poppets showed definite deformation in the center between the hinge struts. The poppet of the first margin valve, S/N 002, which was tested in H<sub>2</sub>O and did not lock, showed no deformation at all, indicating that inertia effects were absent.

The poppet of the second margin valve S/N 003 revealed slight deformation in the center indicating that inertia effects were present. (See Figure 13.) The poppet of the third margin Valve, S/N 004, which was tested in LH<sub>2</sub> and which had a reduced pre-actuation volume, showed very pronounced deformation in the center. In fact, this deformation was more severe than that of the poppet used in the fourth margin valve, S/N 006, which had the 130% pre-actuation volume. (See Figure 14.)

The deformation of the center of the poppets was due to the rapid deceleration on impact with the outlet seat. Inertia forces on the steel coupon were transmitted to the poppet by the socket head cap screw and resulted in the observed deformation. There was a direct correlation between the severity of deformation and the pressure required to unseat the poppet after valve actuation. Since the poppet deformation was due to inertia forces it was concluded that the hinged poppet acquired a much higher velocity in LH<sub>2</sub> than in H<sub>2</sub>O and that this was a direct result of the difference in fluid density.



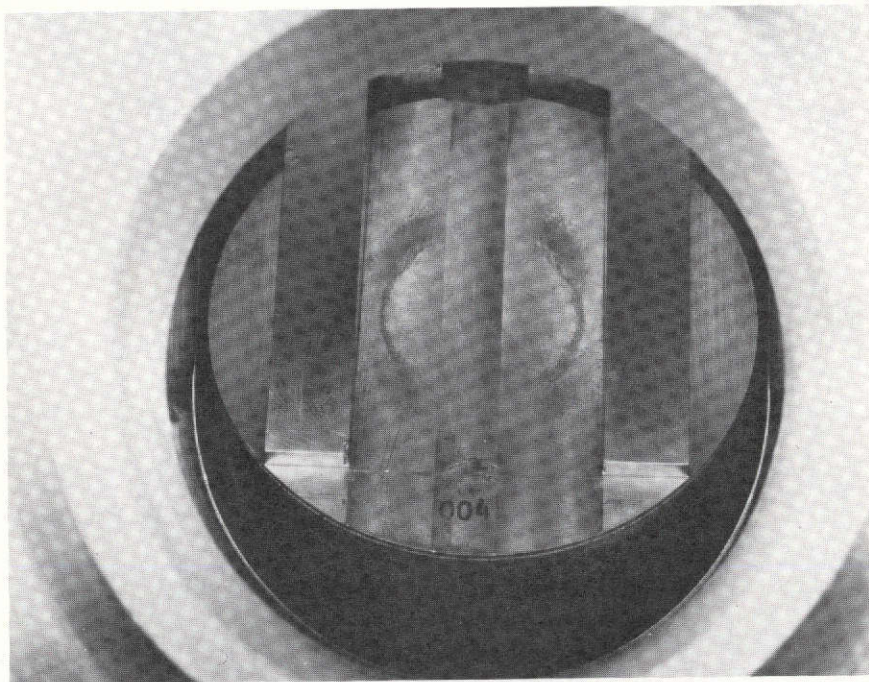
VALVE S/N 002



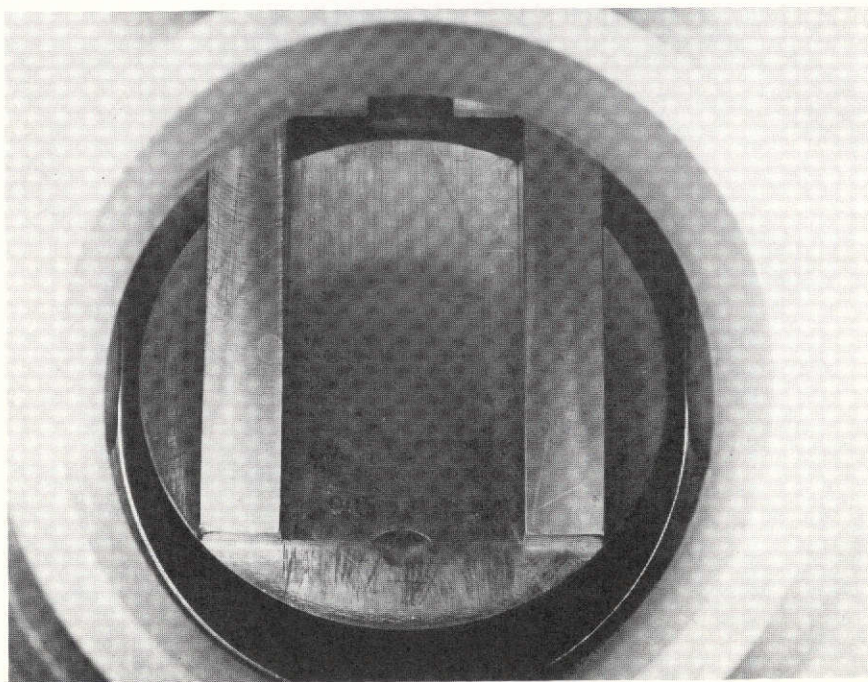
VALVE S/N 003

FIGURE 13. HINGED POPPET AFTER ACTUATION  
(FLOW MEDIUM: WATER)





VALVE S/N 004



VALVE S/N 006

FIGURE 14. HINGED POPPET AFTER ACTUATION  
(FLOW MEDIUM: LIQUID HYDROGEN)

## 4.2 Orifice Effects

Up to this point in the program two instances of valve failure had occurred which were attributed to restriction in the downstream line. In both instances the poppet failed to wedge itself into the outlet seat with sufficient force to withstand an unseating or back pressure of 250 psig (172.41 N/cm<sup>2</sup>). In the case of the full flow development test the restriction was caused by a flow meter, and in the case of the first valve margin test the restriction was due to a fast acting relief valve. To investigate the effect of downstream line restriction a special orifice test valve was manufactured. The valve was designed to be reusable for a limited number of tests. Reusability was verified prior to each subsequent test by disassembly of the valve and by inspection of the component parts. The orifice test valve differed from the standard design in the following areas:

1. The cartridge utilized was a Horex Cartridge P/N 6304 . The use of these cartridges was considered to be acceptable in light of the fact that they would be used under ambient conditions and because the primary purpose of the test was to gather comparative data on the effect of line restriction.
2. Isolation of the products of combustion of the explosive cartridge was not considered to be necessary since the valve was to be tested in H<sub>2</sub>O. For this reason the explosive actuator was not provided with a metallic bellows.
3. The orifice test valve was provided with a steel hinged poppet, machined of A-286 alloy steel. The selection of this material was made necessary in order to minimize wear of the sealing surfaces.
4. A .063 inch (.160 cm) diameter hole was drilled through the valve housing and the poppet hinge struts with the poppet held in the open position by the aluminum shear pins. A second .063 inch (.160 cm) diameter hole was drilled through the outlet, just below the sealing area. These holes provided access for installation of carbon rods which were to be used for poppet closure time measurements.

The orifice test valve was installed in the test setup shown schematically in Figure 15.

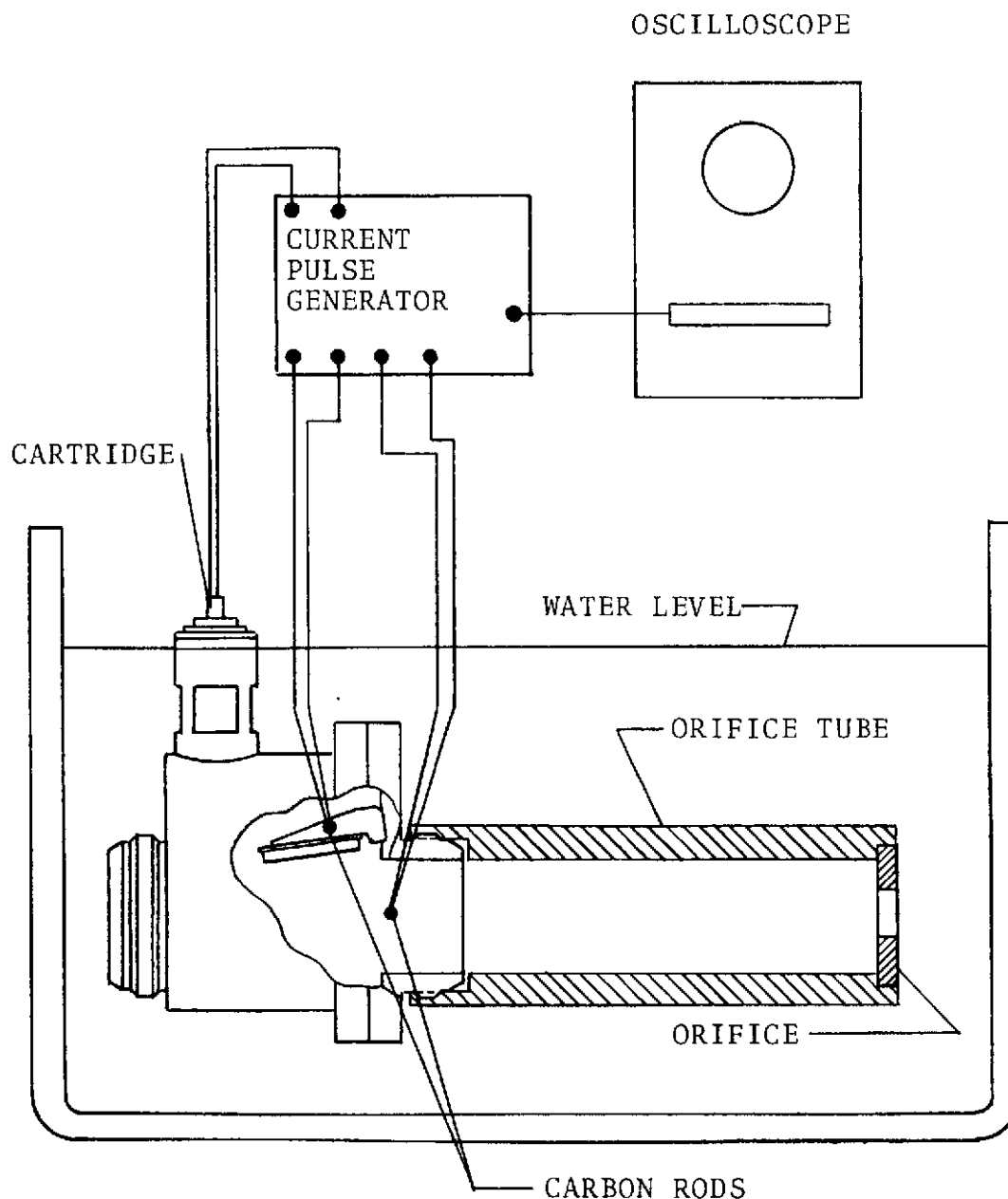


FIGURE 15. ORIFICE EFFECT TEST SCHEMATIC

The test setup consisted of a 24.00 inch (60.96 cm) long straight tube with an inside diameter of 2.500 inch (6.35 cm). The outlet of the straight tube was designed to accept sharp edged orifice plates. The orifice test valve was connected to the straight tube and submerged in  $H_2O$ . The results of the orifice effect tests are summarized in Table 3.

TABLE 3. ORIFICE EFFECTS TEST DATA

TEST NO.	ORIFICE DIAMETER		BACK PRESSURE		VALVE CLOSING TIME
	IN	CM	PSI	N/CM <sup>2</sup>	MSEC
1	2.50	6.35	500	345	No Data
2	1.25	3.17	50	34	11.20
3	1.50	3.81	100	69	11.50
4	1.75	4.44	245	169	11.00
5	2.50	6.35	425	293	No Data

A graphical representation of the test data is shown in Figure 16. The measured pressure to unseat the poppet (back pressure) was plotted against the area of the orifice installed in the test setup. Total drag on the poppet is a function of rotational velocity, fluid density and orifice effects. The data must therefore be interpreted in terms of these variables and cannot be assumed to be valid in other fluids of differing density. The data did show, however, that when the downstream restriction approached 1.00 inch (2.54 cm) diameter the poppet could no longer be locked into the outlet seat provided that the density of fluid is 62.4 lb/ft<sup>3</sup> (1 gm/cm<sup>3</sup>).

There appeared to be no correlation between the closing time of the poppet and the back pressure. It was expected that the higher the velocity of the poppet the greater the pressure necessary to lift the poppet from the seat. A possible explanation for the discrepancy in closing time was the possibility that the drag due to orifice effects occurs in the last stage of rotational displacement and that therefore the impact on time was so small that it could not be measured by the graphite rod method.

In summary, the orifice effects tests verified the two valve failures previously mentioned. An analytical model describing the orifice effects on valve closure is presented in Section 7.0. The analytical data correlates well with the observed test points.

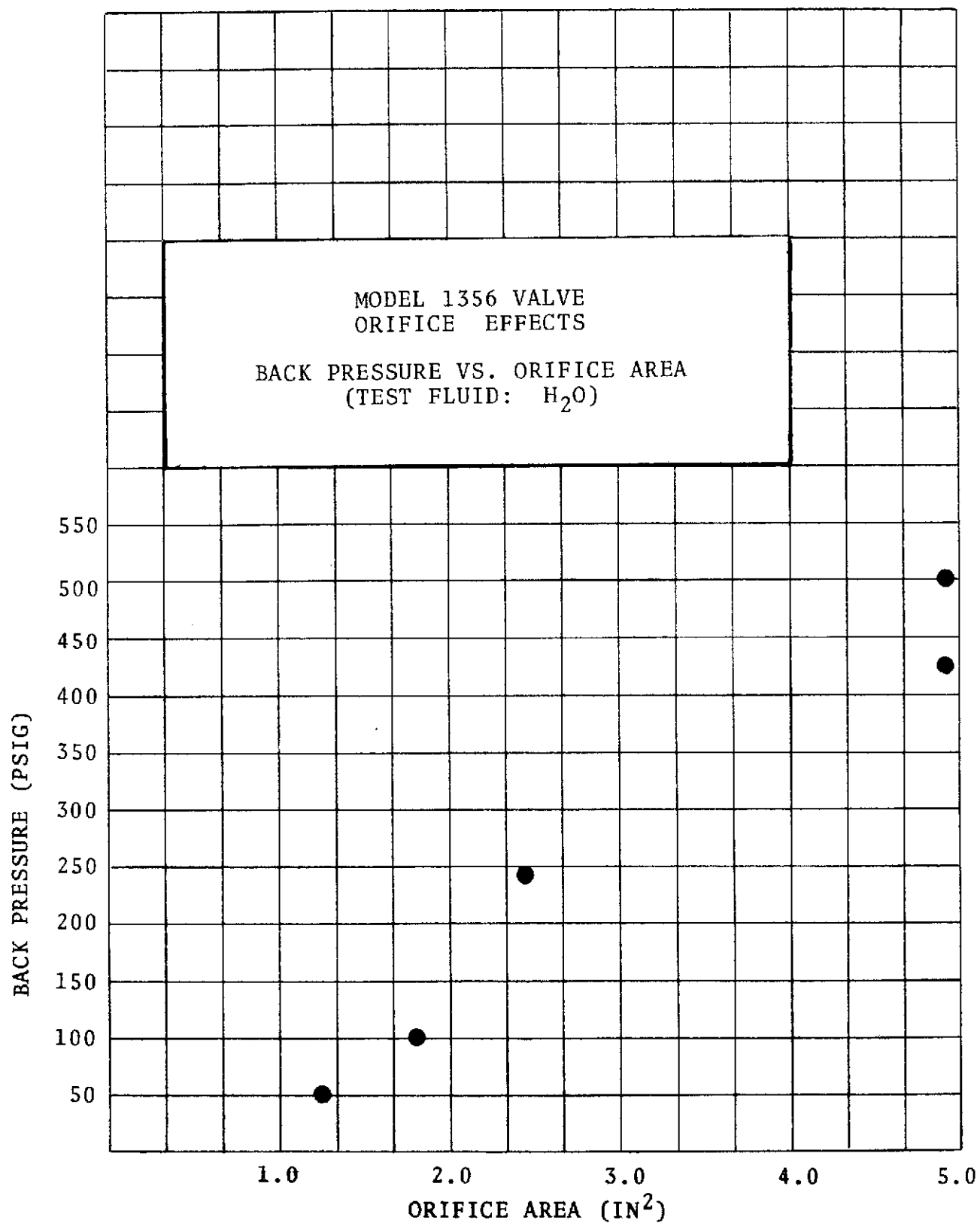


FIGURE 16. ORIFICE EFFECTS, GRAPHICAL REPRESENTATION

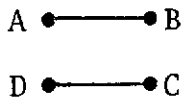
### 4.3 Cartridge Verification Testing

Because of the potential problem areas of low temperature effects on the burning rate of the explosive cartridge, and shrinkage or cracking of the charge due to vibrational loads, a formal cartridge verification test program was conducted. The cartridge verification tests were conducted by the Martin Marietta Corporation, Engineering Propulsion Laboratory, Denver, Colorado, with cartridges furnished by the NASA. The cartridge performance specifications are summarized in Table 4, and the cartridge external envelope is shown in Figure 17.

During the proposal stage, initial design calculations were conducted which indicated that a cartridge manufactured under the auspices of the Jet Propulsion Laboratory, Pasadena, California, would be suitable for this application. Preliminary evaluation firings were conducted in a 10 cm<sup>3</sup> bomb at -423°F (-253°C) with three cartridges (JPL P/N 10028049). These initial tests indicated that cartridge output pressure at cryogenic conditions was consistent and that the output charge would not be affected by the low temperature environment. Peak Pressures measured during these initial tests were 5200 psig, 5450 psig (3586 N/cm<sup>2</sup>, 3758 N/cm<sup>2</sup>) respectively. Data were lost during the third firing due to O-Ring failure.

The purpose of the cartridge verification tests was to establish the variation, if any, in cartridge output pressure due to vibration and thermal shock at 120°F, -320°F, -423°F (49°C, -196°C, -253°C). This was accomplished by establishing pressure traces at the above temperatures and comparing the traces with those obtained at the respective temperatures after exposure to vibration and thermal shock.

TABLE 4. CARTRIDGE PERFORMANCE SPECIFICATIONS

PRESSURE CARTRIDGE JPL P/N 10028049	
Bridgewire Resistance [70°F, (21°C)]	1.0 $\pm$ .10 ohm
Insulation Resistance (Shorted Pins to Case, Pin to Pin)	10,000 ohm at 500 vdc
Dielectric Strength (Shorted Pins to Case, Bridge to Bridge)	150 v for 60 sec
No-Fire Current	1.0 amp, 1.0 watt for 5 minutes
All-Fire Current [-65°F to +165°F (-54°C to 74°C)]	3.5 amps at .999 Reliability and .90 Confidence
Functioning Time (From Application of Current to Peak Pressure) [-65°F to +165°F (-54°C to +74°C)]	10.0 msec (max) at .999 Reliability and .90 Confidence
Electrostatic Sensitivity	Cartridge shall not ignite or be degraded with application of 25,000 v from 500 pico-farad capacitor across shorted pins to case or bridge to bridge
Electrical Circuit Schematic	 <p>A —●— B D —●— C</p>
Output Pressure In .200 in <sup>3</sup> Bomb [70°F, (21°C)]	9,350 to 12,650 psig (6,448 to 8,724 N/cm <sup>2</sup> )

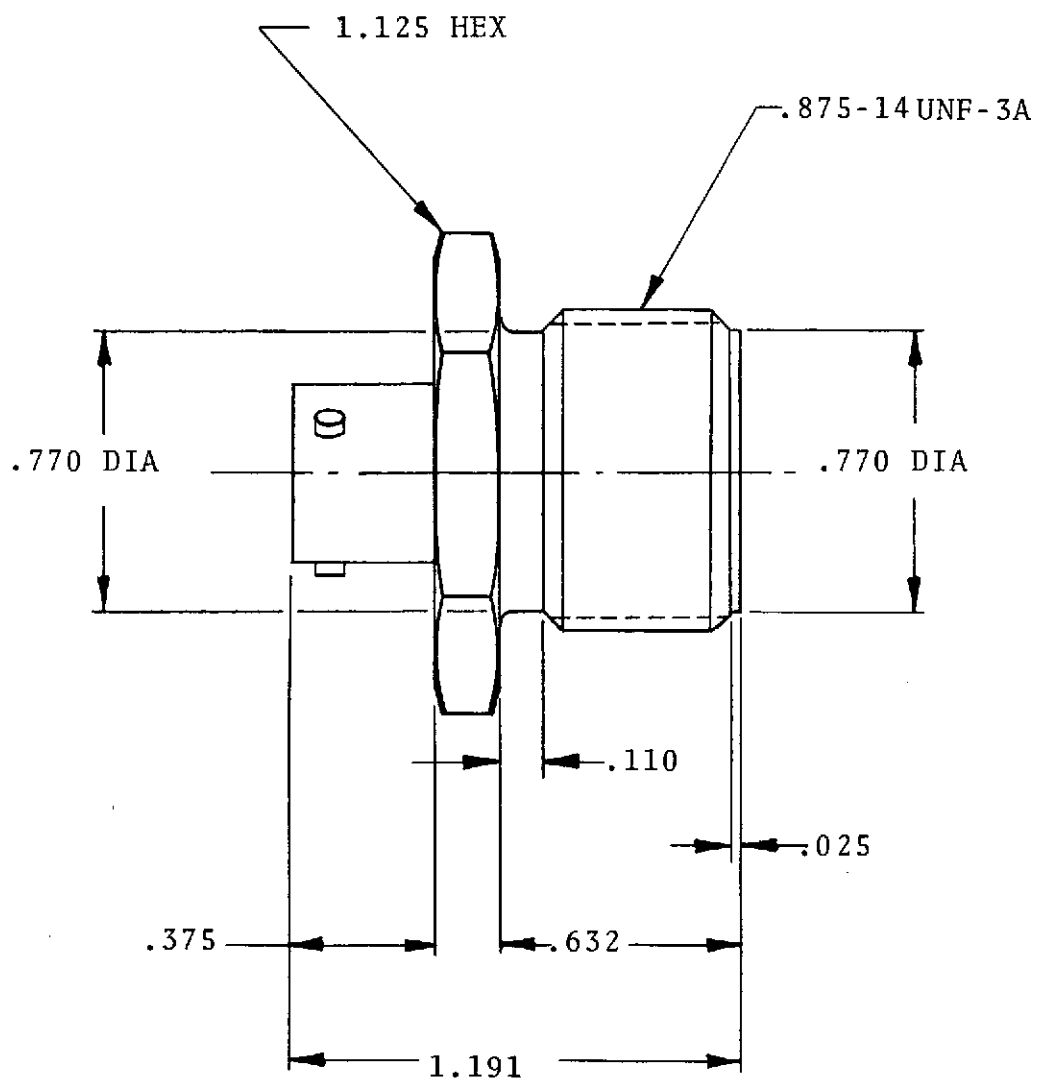


FIGURE 17. CARTRIDGE EXTERNAL ENVELOPE  
(JPL P/N 10028049)



## Special Test Conditions

All measurements were made with laboratory precision type instruments. All calibrations were current at the time of the test. The volume of the firing chamber of each bomb was verified dimensionally and was measured as 10.0 cm<sup>3</sup> using a graduated beaker. A list of equipment used, including model number, serial number and calibration date is included as Figure 39.

During all testing operations the equipment was operated according to Martin Marietta "Standard Environmental Laboratory Operating Procedure". During Vibration Testing, two accelerometers were monitored to detect any defect or malfunction of the vibration control system. Due to the hazardous nature of testing ordnance devices under liquid hydrogen conditions, the Martin Marietta Safety Department was advised of all test activities and had final approval over all test activities. All cartridge installations and firings were performed by Martin Marietta Ordnance Certified Personnel.

## Cartridge Firing Data Nomenclature

The terms used in Figure 18, Cartridge Firing Data Nomenclature, for presenting cartridge firing data are summarized and defined below:

Time of Burn	:	The time required for bridgewire burn out
Time to $\Delta P$	:	The time from the initiation of bridgewire burn to the initial pressure rise in the bomb
Pressure, Peak	:	The maximum pressure recorded during cartridge firing.
Time of $\Delta P$		The rise time of the first pressure spike
Time to Front	:	The time from initial pressure rise to the time that the cartridge output pressure appears to initially damp the peak pressure
Stable Pressure	:	The indicated pressure in the bomb after the initial shockwave dampening has subsided
Decay Pressure	:	The pressure in the bomb 20 milliseconds after initial pressure indications

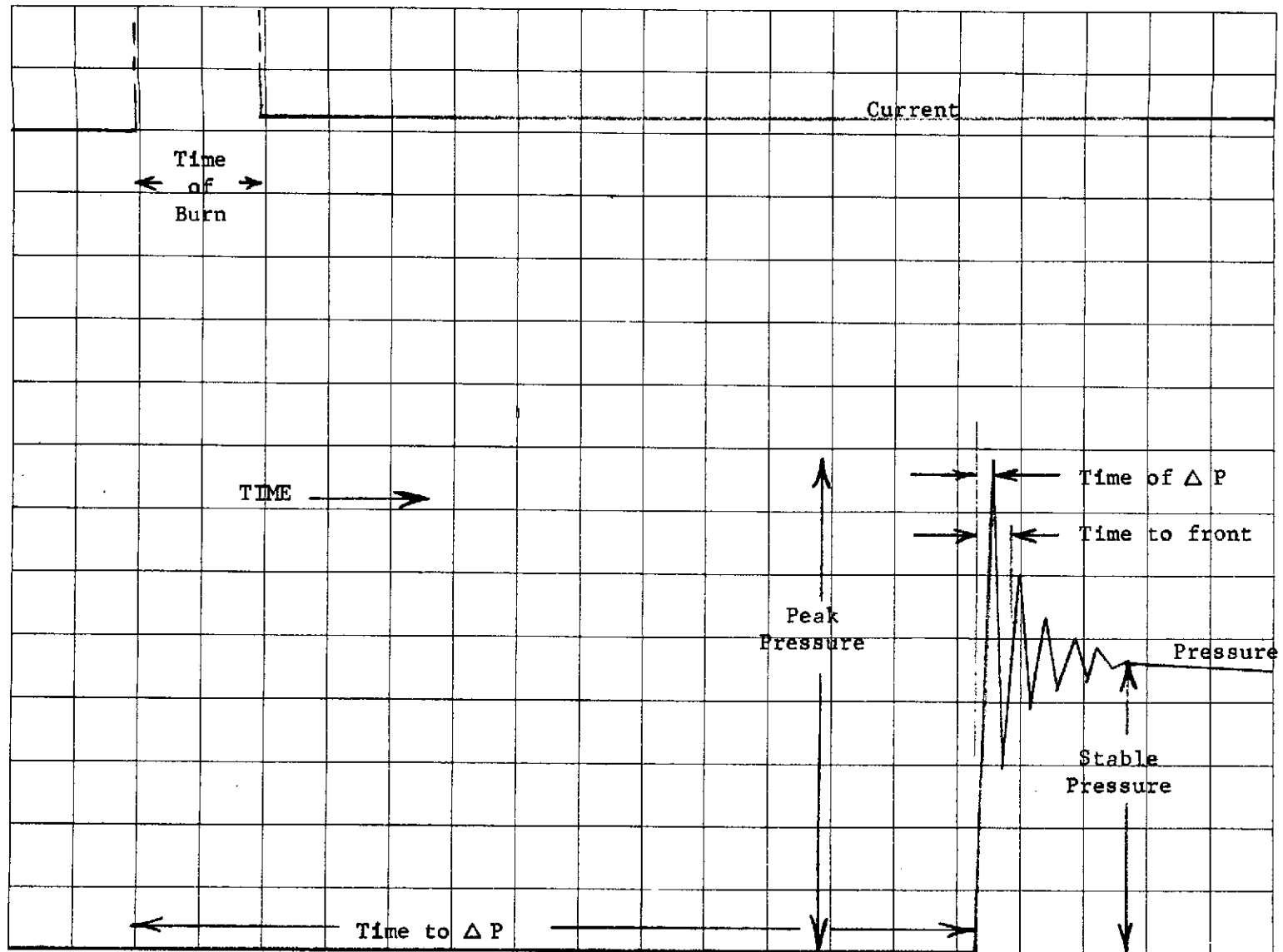


FIGURE 18. CARTRIDGE FIRING DATA NOMENCLATURE

### Firing Test at 120°F (49°C)

The cartridge (ID 11) and transducer were installed in the cartridge firing bomb (Figure 19) and conditioned to 120°F (49°C) by flowing hot GN<sub>2</sub> through the conditioning ports of the bomb. The direct writing and tape recorders were started and the cartridge actuated.

The cartridge firing recording is shown in Figure 20 and the test data are summarized in Table 5. The cartridge firing data were recorded using direct writing and magnetic tape recording equipment. In order to analyze the data, the tape was played back to a high speed oscillographic recorder for visual read out. The initial playback of data for cartridge ID 11 and 12 was made using light sensitive paper which tended to fade when exposed to room lighting. Due to this fading, the time of burn was indeterminate due to blurring. A second playback was attempted and the tape data was inadvertently erased. Subsequent playback of firing data was made using a photographic oscillograph which provided permanent records after development and eliminated the blurring problems. As a result of this problem, the data for ID 11 and ID 20 test articles presented are tracings of the initial playback record. Other firing traces presented are actual reproductions of the developed oscillographic records.

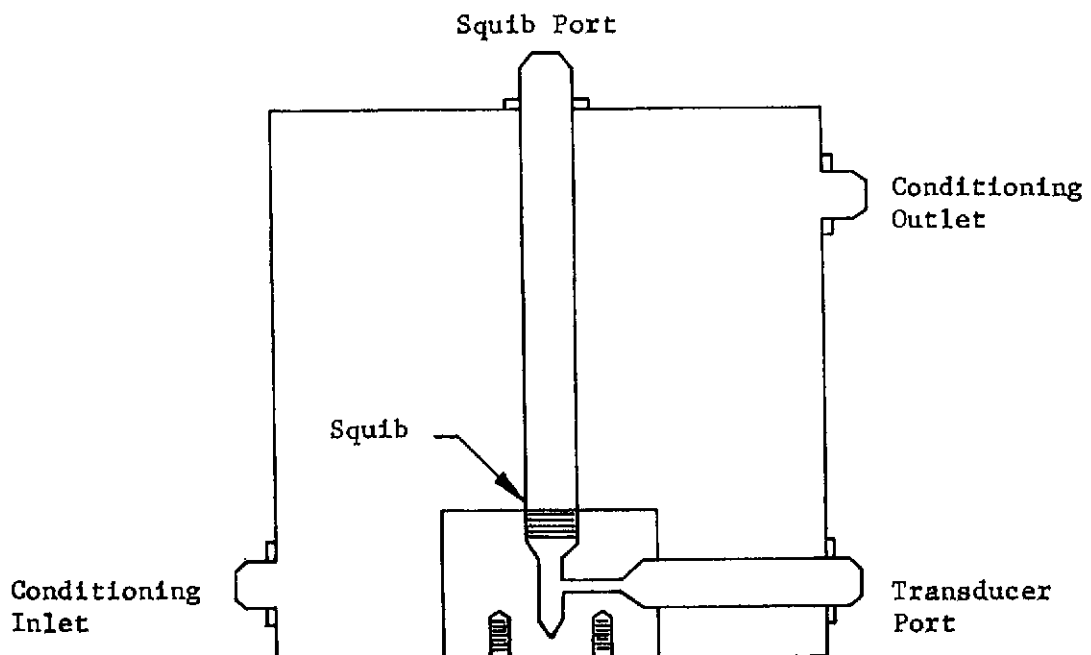


FIGURE 19. CARTRIDGE FIRING BOMB  
& CONDITIONING CHAMBER

NOTE: This figure was traced from the only tape playback made before the tape was inadvertently erased. The playback is on light sensitive paper and could not be reproduced directly due to fading.

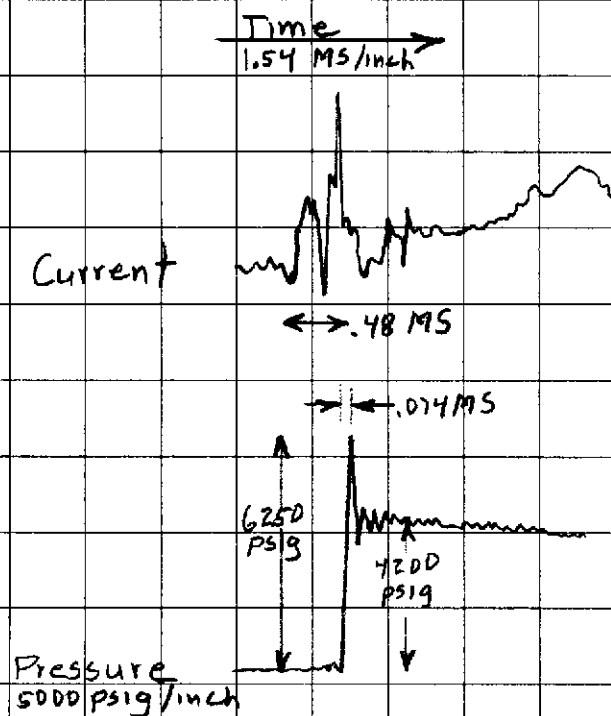


FIGURE 20. CARTRIDGE FIRING TRACE (ID 11)

TABLE 5. CARTRIDGE FIRING DATA

Cartridge ID			11					
Test Condition			120°F (49°C)					
Time of Burn	Time to $\Delta P$	Time of $\Delta P$	Peak Pressure		Stable Pressure		Decay Pressure	
Milliseconds			psig	N/cm <sup>2</sup>	psig	N/cm <sup>2</sup>	psig	N/cm <sup>2</sup>
----	.48	.074	6250	4310	4200	2896	1520	1048

#### Firing Test at -320°F (-196°C)

The cartridge (ID 12) and transducer were installed in the cartridge firing bomb (Figure 19) and conditioned to -320°F (-196°C) by flowing LN<sub>2</sub> through the conditioning ports of the bomb. The direct writing and tape recording equipment was started and the cartridge actuated. Test data are shown in Table 6 and the cartridge firing recording is shown in Figure 21.

TABLE 6. CARTRIDGE FIRING DATA

Cartridge ID			12					
Test Condition			-320°F (-196°C)					
Time of Burn	Time to $\Delta P$	Time of $\Delta P$	Peak Pressure		Stable Pressure		Decay Pressure	
Milliseconds			psig	N/cm <sup>2</sup>	psig	N/cm <sup>2</sup>	psig	N/cm <sup>2</sup>
.76	1.54	.051	7650	5275	4820	3324	4200	2896

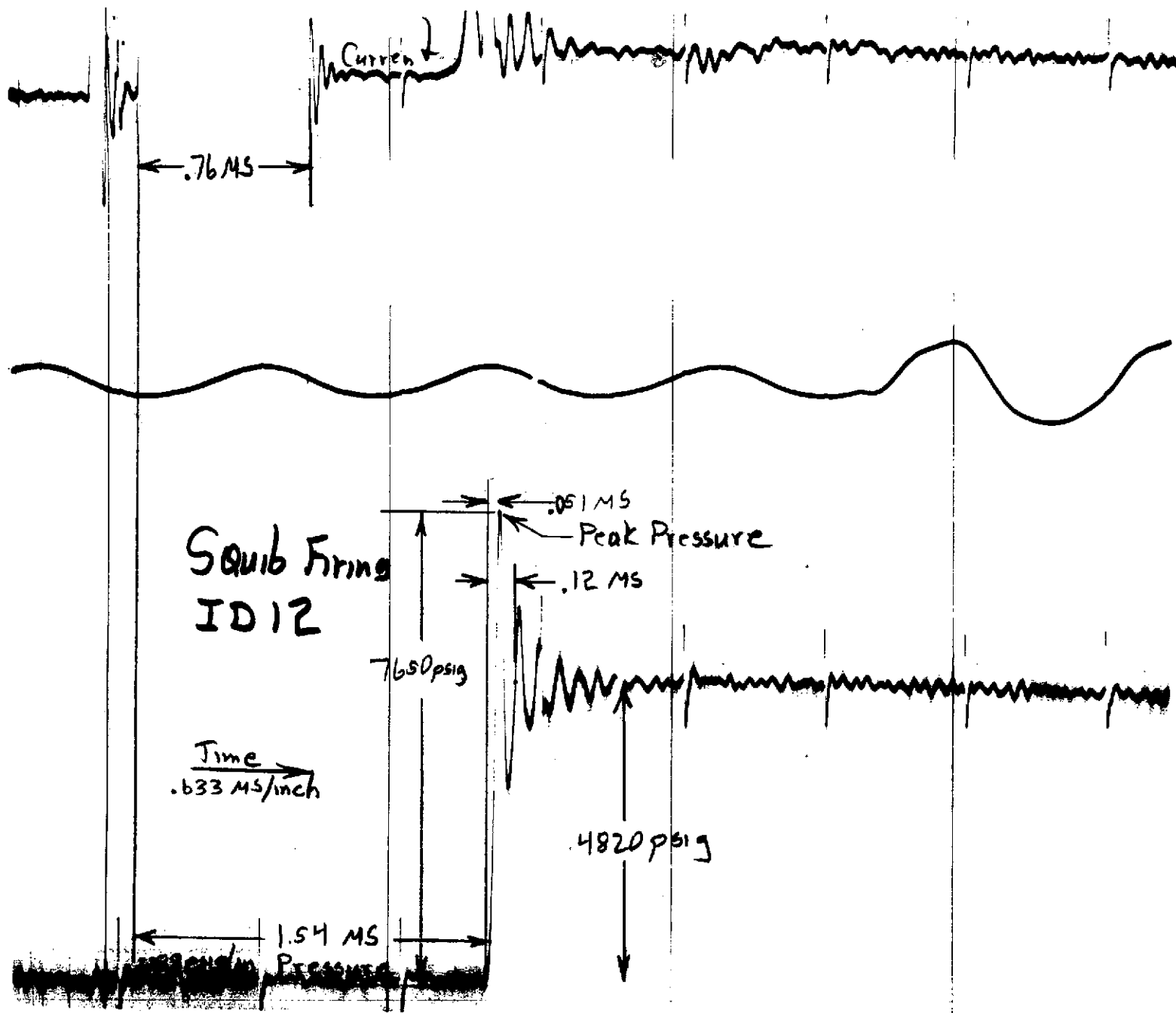


FIGURE 21. CARTRIDGE FIRING TRACE (ID 12)

### Firing Test at -423°F (-253°C)

Two cartridges (ID 13, ID 14) were tested at liquid hydrogen temperatures. The cartridge and the transducer were installed in the cartridge firing bomb (Figure 19) and conditioned to -423°F (-253°C) by flowing LH<sub>2</sub> through the conditioning ports of the bomb. The test setup is shown pictorially in Figure 22. The direct writing and tape recorders were started and the cartridge was actuated. The cartridge firings were successful. Test data are summarized in Table 7 and the cartridge firing recording is shown in Figure 23 and Figure 24.

TABLE 7. CARTRIDGE FIRING DATA

Cartridge ID			13, 14					
Test Condition			-423°F (-253°C)					
Time of Burn	Time to ΔP	Time of ΔP	Peak Pressure		Stable Pressure		Decay Pressure	
			psig	N/cm <sup>2</sup>	psig	N/cm <sup>2</sup>	psig	N/cm <sup>2</sup>
.51	1.81	.066	8370	5772	5600	3862	4200	2896
.51	2.59	.063	10400	7172	9880	6813	7850	5413

### Thermal Shock and Firing at -423°F (-253°C)

Two cartridges (ID 16, ID 17) were tested after being exposed to thermal shock. The cartridge and transducer were installed in the bomb (Figure 19). The bomb was then submerged into a LH<sub>2</sub> bath. When bomb temperature reached -400°F (-240°C) or lower, the direct writing and tape recorders were started and the cartridge was fired. The test setup is shown schematically in Figure 25 and pictorially in Figure 26.

The cartridge firings were successful. Cartridge shock temperature is plotted in Figure 27. Test data are summarized in Table 8, and cartridge firing recordings are shown in Figures 28 and 29.



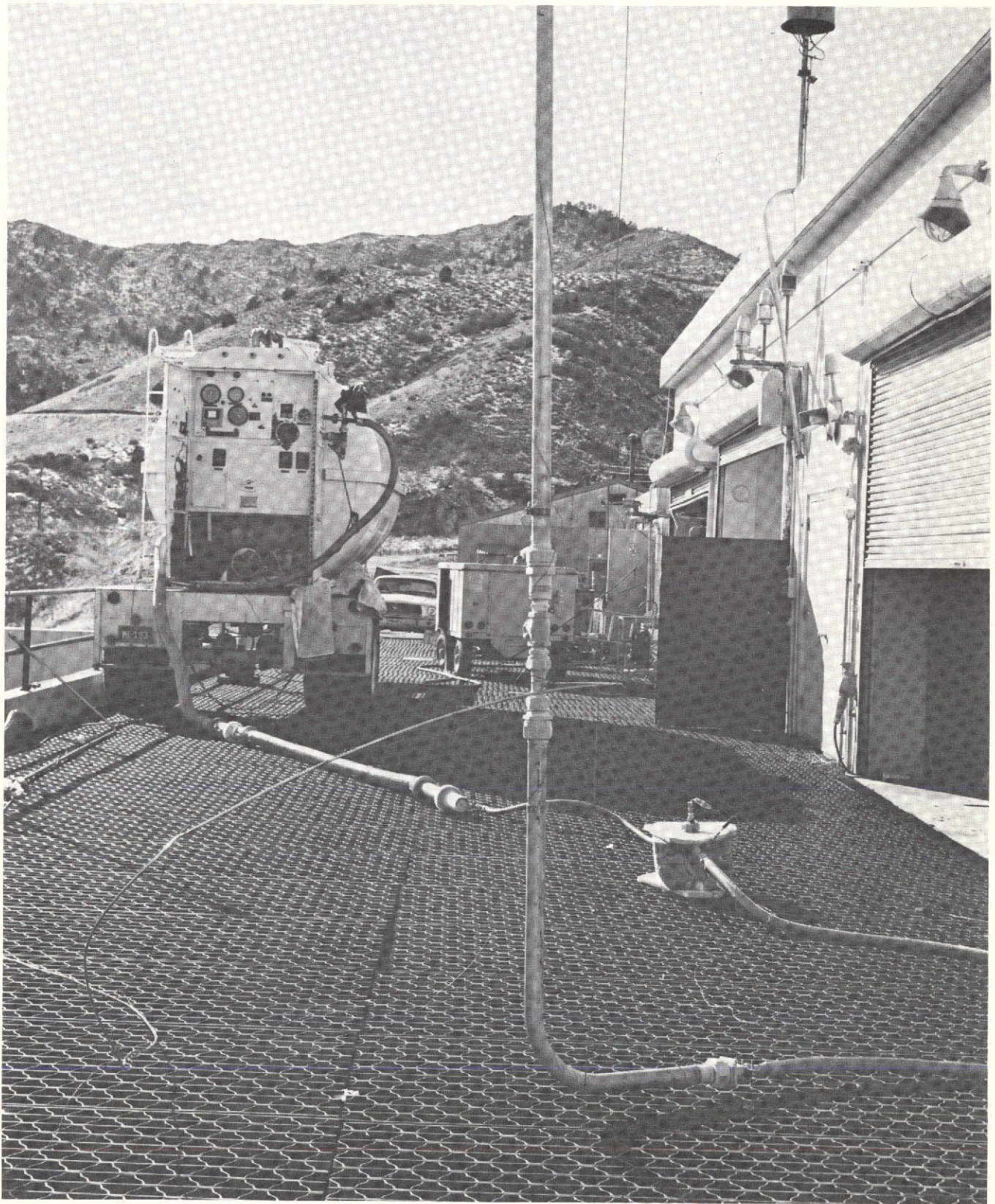


FIGURE 22. LIQUID HYDROGEN CARTRIDGE FIRINGS  
TEST SET UP--GENERAL VIEW



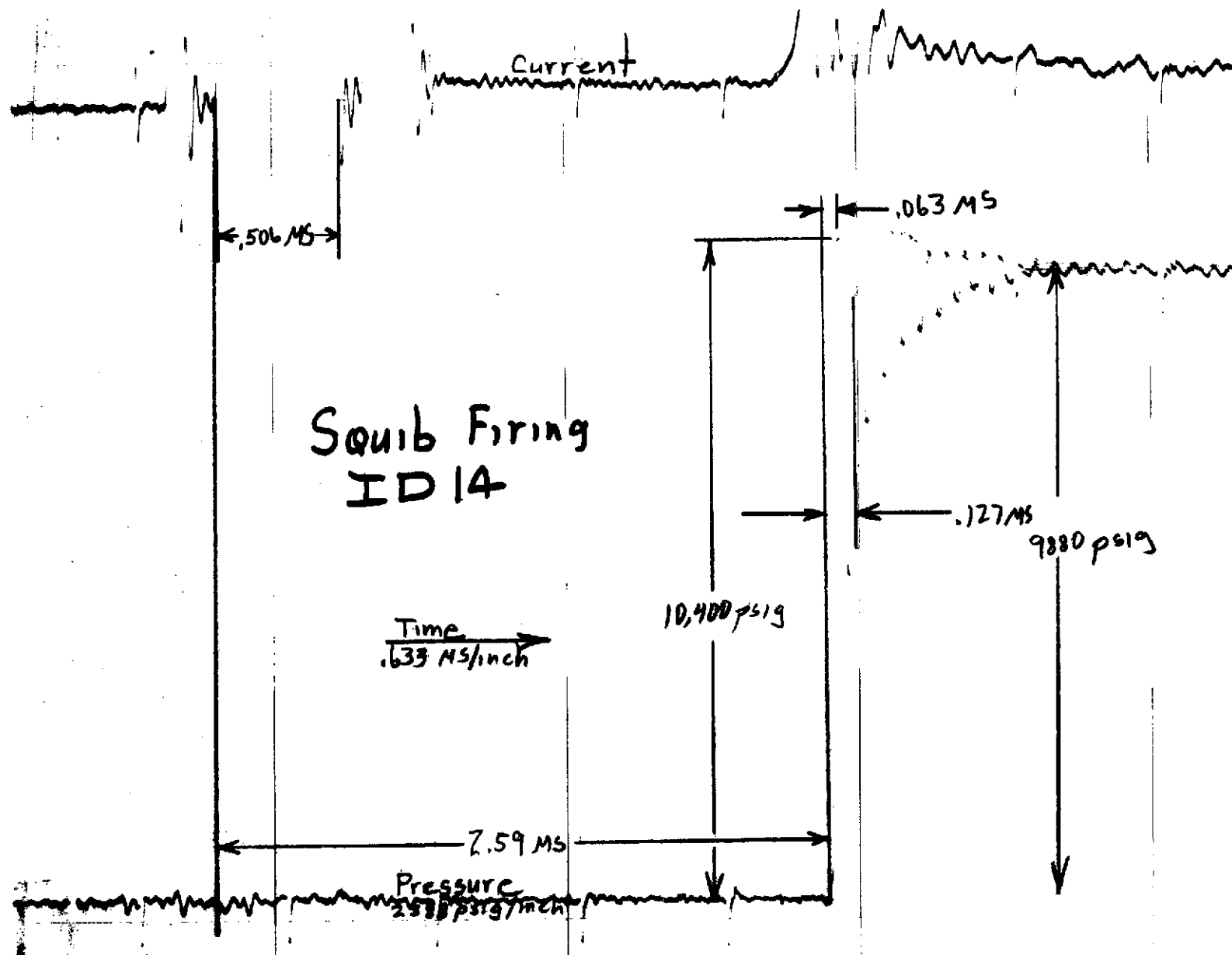


FIGURE 23. CARTRIDGE FIRING TRACE (ID 14)

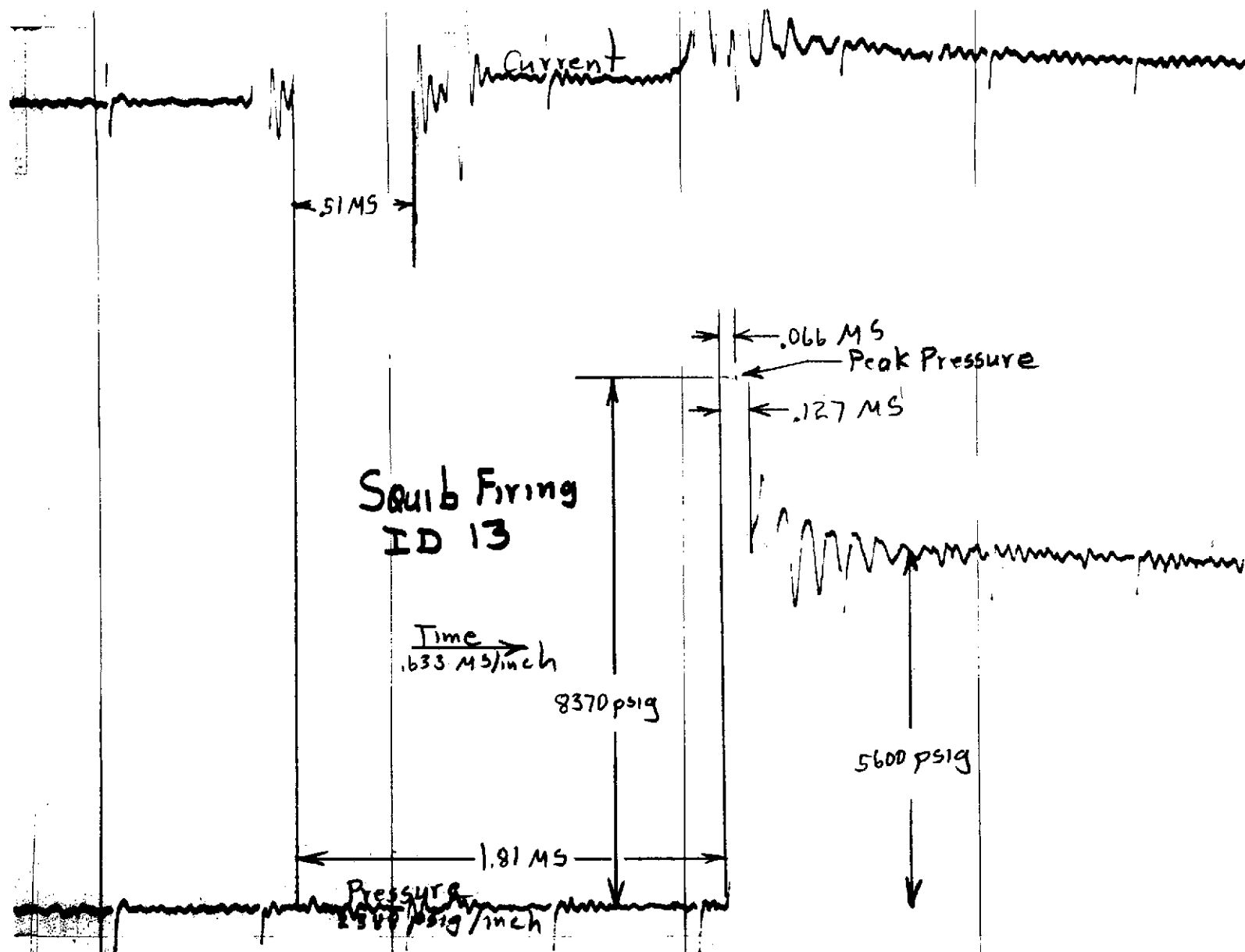


FIGURE 24. CARTRIDGE FIRING TRACE (ID 13)

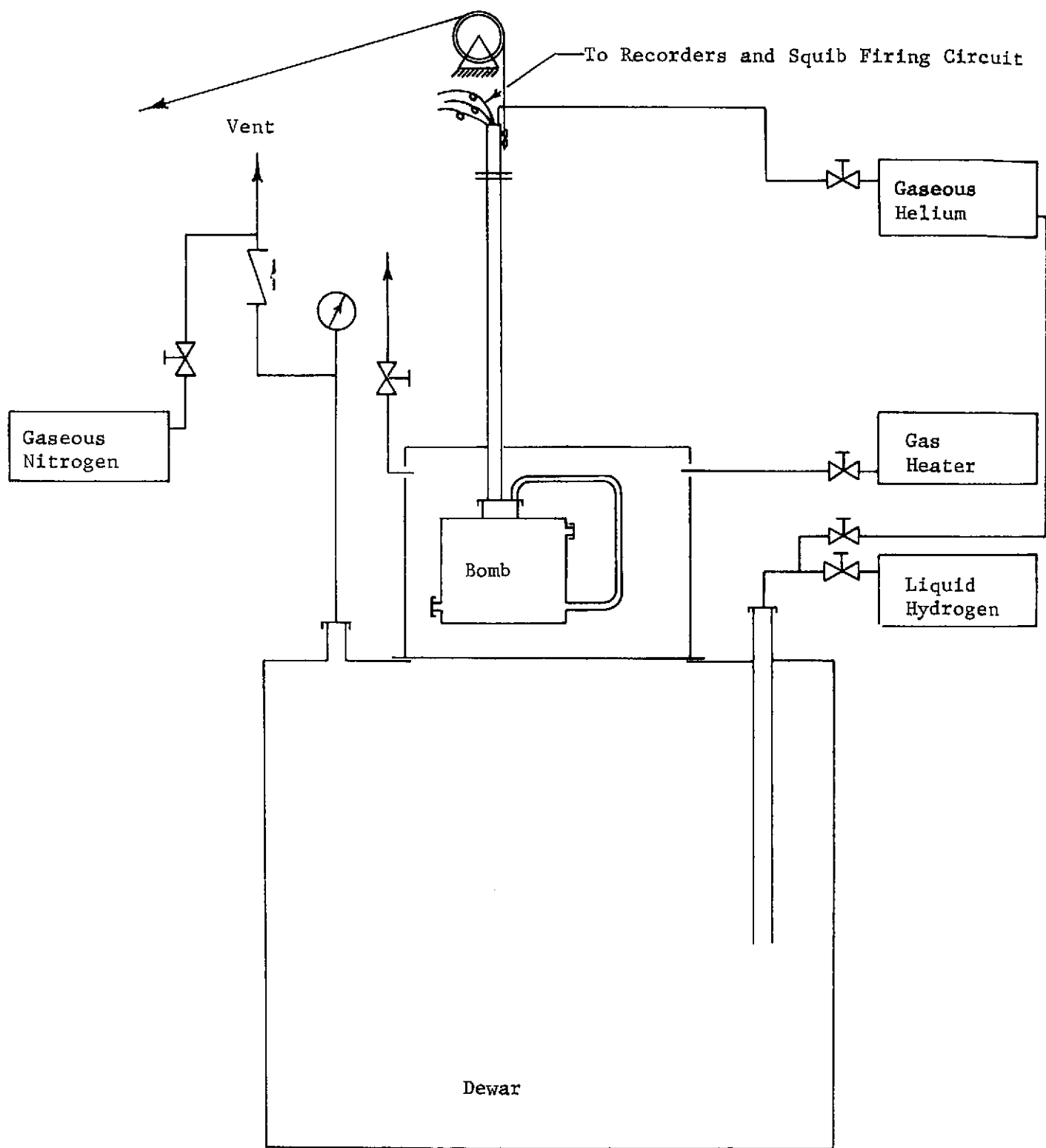


FIGURE 25. FIRING INSTALLATION, THERMAL SHOCK TEST



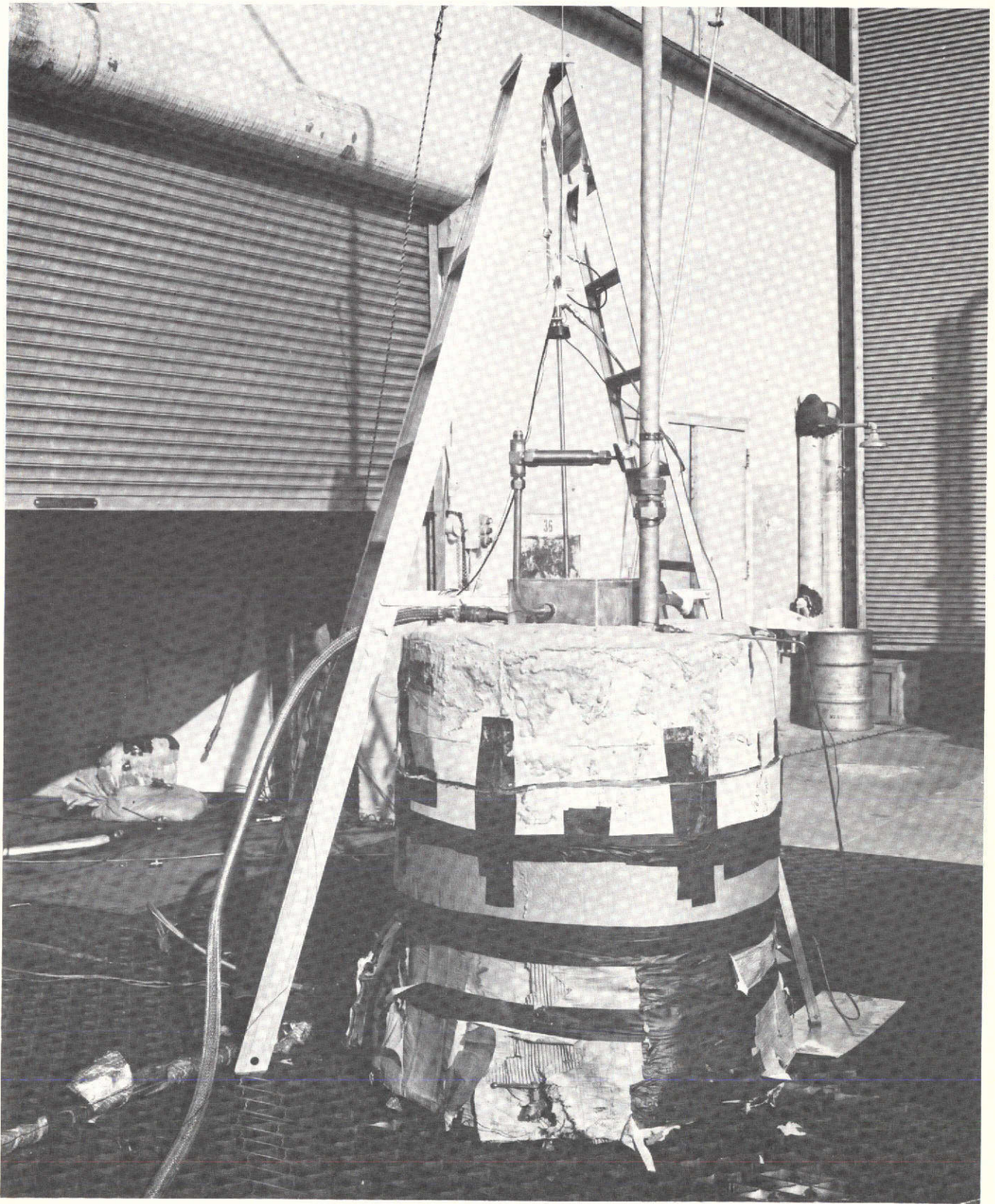


FIGURE 26.  $\text{LH}_2$  THERMAL SHOCK TEST SETUP



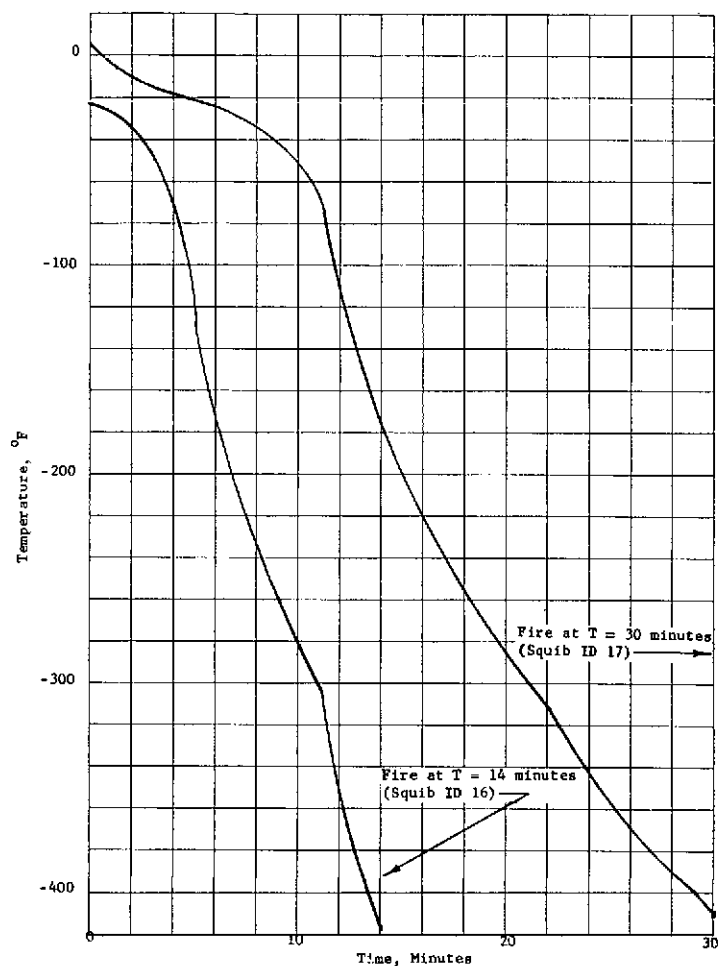


FIGURE 27. THERMAL SHOCK TEMPERATURE PLOT

TABLE 8. CARTRIDGE FIRING DATA

Cartridge			16, 17					
Test Condition			Thermal Shock at -423°F (-253°C)					
Time of Burn	Time to ΔP	Time of ΔP	Peak Pressure		Stable Pressure		Decay Pressure	
Milliseconds			psig	N/cm <sup>2</sup>	psig	N/cm <sup>2</sup>	psig	N/cm <sup>2</sup>
.52	2.01	.042	8380	5779	5390	3716	1870	1290
.58	2.14	.057	9396	6479	6932	4780	4875	3362

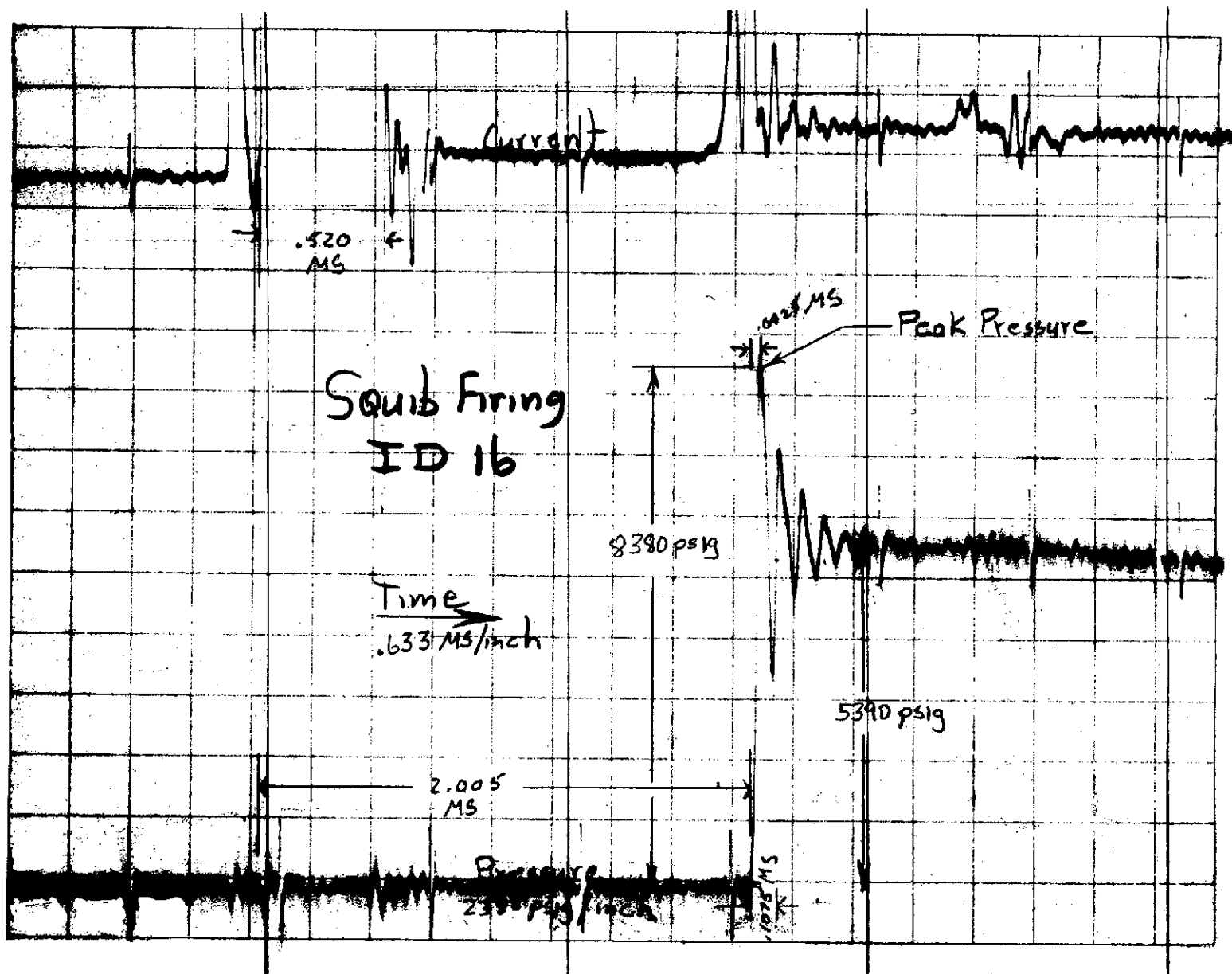


FIGURE 28. CARTRIDGE FIRING TRACE (ID 16)

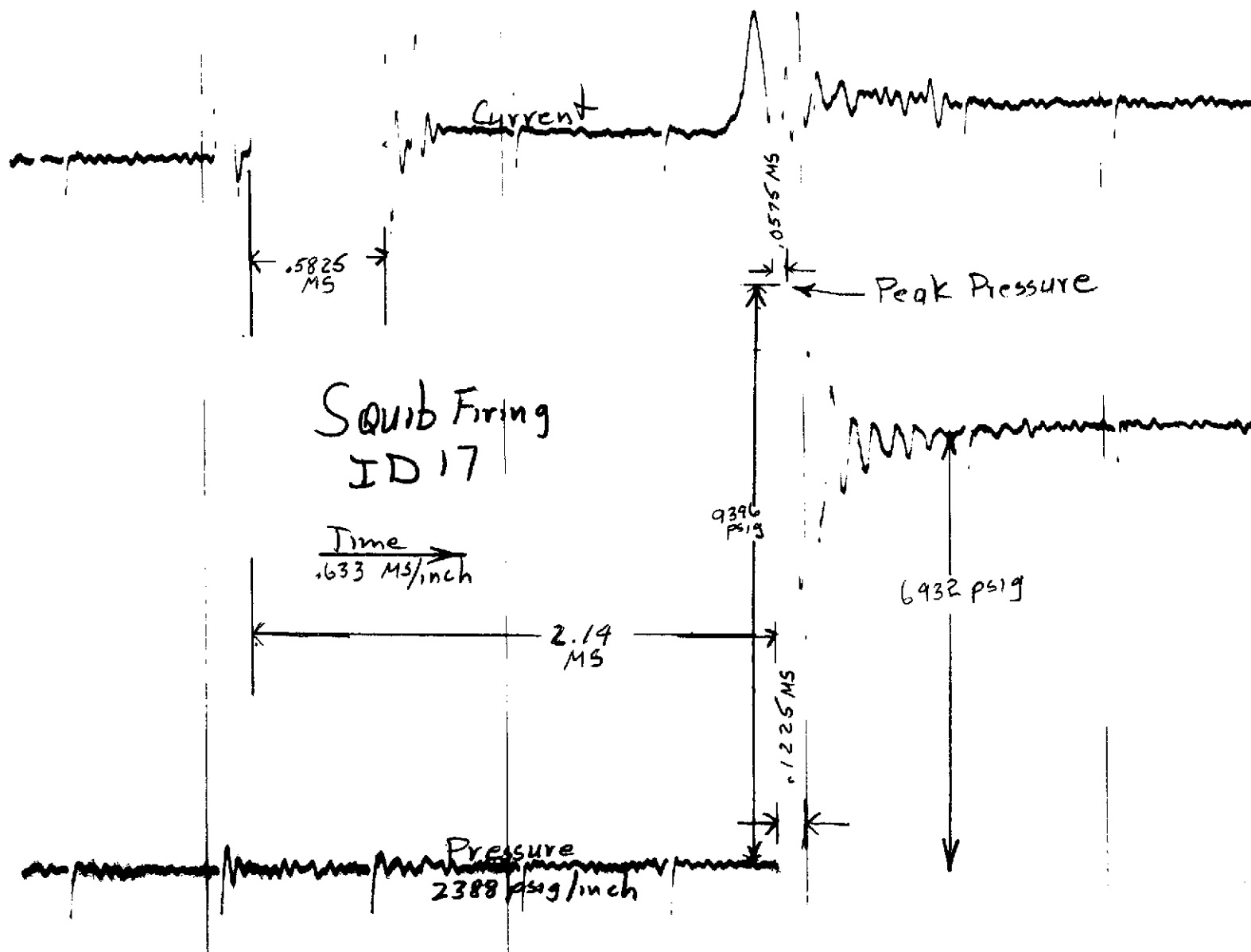


FIGURE 29. CARTRIDGE FIRING TRACE (ID 17)

### Vibration, Leakage and Firing Test (Ambient)

The cartridge (ID 20) was installed in the bomb as shown in Figure 19. The bomb was attached to the vibration exciter and subjected to a 6.4 g peak vibration as detailed in the test procedure. The bomb was removed from the vibration exciter and connected as shown in Figure 30 to a helium supply, and a mass spectrometer leak detector. The bomb was then pressurized to 238 psig (164 N/cm<sup>2</sup>) and the cartridge hermetic seal leakage was measured. The pressure transducer was then installed and the firing circuit connected. The direct writing and tape recorders were started and the cartridge was fired. The cartridge was subjected to the vibration spectrum and no inadvertent firing or visible damage occurred as a result of the test. An ambient leak test was performed and leakage was less than  $2 \times 10^{-10}$  sec/sec of helium.

The cartridge firing was successful. Test data are summarized in Table 9 and the cartridge firing record is shown in Figure 31.

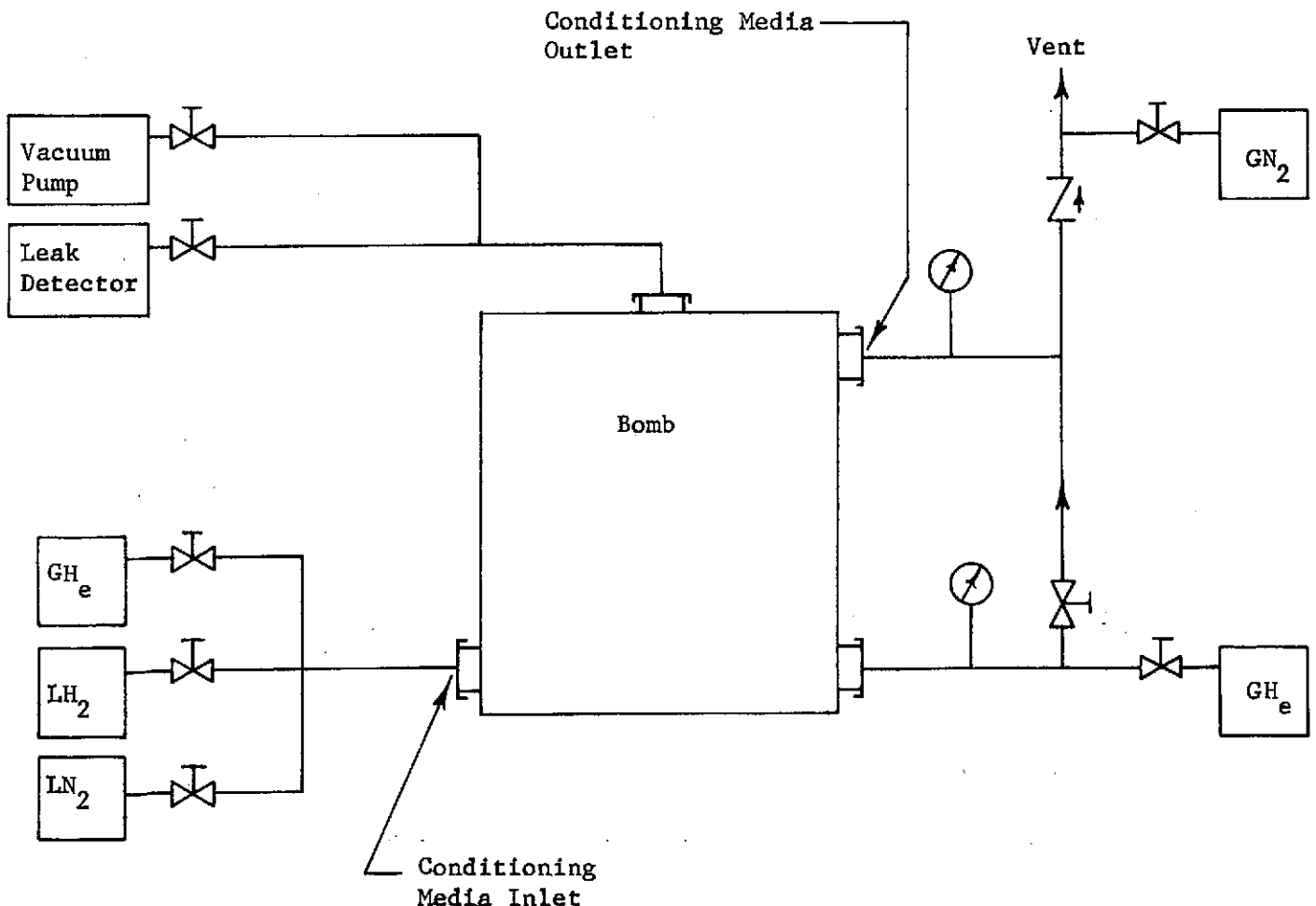


FIGURE 30. CARTRIDGE LEAK TEST INSTALLATION



NOTE: This figure was traced from the only tape playback made before the tape was inadvertently erased. The playback is on light sensitive paper and could not be reproduced directly due to fading.

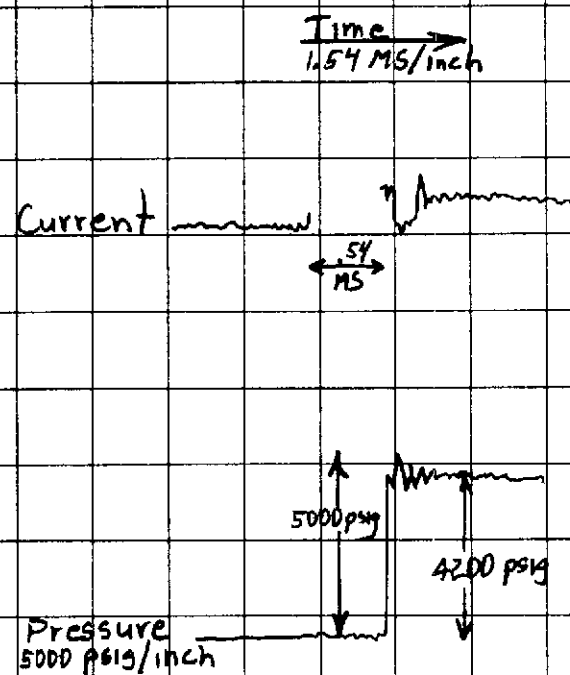


FIGURE 31. CARTRIDGE FIRING TRACE (ID 20)

TABLE 9. CARTRIDGE FIRING DATA

Cartridge ID			20					
Test Condition			Ambient Vibration					
Time of Burn	Time to $\Delta P$	Time of $\Delta P$	Peak Pressure		Stable Pressure		Decay Pressure	
Milliseconds			psig	N/cm <sup>2</sup>	psig	N/cm <sup>2</sup>	psig	N/cm <sup>2</sup>
----	.54	.068	5000	3448	4200	2896	----	----

#### Vibration, Leakage, and Firing Test at -320°F (-196°C)

Two cartridges (ID 21, ID 22) were subjected to vibration testing at -320°F (-196°C). The bomb was attached to the vibration exciter and LN<sub>2</sub> was metered through the conditioning chamber as required to maintain the bomb temperature at -320°F (-196°C). While the bomb was at the above temperature it was subjected to a 6.4 g peak vibration as detailed in the test procedure. The bomb was removed from the vibration exciter and connected to a helium supply, a mass spectrometer leak detector, and the conditioning media. The bomb was then conditioned to a temperature of -320°F (-196°C) and pressurized to 238 psig (164 N/cm<sup>2</sup>).

The leakage tests could not be performed at -320°F (-196°C) as planned because the cartridge thread O-Ring seal could not be sealed to allow a measurement of leakage through the hermetic seal. This leakage problem is discussed in detail in paragraph 4.4. Ambient leak tests were performed, however, and leakage of each cartridge was less than  $2 \times 10^{-10}$  scc/sec of helium.

The cartridge firings were successful. Test data are summarized in Table 10 and the cartridge firing records are shown in Figure 32 and Figure 33. A photograph of the test setup is shown in Figure 34.

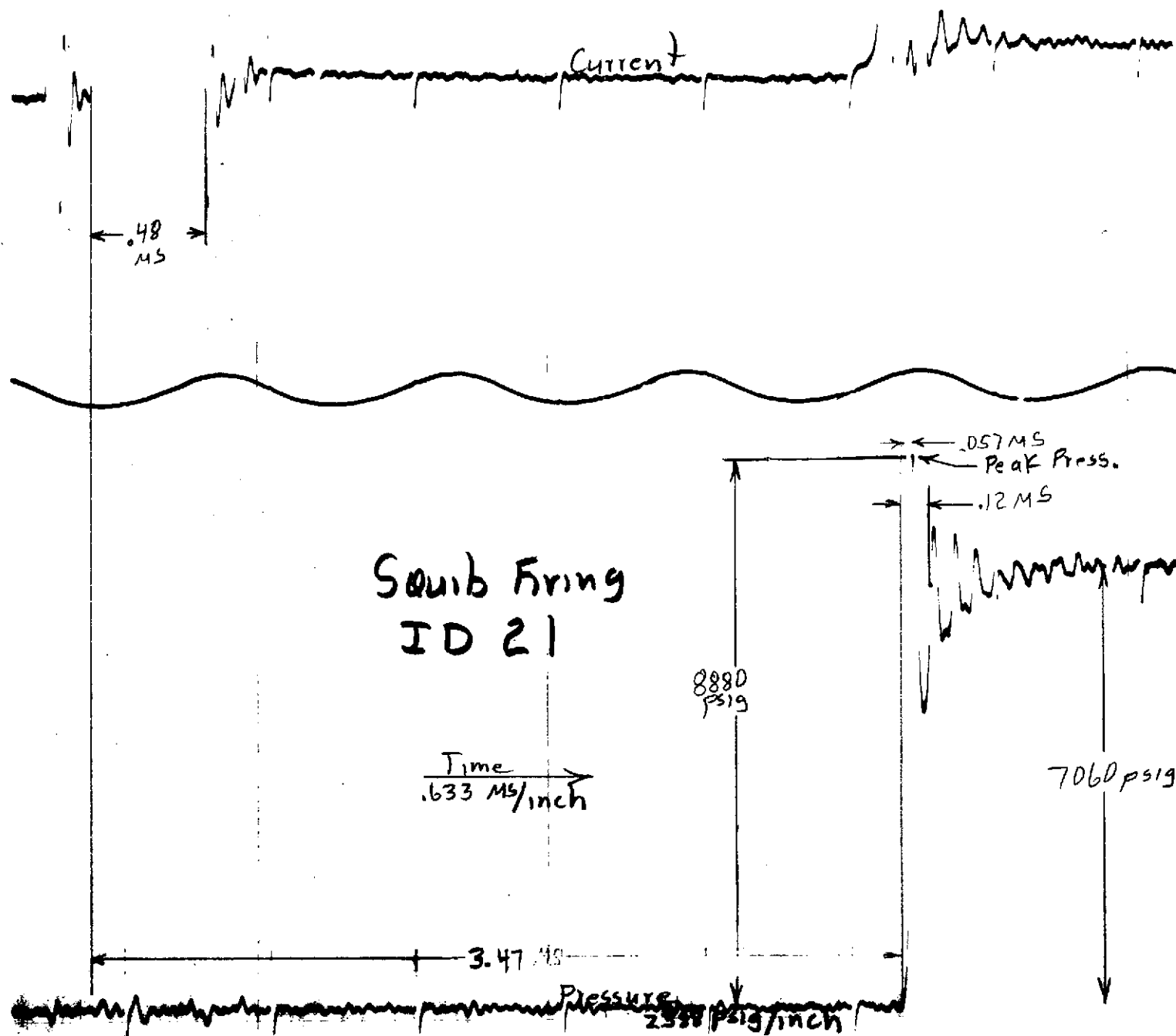


FIGURE 32. CARTRIDGE FIRING TRACE (ID 21)

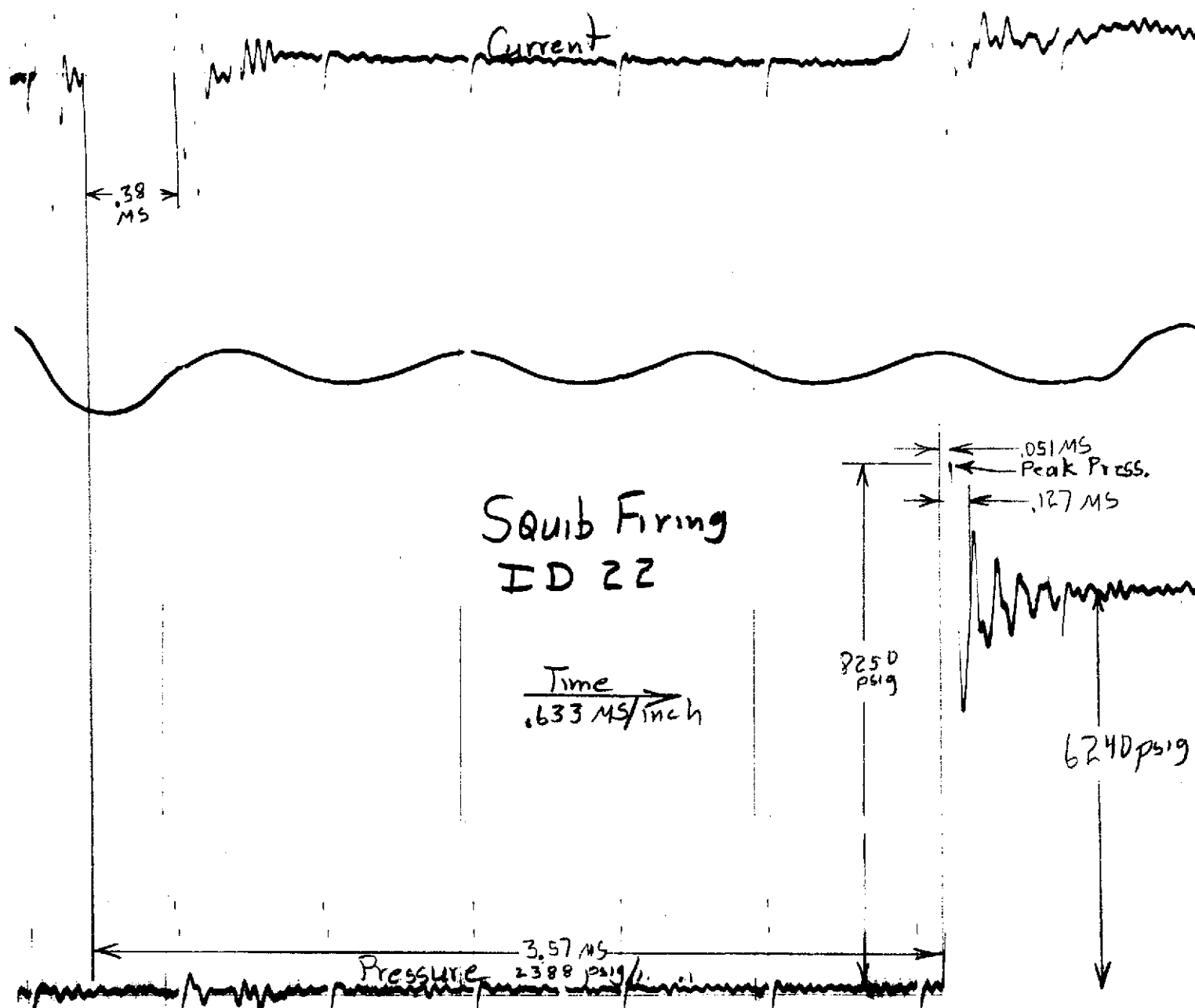


FIGURE 33. CARTRIDGE FIRING TRACE (ID 22)

TABLE 10. CARTRIDGE FIRING DATA

Cartridge ID			21, 22					
Test Condition			Vibration at -320°F (-196°C)					
Time of Burn	Time to ΔP	Time of ΔP	Peak Pressure		Stable Pressure		Pressure	
Milliseconds			psig	N/cm <sup>2</sup>	psig	N/cm <sup>2</sup>	psig	N/cm <sup>2</sup>
.48	3.47	.057	8880	6124	7060	4869	5740	3958
.38	3.57	.051	8250	5689	6240	4303	5824	4016

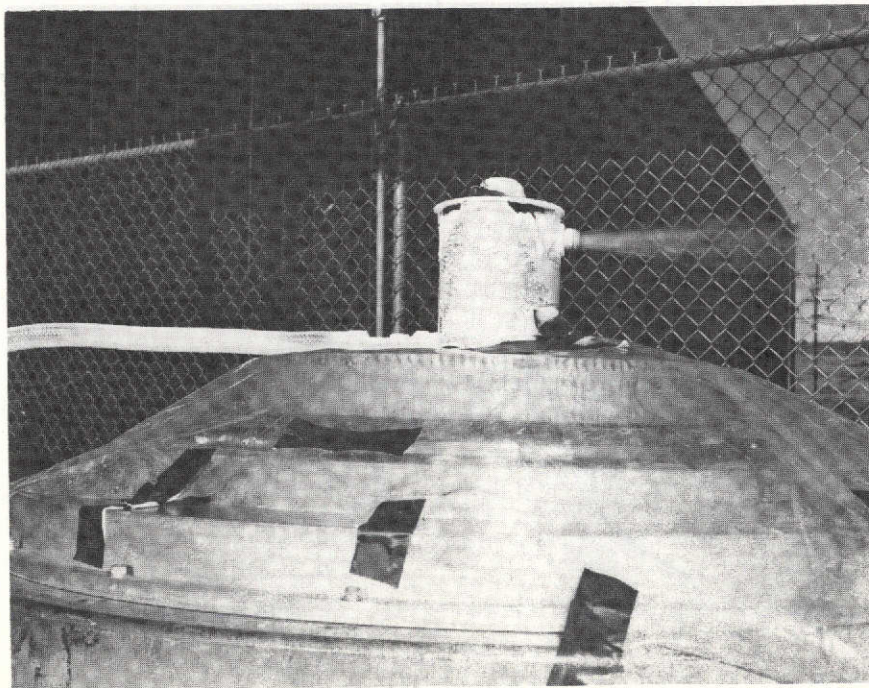


FIGURE 34. VIBRATION SETUP

### Vibration, Leakage, and Firing at -423°F (-253°C)

Three cartridges were subjected to this test (ID 23, 24, 25). The applicable portion of the test procedure follows:

"Install the cartridge in the bomb. Attach the bomb to the vibration exciter and flow LH<sub>2</sub> through the conditioning chamber of the bomb as required to maintain the bomb temperature at -350°F (-212°C) with evidence of LH<sub>2</sub> in the vent system. While the bomb is at the above temperature subject it to a 6.4 g peak vibration as detailed in the test procedure. Remove the bomb from the vibration exciter and connect the bomb to a helium supply, a mass spectrometer leak detector, and conditioning media. Condition the bomb to a temperature of -410 ± 20°F (-246 ± 6.7°C), pressurize the cartridge to 238 psig (164 N/cm<sup>2</sup>), and measure the cartridge hermetic seal leakage. Install the pressure transducer and connect the firing circuit. Condition the bomb to a temperature of -410 ± 20°F (-246 ± 6.7°C), start the direct writing and tape recorders and fire the cartridge."

The cartridges were subjected to the vibration spectrum at the specified temperature and no inadvertent firing or visible damage occurred as a result of the test. The leakage tests could not be performed at -423°F (-253°C) as planned because the cartridge thread O-Ring could not be sealed to allow a measurement of leakage through the hermetic seal. This leakage problem is discussed in detail in paragraph 4.4. Ambient leak tests were performed, however, and leakage of each cartridge was less than 2 x 10<sup>-10</sup> scc/sec of helium. The cartridge firings were successful. The test data are summarized in Table 11 and the cartridge firing records are shown in Figures 35, 36, and 38.

TABLE 11. CARTRIDGE FIRING DATA

Cartridge ID			23, 24, 25					
Test Condition			Vibration at -423°F (-253°C)					
Time of Burn	Time to ΔP	Time of ΔP	Peak Pressure		Stable Pressure		Decay Pressure	
Milliseconds			psig	N/cm <sup>2</sup>	psig	N/cm <sup>2</sup>	psig	N/cm <sup>2</sup>
.51	4.58	.042	10642	7339	6110	4213	4187	2887
.50	4.41	.040	10700	7379	4601	3173	3362	2318
.50	3.35	.053	7450	5138	4102	2829	2707	1867

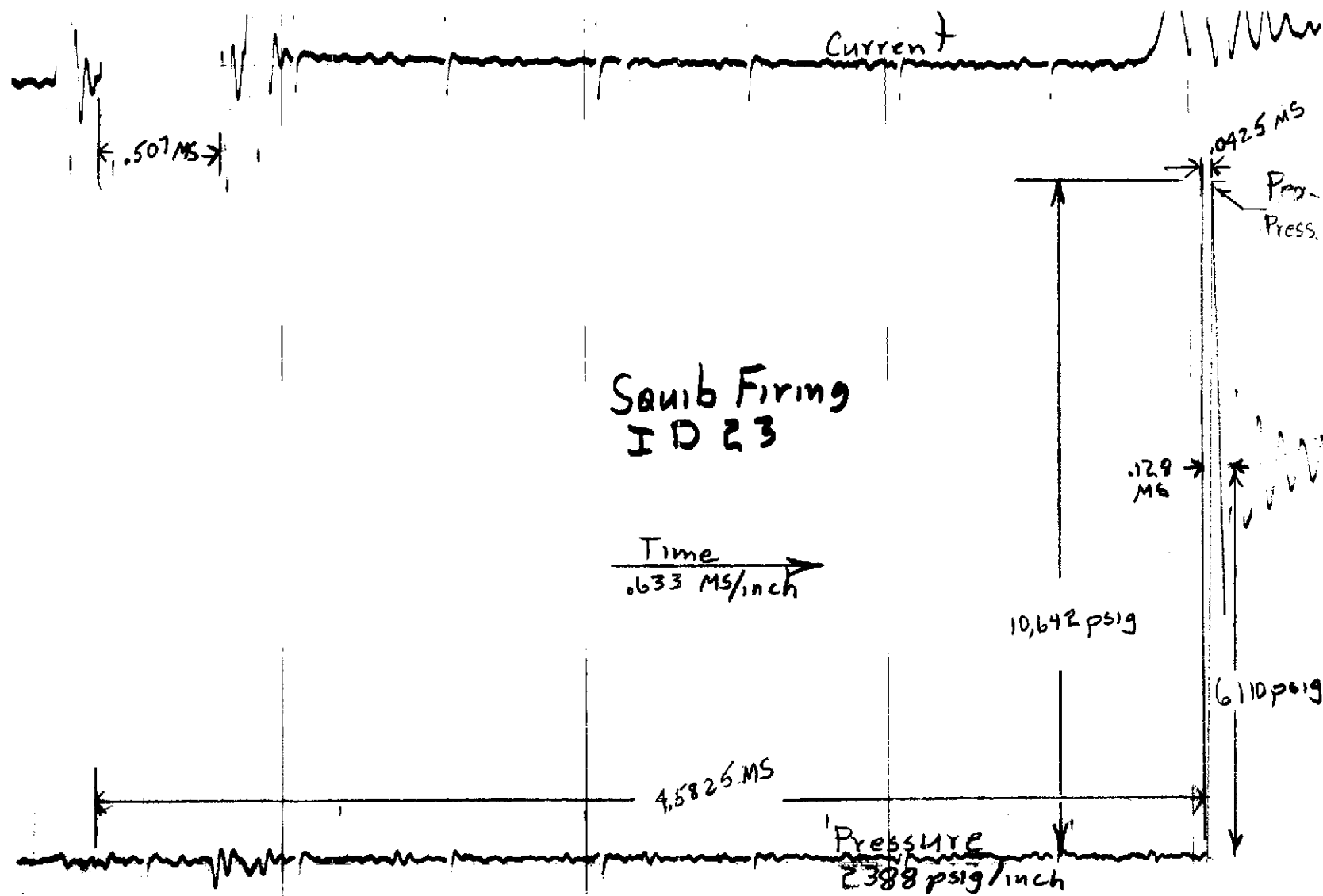


FIGURE 35. CARTRIDGE FIRING TRACE (ID 23)

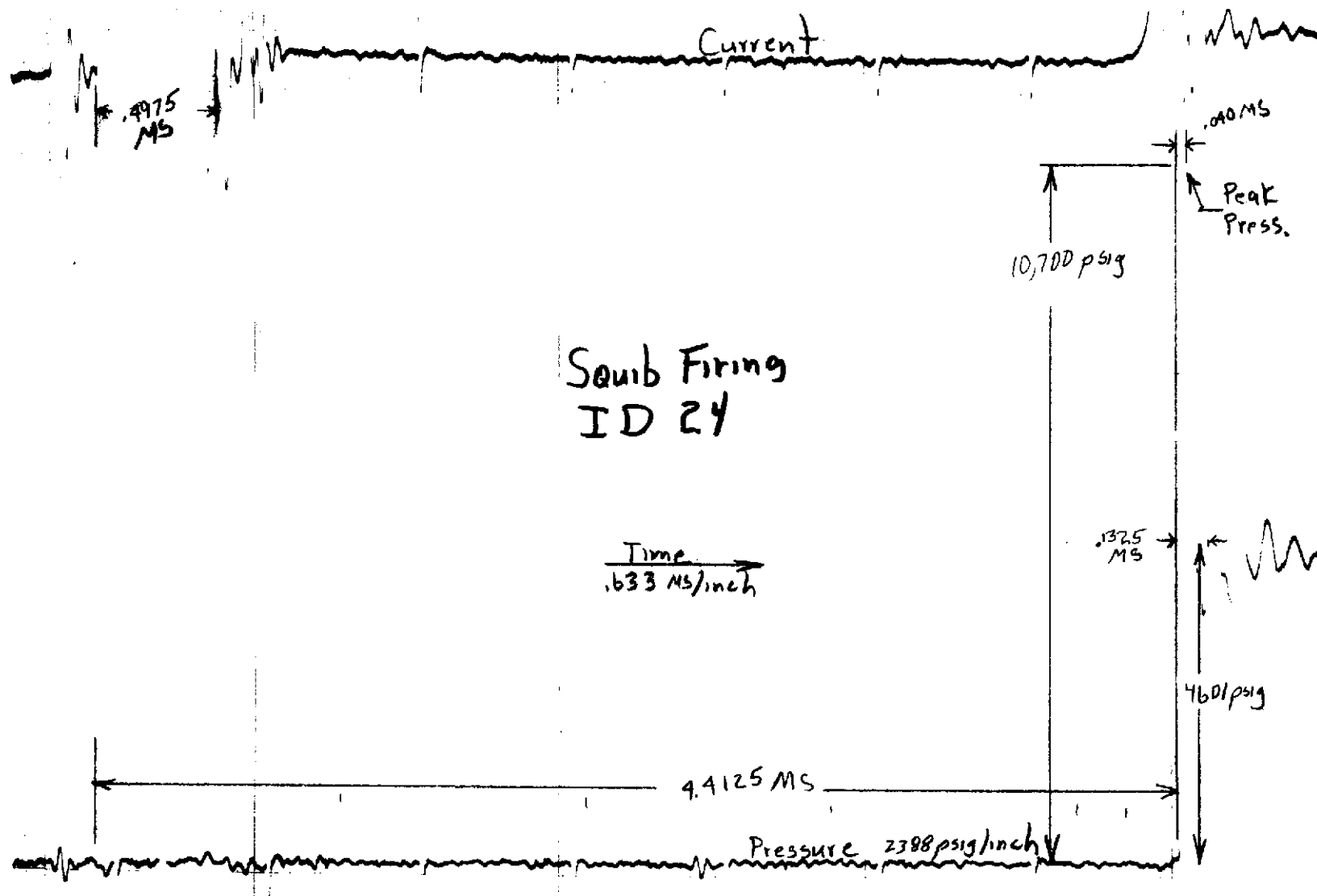
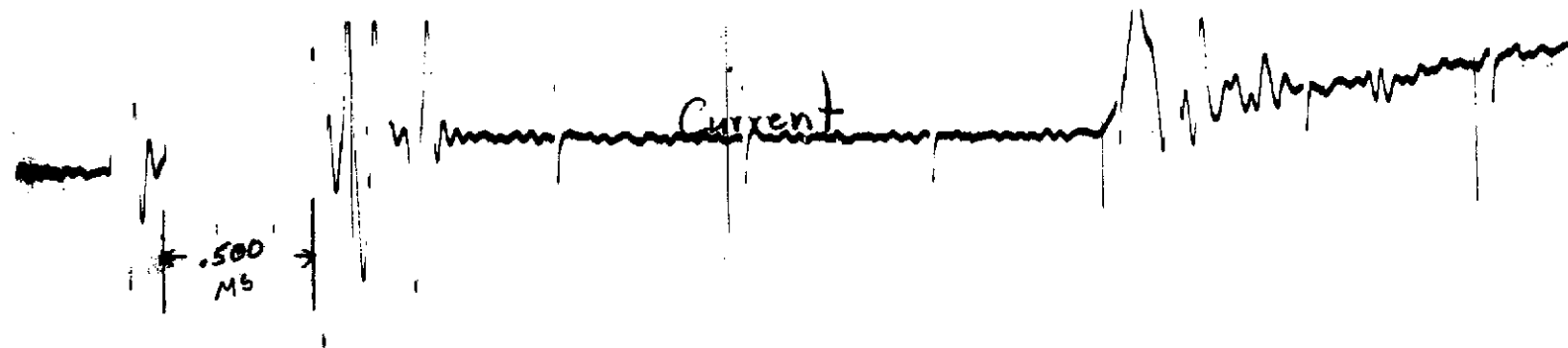


FIGURE 36. CARTRIDGE FIRING TRACE (ID 24)





Snub Firing  
ID 25

Time  
 $.633 \text{ MS/inch}$

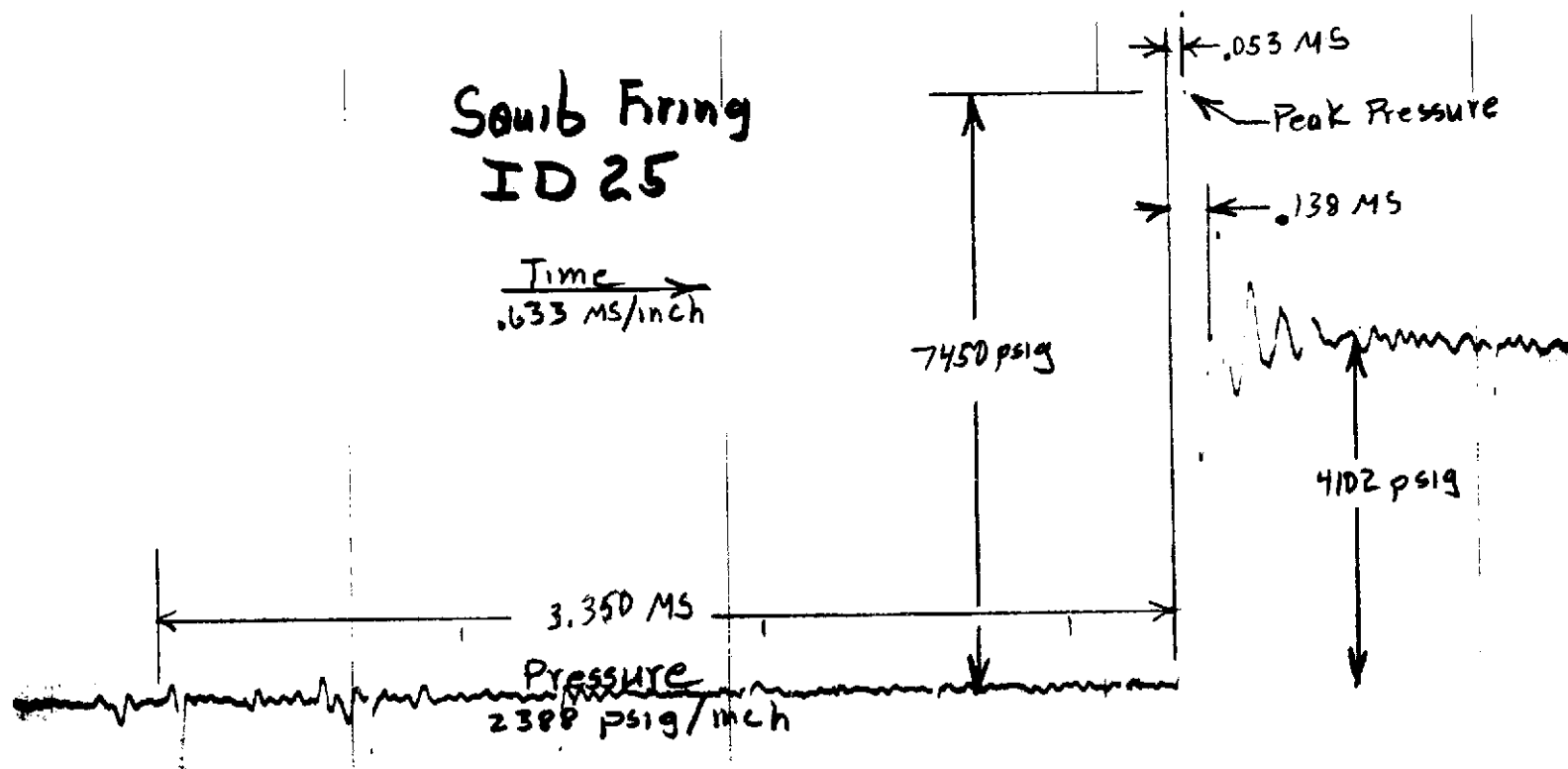


FIGURE 37. CARTRIDGE FIRING TRACE (ID 25)

#### 4.4 Discussion of Results

The purpose of this test program was to establish the effect of vibration, thermal shock, and temperature on cartridge output pressure, and to verify that the cartridge would fire under those conditions. The cartridges performed satisfactorily during all tests to which they were subjected, i.e., all cartridges fired and produced pressure. The effects of vibration, thermal shock and temperature on the cartridge output pressure were pronounced.

##### Cartridge Firing Pressure Traces

In the Cartridge Firing Trace figures it was noted that a certain time after cartridge voltage was applied, the pressure in the firing chamber increased rapidly to a peak and then oscillated at constant frequency of 10,500 Hz as the amplitude decayed exponentially with time. Because this oscillation was viscous in nature and because its frequency was approximately the same as that of a sound wave resonating within the cavity, it was concluded that the pressure actually oscillated as indicated and that the oscillations were due to the shock wave resonating within the cavity. These oscillations were not caused by "transducer ringing" because the rapid response of the transducer at -423°F (-253°C) was 130,000 Hz and the "slowest" component in the data acquisition train was 20,000 Hz whereas the frequency of the oscillations were 10,500 Hz.

A comparison of all pressure traces is presented in Figure 38. Although a certain pattern in the test data is definitely present, it should be recognized that the sample number of each test population was extremely small, due to the high cost of the cartridges. Nevertheless several general observations can be made with regard to the environmental effects on the cartridge pressure output.

1. Peak pressures obtained were considerably higher at cryogenic temperatures than at the ambient temperature.
2. First indication of pressure occurred significantly later under cryogenic conditions than under ambient conditions.
3. Vibration resulted in an additional delay of first indication of pressure.
4. Data scatter was more apparent at -423°F (-253°C) than at the other temperature regimes.
5. There is good correlation of the pressure rise times under all environmental conditions.

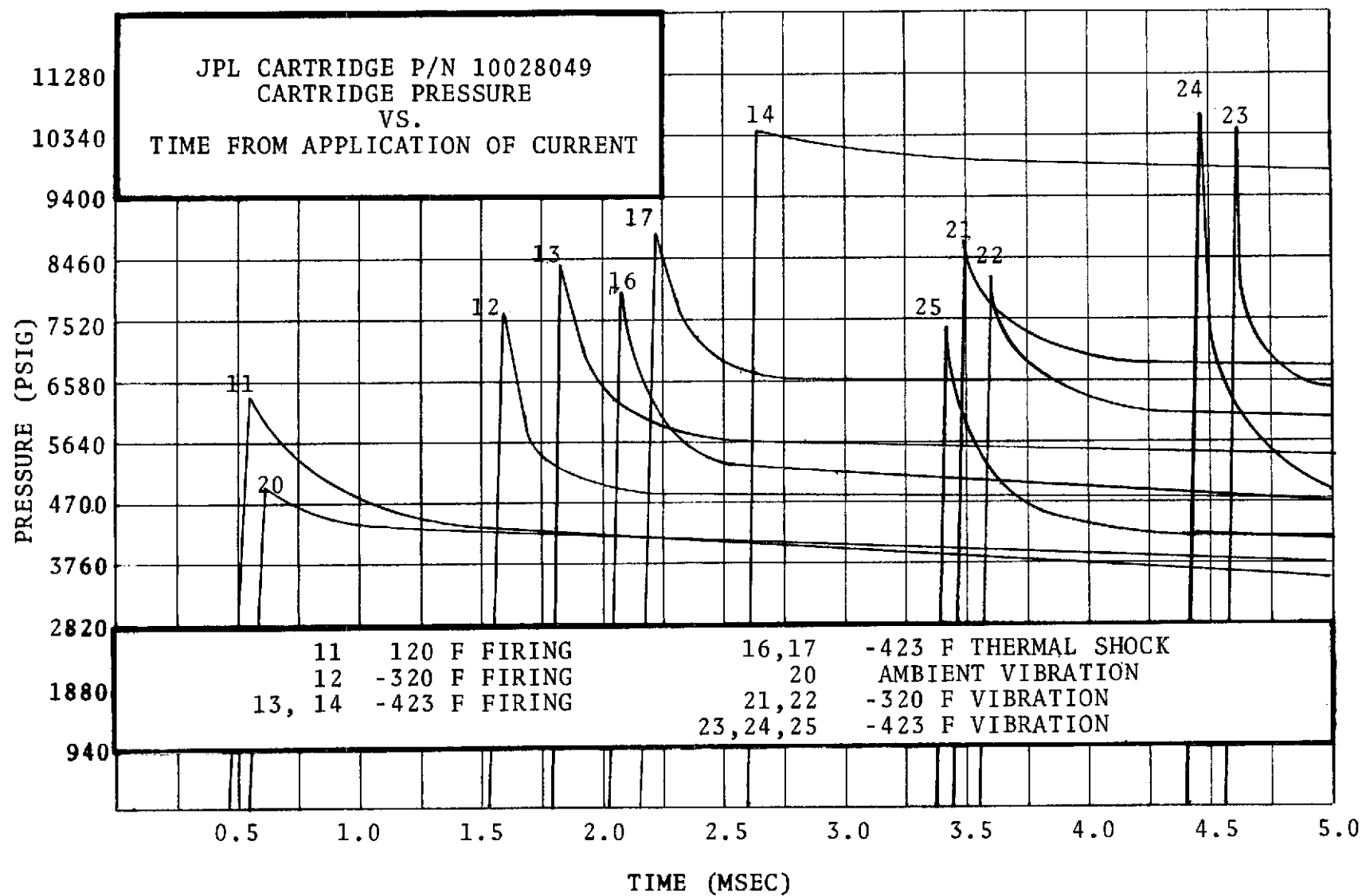


FIGURE 38. CARTRIDGE FIRING TEST SUMMARY

The effect of temperature on cartridge output pressure could be seen from the pressure traces of cartridges ID 11, 12, 13, and 14. ID 11 and 12 were fired at 120°F (49°C) and -320°F (-196°C) respectively. ID 13 and 14 were fired at -423°F (-253°C). A definite increase both in the time to first pressure indication and in peak pressure could be observed.

Comparing the traces of cartridges ID 11 and 20 the effect of vibration could be observed. ID 11 was fired at 120°F (49°C) and ID 20 was vibrated at ambient temperature and then fired. Vibration appeared to have had little effect on the time to first pressure indication but peak pressure was slightly less in the vibrated cartridge. This was probably due to normal cartridge pressure variation.

The effect of vibration at -320°F (-196°C) on the output pressure could be observed by comparing the traces of cartridge ID 12, 21, and 22. Cartridge ID 12 was fired at -320°F (-196°C) and ID 21 and 22 were vibrated and fired at -320°F (-196°C). A very definite increase in the time to first pressure indication could be observed. The two vibrated cartridges also exhibited slightly higher peak pressure. Good correlation existed between the traces of the vibrated cartridges. A possible explanation for the increased time to first pressure indication might be that the ignition mix around the bridgewire was loosened and therefore required more time to reach the ignition point.

Comparing the traces of cartridges ID 13 and 14 which were fired at -423°F (-253°C) and those of cartridges ID 23, 24, and 25 which were first vibrated at -423°F (-253°C) and then fired it could be seen again that vibration resulted in an increase in time to first pressure indication (see particularly the traces of ID 23, 24 as compared to ID 13 and 14). However, the data at -423°F (-253°C) were much more scattered than the data obtained at the higher temperatures.

Thermal shock appeared to have had negligible effect on cartridge output pressure. ID 16 and 17 were subjected to thermal shock at -423°F (-253°C) and these traces compared well with the traces of ID 13 and 14 which were conditioned at -423°F (-253°C) and then fired.

The stable pressure obtained from all cartridges fell into a rather narrow band from approximately 6,580 psig (4537 N/cm<sup>2</sup>) to 3,760 psig (2593 N/cm<sup>2</sup>) and the peak pressures ranged from 5,000 psig (3448 N/cm<sup>2</sup>) to 10,700 psig (7379 N/cm<sup>2</sup>). The longest time measured from first application of current to peak pressure was 4.58 milliseconds. The pressure variations and the time variations noted in the test program had no effect on the function of the valve and

it was therefore concluded that the cartridge was acceptable for this program.

### Cartridge Leakage

The original test plan and test procedure required that the leakage through the cartridge hermetic seal be determined at ambient and cryogenic temperatures. That is, leakage past the cartridge threads was not considered to be cartridge leakage and leakage through the cartridge by any other route was classified as cartridge hermetic seal leakage. The cartridge thread seal was designed for an O-Ring seal, but O-Rings do not seal well at cryogenic temperatures because they contract and become brittle. Various metal devices, such as "K" seals are designed to seal under these temperature conditions using the design sealing surfaces. The Harrison "K" seals (A-286 CRES, K6 nickel-lead alloy plated) purchased and used by Martin Marietta, in an attempt to eliminate the leakage problem, also failed to seal with repeatability at ambient or cryogenic temperatures. All leak tests, therefore, were performed at ambient temperatures using Teflon O-Rings and no leakage was detected in any cartridge at these test conditions.

ITEM	MANUFACTURER	MODEL	S/N	CAL. DATE DUE
Press. Transducer	Kistler	KIC 601H	33336	Calibrated
Press. Transducer	Kistler	KIC 601H	33332	Prior to
Press. Transducer	Kistler	KIC 601H	33333	Each Test
Press. Transducer	Kistler	KIC 601H	33329	↓
Press. Transducer	Kistler	KIC 601H	33330	
Press. Gage	Master Guage	ME124-634	N/A	9/24/71
Press. Gage	Maxi Safe	ME124-926	N/A	5/1/71
Dead Weight Tester	Mansfield-Green	T-10	N/A	3/5/71
Power Supply	Martin Marietta	327-1000100-9	004	↑
Battery	Sonotone	804-1000-000	4X	Calibrated
Amplifier	Kistler	No. 504 A	N/A	Prior to
Recorder (Magnetic Tape)	Ampex Recorder	FR1260	0090150	Each Test
Oscillograph	CEC Recorder	5-119	744986	↓
Leak Detector	CEC	24-120A	TO402303	12/7/71 and daily
Bomb (3)	Martin Marietta	CFL6300700	1, 2, 3	N/A
Cryostat	Martin Marietta	CFL6300705	1	N/A
Vacuum Pump	Kinney	Portable	AF-001205	N/A
Vibration System	Ling	A-249	AF001151	Maintenance
Accelerometer	Endevco	2272	ME125732	1/29/71
Accelerometer	Endevco	2272	ME126749	1/29/71
Charge Amplifier	Unholtz-Dickie	D-11	EQ526969	1/28/71
Charge Amplifier	Unholtz-Dickie	D-11	EQ525749	1/28/71
VTVM RMS	Ballantine	Mod 320	EQ504946	3/10/71
Sweep Oscillator	Spectral Dynamics	SD104A-5	AF006409	2/18/71

FIGURE 39. EQUIPMENT LIST

## 5.0 MANUFACTURING

After successful completion of Task I and Task II the original work statement called for the fabrication of nineteen (19) valves. Fabrication of the valves was to occur in four (4) phases as follows:

- Phase AA     One normally open valve was to be allotted for preliminary liquid fluorine testing.
- Phase A      Six (6) normally open valves were to be fabricated for Valve Functional Acceptance Testing
- Phase B      Six (6) normally open valves were to be fabricated for Fluorine Compatibility Testing. These valves were to have all design modifications resulting from Valve Functional Acceptance Testing.
- Phase C      Six (6) normally open valves were to be fabricated for delivery to the NASA-Lewis Research Center. These valves were to have all design modifications which may have resulted from Fluorine Compatibility Testing.

The change of scope in the program effort which resulted from the difficulties encountered during Valve Functional Acceptance Testing described in Section 6.0, made it necessary to eliminate Phase C of valve fabrication. However, a total of thirteen (13) valves were manufactured and several important fabrication and assembly techniques were developed.

### 5.1 Contamination Control

The Model 1356-1 Explosively Actuated Valve was designed to be used in liquid fluorine, liquid hydrogen and liquid nitrogen. Liquid fluorine is one of the most reactive oxidizers presently known; contamination of even a very minor nature can result in combustion of any material in the fluorine environment, with the obvious disastrous results. A comprehensive Process and Assembly Procedure was therefore established which covered all areas of valve fabrication. The maintenance of the very high cleanliness levels specified in this document were observed at all times. In the event of doubt regarding the integrity of any detail part or sub-assembly of the Model 1356-1 Valve, the detail part or the

subassembly were rejected and submitted to the Material Review Board for disposition.

The following general precautionary measures applied to all components of the valve.

### Machining

Commonly used coolants can result in surface contamination which is extremely difficult to remove. Only the following coolants were used during manufacture of components:

Hocut SS  
Cincool T-10  
Pems 1755

To be assured removal of surface contamination, all parts had a minimum of .062 inch (.157 cm) stock removal before starting machining of actual part dimensions.

To prevent surface damage and contamination, each component was kept in individual polyethylene bags between machine operations.

### Heat Treatment

Heat treatment, stress relieving, and normalizing of any component was done in the premachined condition.

### Assembly

No lubricants of any kind were used during assembly of the valve.

### Inspection

Surfaces which had a finish of 32  $\mu$ in. rms or better were not inspected with a stylus instrument. This applied to the sealing surfaces. Welds were inspected visually and radiographically. Dye penetrants were not used.

### Identification

Component identification was accomplished only by electro-etching or tagging.



## Pre-Cleaning

Components requiring pre-cleaning were processed outside the clean room. This included removal of dirt, grit, chips, grease and other major contaminants. Preparatory processes including degreasing, summa and passivation were performed on metal parts prior to this pre-cleaning operation.

## Final Cleaning

All final cleaning, inspection, assembly and preservation of cleaned components were performed within a clean room meeting the requirements of Federal Standard 209, Class 100,000.

## 5.2 Special Manufacturing Techniques

The design of the valve was such that all fabrication could be accomplished on standard machine tools. However, the fabrication of the outlet assembly which consisted of the hinged poppet, the outlet, the hinge pins and the shear pins required a procedure which would assure that the poppet could contact the outlet seat absolutely perpendicularly.

The procedure which was followed and which proved to be very effective is outlined below.

The poppet was pre-machined to the configuration shown in Figure 40, and installed in the outlet.

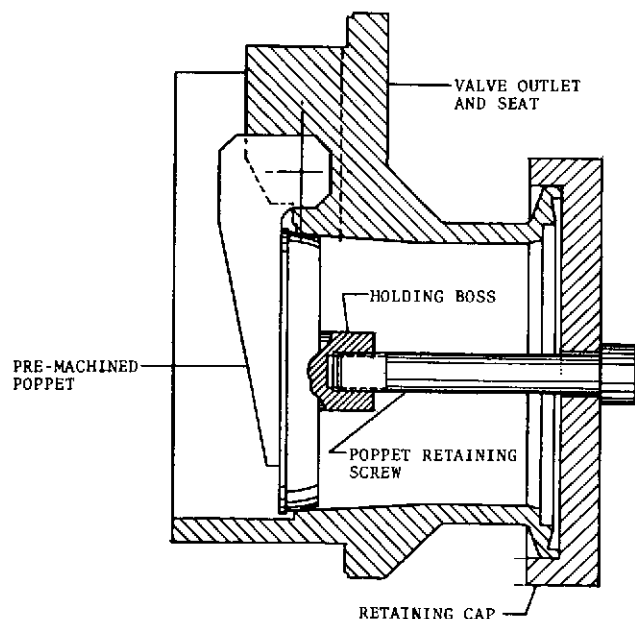


FIGURE 40. HINGED POPPET, PRE-MACHINED

Perpendicularity of the poppet with respect to the outlet was then verified by inspection. The holes for the hinge pins were drilled next. Installation of "tool" hinge pins followed. The "tool" hinge pins were slightly smaller in diameter than the assembly pins since the latter were to be press fitted. The poppet was then rotated into the open position and held in this position by a holding fixture. Then the holes for the shear pins were drilled. The poppet and the outlet were then identified as a matched set. Final machining of the poppet, i.e., the removal of the holding boss, followed by passivation and cleaning completed the Outlet Match Drill Procedure.

#### 6.0 TASK IV: VALVE FUNCTIONAL ACCEPTANCE TESTING

As originally conceived it was the purpose of Task IV to verify the valve design in several important areas prior to committing any future hardware to fluorine testing. The parameters which were to be investigated were:

- a. Valve Actuation Time
- b. Ability of the valve to meet the leakage limit specifications at earth ambient, liquid nitrogen and liquid hydrogen temperatures
- c. Minimum solid propellant charge to ensure full actuation of the valve
- d. Verification of proof conditions
- e. Verification of fluorine compatibility with one valve

The projected scope of Task IV testing and the test sequence is shown in the table below.

TABLE 12. TASK IV TEST SCHEDULE

NUMBER OF VALVES	TEST TEMPERATURE		FLOW RATE		TEST MEDIUM
	°F	°C	GPM	l/sec	
1	-320	-196	0	0	LF <sub>2</sub>
2	70	21	5	.31	H <sub>2</sub> O
2	-320	-196	60	3.78	LN <sub>2</sub>
2	-423	-253	5	.31	LH <sub>2</sub>

## 6.1 Zero Flow Fluorine Test

The primary purpose for this zero flow fluorine test was to verify material compatibility during a pre-actuation holding period and during valve actuation. In light of the high impact velocity with which the valve poppet during previous tests had contacted the valve seat, the possibility existed that a fluorine reaction would occur. The developmental nature of the valves and the hazards associated with fluorine testing in general made it necessary to test this valve in a low volume liquid fluorine test system.

The zero flow test system was completely isolated from the full flow test facility in order to minimize potential damage which might result from a valve failure. The valve was installed in the test set-up shown in Figure 41 below.

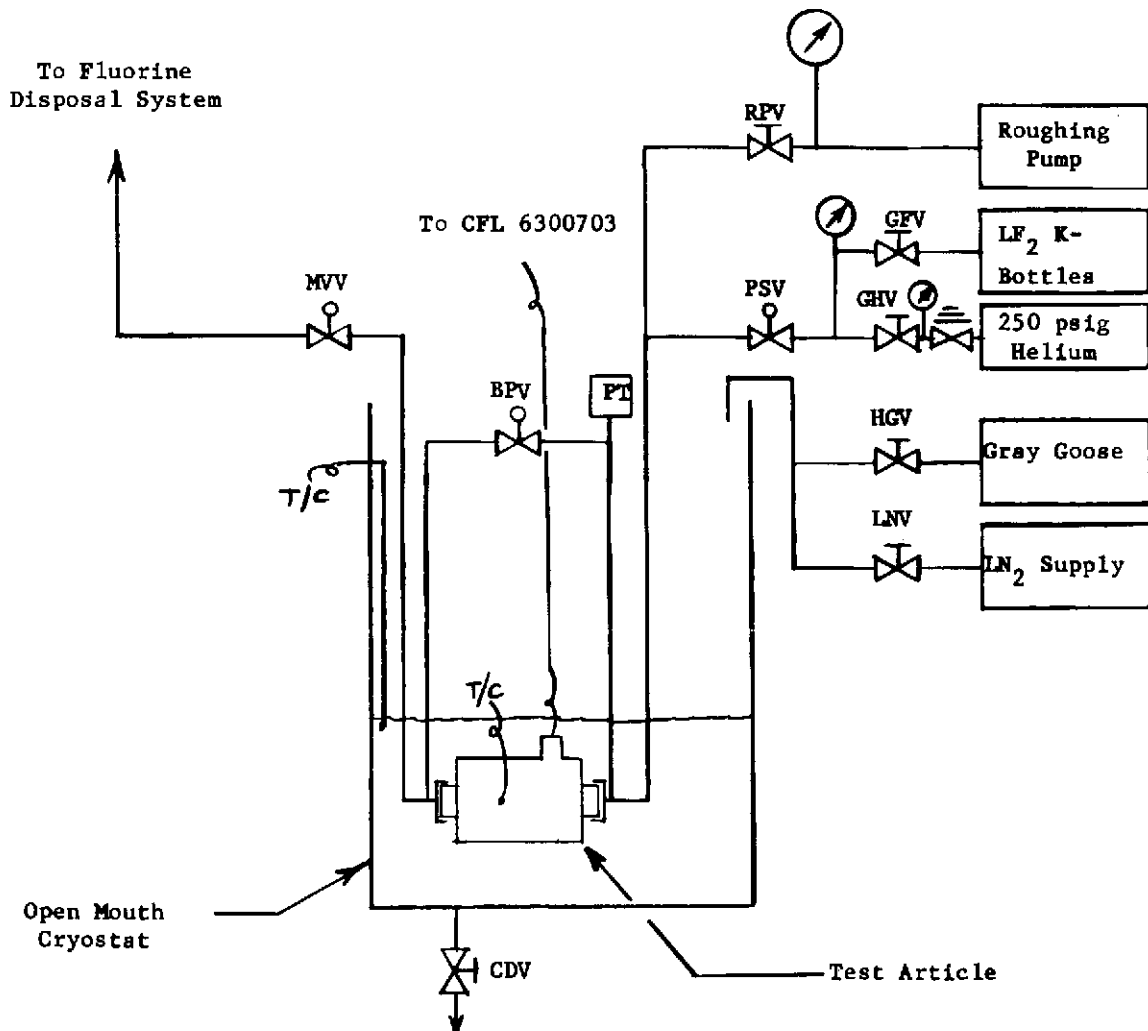


FIGURE 41 . ZERO FLOW FLUORINE TEST SET-UP

The valve was installed in the zero flow fluorine test fixture and actuated according to test plan under 250 psig (172.41 N/cm<sup>2</sup>) nominal pressure. The cartridge fired but the valve failed to lock, however, the primary objective of the test, namely to establish valve actuation without precipitating a reaction in the fluorine was met.

A failure analysis conducted on the zero flow fluorine valve revealed that the separation screw and the actuation piston had not stroked the full distance. This condition is shown in Figure 42.

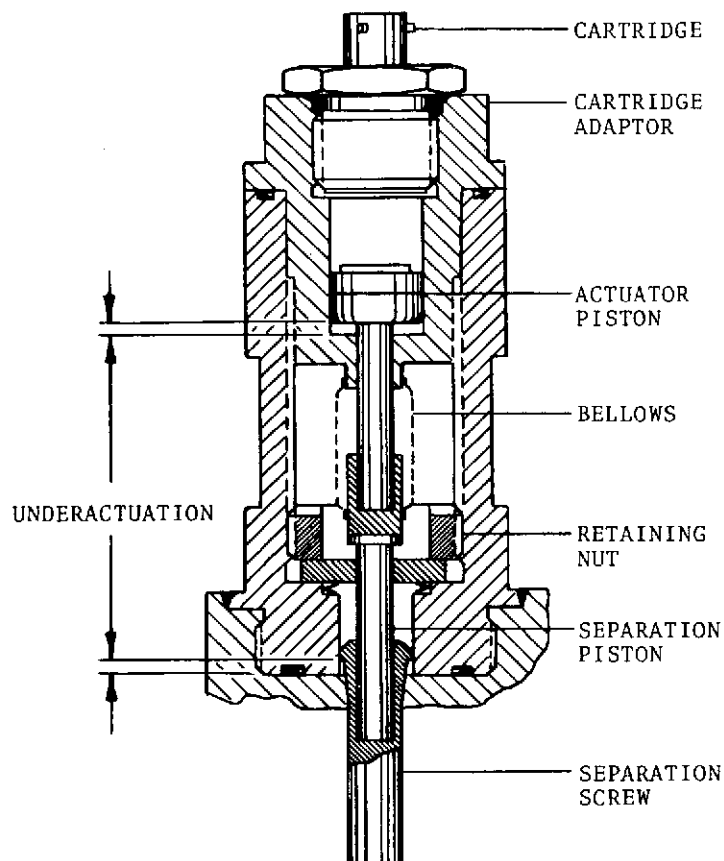


FIGURE 42. UNDERACTUATION OF PISTON

Analysis showed that during the last 1/16 inch (.157 cm) increment of stroke a significant portion of total energy was imparted to the valve poppet. Failure of the valve actuator to stroke the full design distance was attributed to energy losses due to the higher density of the liquid fluorine. In consultation with the NASA Lewis Program Manager it was decided to verify the failure mode using the identical test method but with carbontetrachloride as test medium.

## 6.2 Failure Mode Verification Tests

In the course of establishing the reason why the zero flow fluorine valve failed to close, all of the valves originally committed to Task IV were consumed.

### Density Verification Test

The first step in determining the probable cause of failure was a valve actuation test in  $\text{CCl}_4$ . The specific weight of  $\text{CCl}_4$  is  $99.6 \text{ lb/ft}^3$  ( $1.595 \text{ gm/cm}^3$ ) which is very nearly equal to the specific weight of  $\text{LF}_2$ , i.e.,  $94.3 \text{ lb/ft}^3$  ( $1.514 \text{ gm/cm}^3$ ).

By using  $\text{CCl}_4$  as the test fluid it was possible to eliminate one possible reason for the valve failure, namely that a reaction had occurred within the valve (even though no visible evidence was present) which might have affected valve closure. A second reason for using  $\text{CCl}_4$  rather than liquid fluorine was the hazard associated with testing the valve in liquid fluorine.

The valve was installed in the identical test setup as the zero flow fluorine valve and the cartridge was actuated. The cartridge fired, but the valve did not close. Again the piston failed to stroke the full distance. It was concluded that the failure was due to the effect of density during the power stroke. The separation screw is designed to form a secondary seal between valve housing and actuator housing after valve actuation. This seal is obtained by forcing the tapered section of the separation screw into the valve housing. In order to compensate for the increased density effects it was decided to reduce the amount of interference between separation screw and valve housing.

### Reduced Separation Screw Interference Test

The separation screw was redesigned to reduce the amount of interference and the new part installed in the valve.

The modified valve was fired under 250 psig ( $172.41 \text{ N/cm}^2$ ) pressure using carbontetrachloride as test medium. This valve also failed to lock in the closed position. X-ray photographs revealed that this valve also did not stroke the full design distance, however, it did stroke further than either of the first two valves.

### Zero Separation Screw Interference Test

A third valve firing was conducted using CCl<sub>4</sub> as the test fluid in order to simulate LF<sub>2</sub>. The modification for this valve consisted of a straight shaft separation screw. The poppet in this valve as in all previous Task IV valves was machined of 304 CRES condition B per QQ-S-763. This valve also failed to close. Post test examination revealed that the hinge struts of the valve poppet were severely deformed.

This test indicated that the straight shaft of the separation screw which caused no interference with the valve housing, transmitted more energy to the hinged poppet. Hinge strut deformation had not been previously encountered.

The poppet must contact the valve seat absolutely perpendicularly, otherwise the spherical sealing surface cannot wedge itself into the tapered seat and form the metal-to-metal seal. It was therefore decided to repeat the test with the zero interference separation screw but to manufacture the poppet from A-286 alloy steel. This alloy when heat treated has a yield strength of 80,000 psi which is much higher than that of 304 CRES, condition B, i.e., 30,000 psi.

### A-286 Poppet Test

In order to take full advantage of maximum energy transfer into the poppet, the poppet material was changed to A-286. This prevented the previously experienced deformation of the hinge struts, however this valve also failed to close. Post test examination showed that the poppet hinge struts did not deform and in fact the poppet locked in place when the valve was actuated manually in air.

A program status review was conducted with the NASA Program Manager to evaluate the test results obtained and to determine the extent of further testing. Briefly, the possible reasons for the failure were determined to be:

1. Density Effects
2. System Effects
3. Defective Hardware
4. Shock Effects
5. Hydraulic Effects

### Density Effects

Density affects valve function in the form of drag on the poppet. Although previous analytical work showed that density should not affect the valve to the extent where the poppet would not lock in the valve seat this variable was considered to be a possible reason for failure.

### System Effects

All previous successful valve tests had been conducted when the valve was submerged in a fluid without the valve being connected to inlet and exit lines. This was done because analysis showed that the valve should theoretically not be affected by external plumbing. This variable had to be considered, however, to represent a possible reason for failure.

### Defective Hardware

Although all valves were 100% inspected and manually functioned to verify free movement of the poppet, the possibility existed that this particular lot of valves for Task IV was in some way defective.

### Shock Effects

The possibility was considered that the valve locked but that a reflected shock wave from the plumbing unseated the poppet.

### Hydraulic Effects

Input energy losses due to fluid friction in the separation screw were also considered to be a possible reason for failure.

### Failure Mode Analysis

In order to eliminate the hardware variable, i.e., to verify that this particular lot of valves was not defective in any way it was decided to test one valve in LH<sub>2</sub>. A total of three valves had previously been tested in LH<sub>2</sub> and these valves had functioned properly. A successful test would have shown that the hardware was not defective, conversely



an unsuccessful test would have been a strong indication of hardware defects.

A closed system test, with the valve installed in the zero-flow fluorine test facility but using water as the test fluid instead of carbontetrachloride would have isolated the following failure areas:

If the valve locked in the closed position density would have to be the reason for failure. System effects, defective hardware, shock effects and hydraulic effects would then be known not to have an appreciable effect on valve function. Conversely, if the valve failed to lock in the closed position density would not be the reason for failure because previously tested valves had successfully locked with water as the test fluid.

An open system test, with the valve submerged in carbontetrachloride, would have provided the same data as the closed system test with water.

If the valve locked then the system effects would be the cause of failure. Conversely if the valve would fail to lock, then the density effect would be the reason for failure.

The decision was made to conduct two tests as a result of this analysis.

- a. Open system test with LH<sub>2</sub>
- b. Open system test with CCl<sub>4</sub>

#### Open System LH<sub>2</sub> Test

The purpose of the open system LH<sub>2</sub> test was to establish that this hardware lot manufactured for Task IV was not in any way defective. Three previous tests conducted with LH<sub>2</sub> had been successful, therefore success or failure of this test would have determined whether this lot of hardware was defective.

The valve was submerged in LH<sub>2</sub> and actuated. The poppet locked and required 1280 psig (883 N/cm<sup>2</sup>) backpressure to unseat. This fact indicated that the valves were not defective.

### Open System CCl<sub>4</sub> Test

The purpose of the open system CCl<sub>4</sub> test was to identify whether density or system effects (i.e., plumbing, etc.) were the dominant failure causes.

Previous tests conducted in a closed system with CCl<sub>4</sub> were not successful. Consequently if an open system test with CCl<sub>4</sub> proved to be successful the reason for the previous failures could be attributed to system effects. Conversely an unsuccessful test in CCl<sub>4</sub> would mean that density effects were definitely the reason for failure.

The valve was submerged in CCl<sub>4</sub> and actuated. The poppet did not lock. Therefore the density effects were considered to be the primary reason for all previous valve failures.

### 6.3 Discussion of Results

The first valve actuation in LF<sub>2</sub> was conducted at Martin Marietta on 11 August 1971. The Model 1356-1 failed to close as anticipated. A second firing was conducted using carbon-tetrachloride as test medium. The purpose of this test was to verify the failure mode with a liquid of approximately the same specific gravity as LF<sub>2</sub>. The second valve also failed to close. This then verified the failure mode, i.e., the reason for the failure was attributed to the increase in density of the test medium. A failure analysis revealed that the actuator piston and separation screw in both valves had not stroked the full design distance. Since the separation screw is designed to wedge itself into a bore in the valve housing to form a secondary seal it was decided to compensate for the increased density effect by reducing the amount of interference between separation screw and valve housing. A third valve was then fired, again in carbontetrachloride, this time with a reduced taper on the separation screw. This third valve also failed to close and the actuator piston and separation screw still failed to stroke the full design distance, although the stroke was longer than on the previous two firings. In order to maximize energy input from the actuator the fourth valve was fired with a straight shaft separation screw. This modification also did not result in a successful valve closure. It was found, however, that the valve poppet was severely deformed after valve firing.

A fifth valve firing was conducted using a poppet machined of A-286 alloy steel. The test medium was CCl<sub>4</sub> and the valve was installed in the zero-flow fixture. This valve also failed to close.

Two additional tests were conducted in order to determine whether defective valve hardware or density/system effects were the cause for the valve failures. One valve was tested in LH<sub>2</sub>. This valve locked shut and the test was considered successful. The second valve was tested in CCl<sub>4</sub>. This latter valve failed to lock. The interpretation of this was that valve hardware is not defective but that density effects prevent successful valve closures if the density of the test medium is in excess of approximately 75 lb/ft<sup>3</sup>.

A summary matrix of all tests conducted since the conclusion of the development phase of the program is shown in Table 13. The valves consumed during tests 1 through 7 inclusive, were equipped with composite poppets as described earlier, which had a moment of inertia slightly less than that of the poppet utilized in the valves consumed during tests 8 through 19. For this reason the poppet unseating pressures measured during tests 1 through 7 are less than the pressures measured during tests 8 through 19.

If the back pressure which is required to unseat the poppet is plotted vs. the density of the test fluid it becomes very obvious how dramatically the density affects valve closure. This is shown in Figure 43. It should be pointed out that this graphical representation is unique for one particular valve design with a given energy input. If the energy input is increased the curve would shift upwards and one could expect that valves of the hinged poppet design can be made to function in relatively high density fluids. Energy input can be increased either by increasing the stroke or by increasing the pressure output of the cartridge or a combination of the two methods.

TABLE 13. SUMMARY TEST MATRIX

TEST NO.	TEST CONDITION	TEST MEDIUM	SYSTEM PRESSURE		UNSEAT PRESSURE		LEAKAGE (He) SCC/SEC	REMARKS
			PSIG	N/CM <sup>2</sup>	PSIG	N/CM <sup>2</sup>		
1	VALVE SUBMERGED	H <sub>2</sub> O	0	0	380	262		LEAKAGE NOT MEASURED
2	VALVE SUBMERGED	LH <sub>2</sub>	0	0	700	483	4.2 X 10 <sup>-6</sup>	
3	60 GPM FLOW FIXTURE	H <sub>2</sub> O	9.5	4.5	---	---	-----	VALVE DID NOT LOCK
4	ZERO FLOW FIXTURE	H <sub>2</sub> O	0	0	---	---	-----	VALVE DID NOT LOCK
5	VALVE SUBMERGED	H <sub>2</sub> O	↑	↑	350	241	1.9 X 10 <sup>-10</sup>	
6	VALVE SUBMERGED	LH <sub>2</sub>			840	579	1.6 X 10 <sup>-9</sup>	
7	VALVE SUBMERGED	LH <sub>2</sub>			740	510	1.6 X 10 <sup>-9</sup>	
8	ORIFICE FIXTURE	H <sub>2</sub> O			500	345		2.50 IN DIA. ORIFICE
9	ORIFICE FIXTURE	H <sub>2</sub> O			50	35		1.25 IN DIA. ORIFICE
10	ORIFICE FIXTURE	H <sub>2</sub> O			100	69		1.50 IN DIA. ORIFICE
11	ORIFICE FIXTURE	H <sub>2</sub> O	↓	↓	245	169		1.75 IN DIA. ORIFICE
12	ORIFICE FIXTURE	H <sub>2</sub> O	0	0	425	293		2.50 IN DIA. ORIFICE
13	ZERO FLOW FIXTURE	LF <sub>2</sub>	250	172	---	---		VALVE DID NOT LOCK
14	ZERO FLOW FIXTURE	CC1 <sub>4</sub>	250	172	---	---		FAILURE VERIFICATION
15	ZERO FLOW FIXTURE	CC1 <sub>4</sub>	250	172	---	---		(1)
16	ZERO FLOW FIXTURE	CC1 <sub>4</sub>	50	34	---	---		(2)
17	ZERO FLOW FIXTURE	CC1 <sub>4</sub>	50	34	---	---		(3)
18	VALVE SUBMERGED	LH <sub>2</sub>	0	0	1280	883		(4)
19	VALVE SUBMERGED	CC1 <sub>4</sub>	0	0	---	---		(5)
NOTES: (1) SEPARATION PISTON WITH REDUCED TAPER TO IMPROVE ENERGY TRANSFER. (2) SEPARATION PISTON WITH STRAIGHT SHAFT TO IMPROVE ENERGY TRANSFER. (3) SEPARATION PISTON WITH STRAIGHT SHAFT AND A-286 POPPET. (4) HARDWARE VERIFICATION TEST. (5) SEPARATION PISTON WITH STRAIGHT SHAFT.								

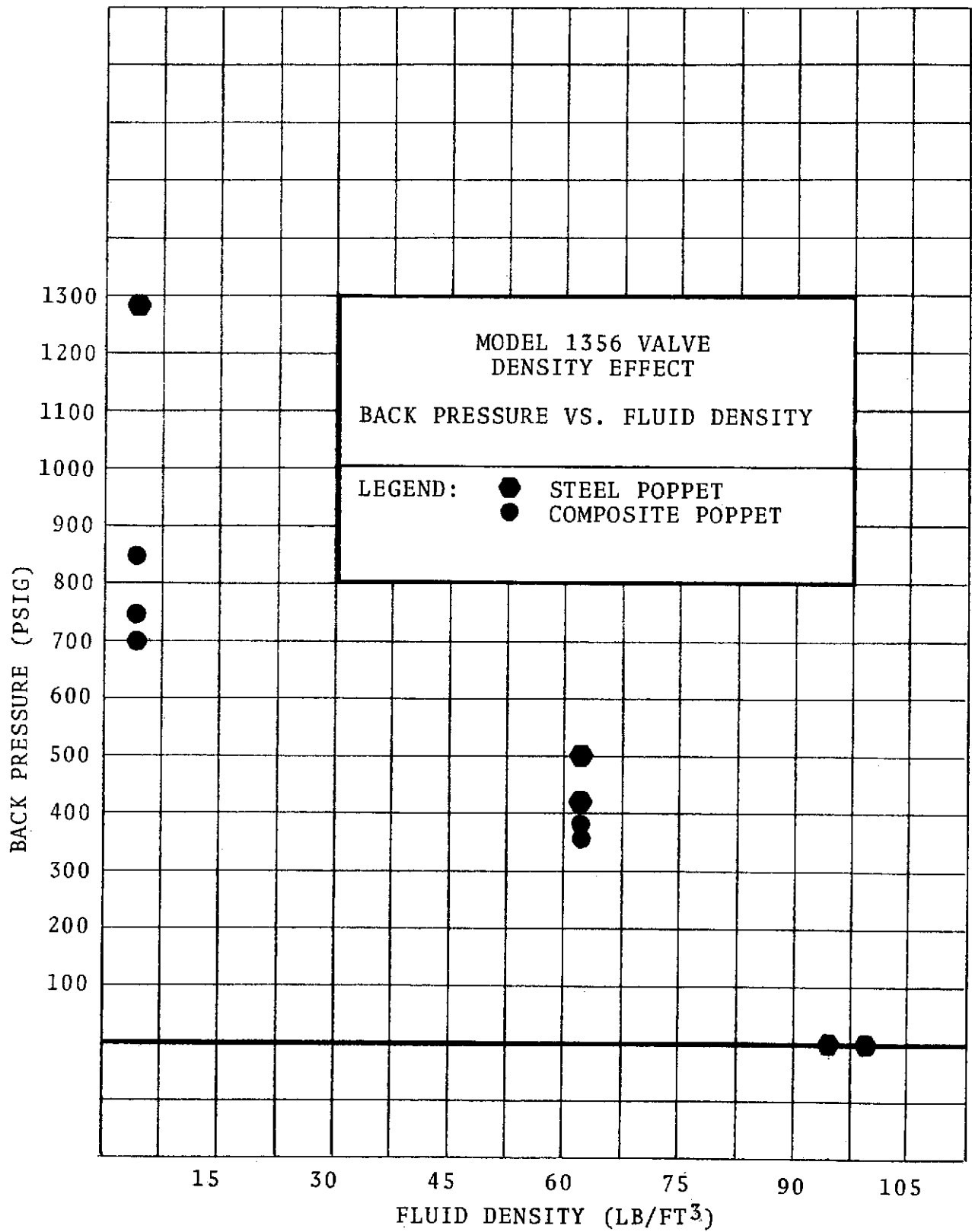


FIGURE 43. DENSITY EFFECTS ON VALVE CLOSURE

## 7.0 ANALYSIS

The hinged poppet of the Model 1356 valve undergoes three phases of motion during its rotational displacement. During the first phase the valve poppet is accelerated by a force provided by the explosive actuator. During the second phase of its rotational displacement the poppet is gradually decelerated by the fluid drag forces. During the last phase of its displacement the poppet is rapidly decelerated on impact into the valve seat.

Expressing the rotational displacement of the valve poppet in terms of its kinetic energy, it can be stated that the poppet obtains a maximum level of kinetic energy at the end of the actuator stroke, the level of kinetic energy is then gradually reduced since energy is given off to the surrounding fluid. On impact, the kinetic energy is finally converted into plastic deformation of the valve seat. A qualitative representation of the kinetic energy of the valve poppet is shown in Figure 44 below. The kinetic energy of the poppet is plotted on the ordinate and the angular displacement is shown on the abscissa.

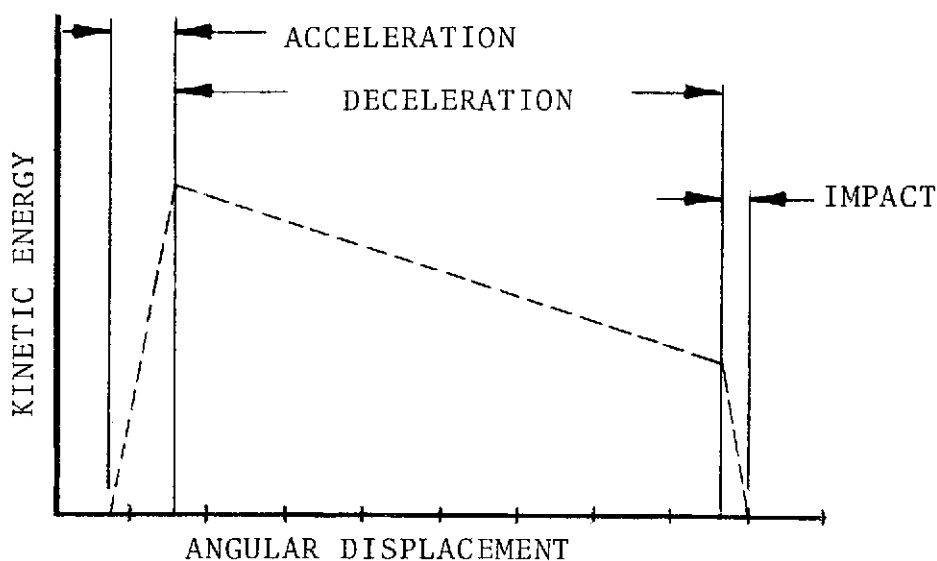


FIGURE 44. KINETIC ENERGY VS. DISPLACEMENT

The poppet is held in position at an initial angle of eight degrees. It is then accelerated through a .500 inch (1.27 cm) stroke, the stroke being equivalent to ten degrees, after which the poppet experiences a deceleration through the remaining 72 degrees. The quality of seal which is formed when the poppet is wedged into the valve outlet

depends entirely on the kinetic energy content of the poppet immediately prior to impact. If the energy content is high, the poppet will wedge itself into the outlet with a much higher velocity and the resultant plastic deformation of both the seat and the poppet results in a better lock. This locking action between poppet and seat is reflected directly by the pressure required to lift the poppet from the seat after actuation.

The analysis of the Model 1356 Valve was conducted by investigating the energy transferred from the cartridge to the poppet. An effort was then made to define the energy losses due to drag in various fluids and comparing the energy retained by the poppet with the energy necessary to effect a strong enough seal in the valve outlet seat.

The mathematical approach taken throughout this analysis has been one of incrementation in order to take full advantage of digital computation. The computer language which was used is "Super Basic". Super Basic was developed by Tymshare, Inc., 334 East Kelso Street, Inglewood, California, as a conversational language, designed specifically for computer time sharing facilities. The language is easily translatable into the more common computer languages.

## 7.1 Cartridge Energy

Accurate estimations of energy transfers within explosive actuators are extremely difficult. Part of the reasons are the high propellant burn rates and the small quantities of propellant generally used in explosive cartridges. A systematic approach, even if not completely accurate, will provide initial design parameters and can be refined as more experimental data becomes available.

The total energy transmitted within the explosive actuator depends entirely on the pressure-time profile of the propellant gas which is contained within the plenum behind the actuator piston. This profile is influenced by the burn rate of the propellant, the pressure at which the system starts to move and the rate at which the propellant gas expands. Thus the profile is determined by the characteristics of the cartridge and the characteristics of the system. An analysis concerned with the estimation of energy transfer must therefore deal both with the rate at which the propellant gas is generated and the rate at which the system moves.

### Instantaneous Change of Pressure

The actuator piston of the Model 1356 Valve is held in its initial position until a pressure value has been reached which is high enough to break the frangible section of the separation piston. The propellant continues to burn while the piston is accelerated until complete consumption has occurred. Then the gas expands until the piston has completed its stroke.

The analytical approach can best be described by reference to Figure 45. The graph on the right side of the figure is an isothermal pressure-volume curve which is based on the pressure obtained when the cartridge is fired into a fixed volume. (This data is generally available from the cartridge manufacturer.) The curve is generated to provide pressure values for the initial volume which exists within the explosive actuator.

The graph on the left side of the figure is the relationship between pressure and total burn time, i.e., the time required for complete consumption of the propellant charge. For this analysis the assumption has been made that the total burn time is independent of pressure. By entering the  $P \cdot V = C$  curve at the initial volume ( $V_i$ ) the pressure ( $P_i$ ) which would exist if the propellant were burned completely within this volume can be found. This pressure value is then projected onto the pressure-time graph. The time required to reach release pressure ( $P_R$ ), i.e., the pressure at which the system starts to move can then be determined. By dividing the time period ( $T - T_1$ ) into suitably small segments the changes in volume which would occur if the release pressure ( $P_R$ ) were to act for one time increment can then be calculated (see the next section for volume changes analysis). The release pressure is then projected onto the  $P \cdot V = C$  curve. A new value for initial volume is then generated ( $V_i + \Delta V = V_i'$ ) and a new initial pressure value ( $P_i'$ ) is found from the pressure-volume curve. This pressure is then again projected onto the pressure-time graph. The point at which the time  $\Delta t + t_1$  intercepts the line  $P_i' - 0$  is the pressure which is assumed to act on the next time increment. The change of volume due to this pressure is then calculated and a new pressure ( $P_i''$ ) at  $V_i' + \Delta V = V_i''$  is found from the  $P \cdot V = C$  curve. This procedure is repeated until the sum of the time increments equals total burn time. In this manner the pressure rise curve can be established. Expansion of the propellant gas after complete consumption has occurred, follows the  $P \cdot V = C$  curve. The area under the curve represents the energy imparted to the system.

$$dW = PdV$$

The procedure described above has been adapted for computer application and is summarized as follows:



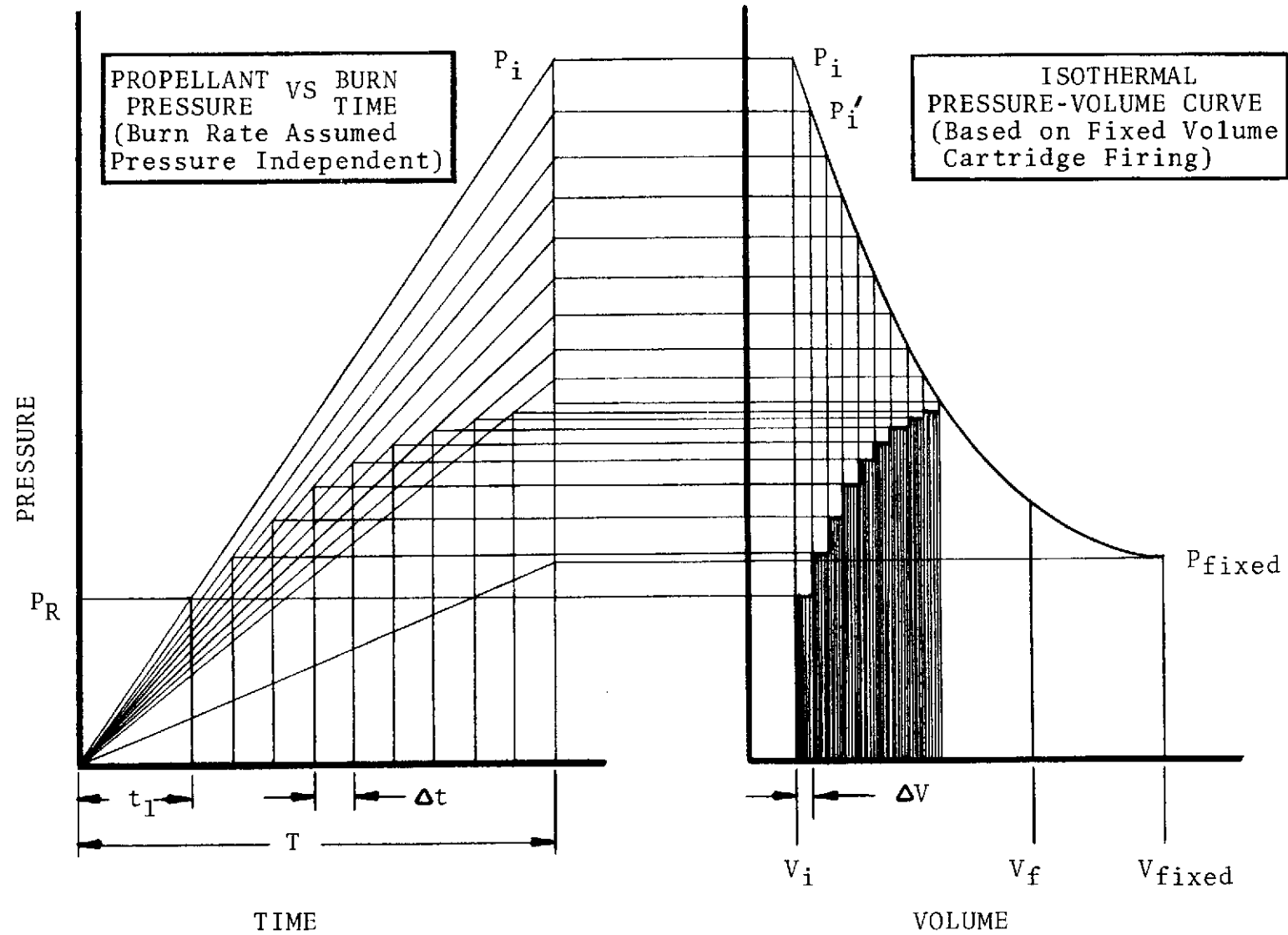


FIGURE 45. THEORETICAL CARTRIDGE PRESSURE CURVE

Definition of Symbols:

$k$  = coefficient of expansion

$\Delta t$  = time increment

$T$  = total burn time

$P$  = pressure in a fixed volume

$V$  = fixed volume

$P_R$  = release pressure

$V_i$  = initial volume in actuator

$\Delta V$  = change of volume

$p$  = instantaneous pressure

$P_i$  = initial pressure

$v$  = instantaneous volume

$t$  =  $(.1)(T)$

$$P_i = \frac{P \cdot V}{V_i}$$

$t_f = t_i + \Delta t$

$$p = \frac{P_i \cdot t_f}{T} \quad \text{when } p \geq P_R$$

$v = V_i + \Delta V$

$V_i = v$  until  $t_f = T$  then

$$p = P \left( \frac{V}{v} \right)^k$$

### Instantaneous Change of Volume

The analytical approach for the establishment of the pressure-stroke curve described above is complete except for the determination of the instantaneous change in volume. The change in volume depends on the system dynamics. A schematic representation of the poppet actuator system is shown in Figure 46:

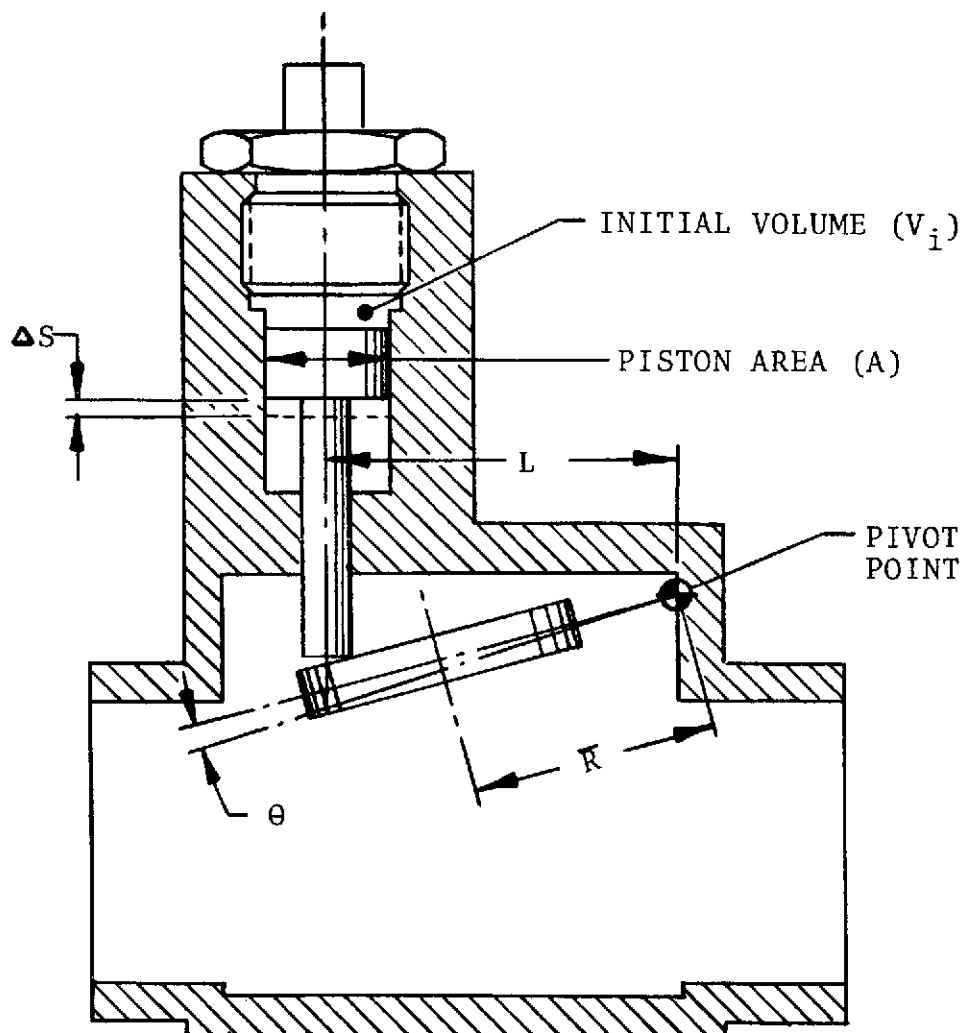


FIGURE 46. POPPET/ACTUATOR SCHEMATIC

The fundamental equation of motion for a rotating body, in terms of the applied moment ( $M$ ), the mass moment of inertia ( $I$ ), and the angular acceleration ( $\alpha$ ) is given by:

$$\Sigma M = I \cdot a \quad (1)$$

By definition, the angular acceleration ( $a$ ) is equal to the change in angular velocity ( $\Delta W$ ) per change of time ( $\Delta t$ ):

$$a = \frac{\Delta W}{\Delta t} \quad (2)$$

The fundamental equation of motion can therefore be expressed in terms of instantaneous cartridge pressure ( $p$ ), the piston area over which it acts ( $A$ ), the distance from pivot point to the application of force ( $L$ ) and the moment of inertia of the system ( $I$ ).

$$\Delta W = \frac{\Delta t \cdot p \cdot A \cdot L}{I} \quad (3)$$

The expression describing angular displacement ( $\theta$ ) with constant angular acceleration ( $a$ ) in terms of initial angular velocity ( $W_0$ ) and final angular velocity ( $W_f$ ) is given by:

$$W_f^2 = W_0^2 + 2a\theta \quad (4)$$

The relationship between initial angular velocity, final angular velocity, and an increase in angular velocity ( $\Delta W$ ) due to constant angular acceleration can be expressed as:

$$W_f = W_0 + \Delta W \quad (5)$$

Equations 2 and 4 can be solved to yield an expression for the angular change in displacement

$$\theta = \frac{\Delta t \cdot (W_f^2 - W_i^2)}{2 \cdot \Delta W} \quad (6)$$

The kinetic energy ( $E$ ) of a rotating body with a mass moment of inertia ( $I$ ) and an angular velocity ( $W$ ) is given by:

$$E = \frac{I \cdot W^2}{2} \quad (7)$$

The change in kinetic energy ( $\Delta E$ ) due to an increase in angular velocity can be expressed as

$$E = \frac{I \cdot (W_f^2 - W_o^2)}{2} \quad (8)$$

Referring to Figure 46, it can be seen that the change in stroke ( $\Delta S$ ) of the actuator piston can be expressed in terms of the change in angular displacement ( $\theta$ ) and the distance ( $L$ ) from the pivot point to the point of application of force:

$$\Delta S = L \cdot \tan (\theta) \quad (9)$$

The resultant change in volume ( $\Delta V$ ) in terms of stroke and piston area ( $A$ ) is then:

$$\Delta V = \Delta S \cdot A \quad (10)$$

The equations derived above can be rearranged to allow for incremental calculation of the kinetic energy of the hinged poppet and the instantaneous change in volume of the plenum behind the actuator piston due to the instantaneous change of cartridge pressure.

$$\Delta W = \frac{t \cdot (p \cdot A \cdot L)}{I}$$

$$W_f = W_i + \Delta W$$

$$\theta = \frac{t \cdot (W_f^2 - W_i^2)}{2 \cdot \Delta t}$$

$$\Delta E = \frac{I \cdot (W_f^2 - W_i^2)}{2}$$

$$\Delta S = L \cdot \tan (\theta)$$

$$\Delta V = \Delta S \cdot A$$

### System Moment of Inertia

The kinetic energy imparted to the hinged poppet by the explosive cartridge is a function of the mass moment of inertia of the poppet and the fluid through which the poppet moves. It can be shown that when a body which is submerged in a liquid is acted upon by a force (F) the body will experience an acceleration (a) of magnitude:

$$a = \frac{F}{(M+M_1)}$$

The term M represents the mass of the body. The term  $M_1$  represents the "hydrodynamic mass" of the fluid in front of the body. The sum  $(M+M_1)$  represents the "virtual mass" of the system. In Appendix B an expression for the hydrodynamic mass of the fluid in front of the poppet has been derived. This expression is given by:

$$M_1 = \left( \frac{8a^3h^3 + 6a^6}{3h^3} \right) \gamma$$

where

a = radius of the poppet

h = distance to the walls

$\gamma$  = density of fluid

The term in the parenthesis in the above equation represents the geometric configuration of the boundary of the fluid.

If the geometric configuration is symbolized by G the hydrodynamic mass of the fluid can be expressed as:

$$M_1 = G \cdot \gamma$$

The hydrodynamic mass of the fluid in front of the hinged poppet can then be calculated for various densities.

If it is assumed that the hydrodynamic mass of the fluid in front of the hinged poppet is in the shape of a flat disc with similar dimensions as the poppet disc the mass moment of inertia of the hydrodynamic mass can be calculated.

$$I_H = \frac{(I_p)(M_1)}{M_p}$$

where

$I_H$  = mass moment of inertia of the hydrodynamic mass

$I_p$  = mass moment of inertia of the poppet disc

$M_1$  = hydrodynamic mass

$M_p$  = poppet mass

For the special case of the Model 1356 Valve the geometric effect reduces to 11.51 in<sup>3</sup>. The hydrodynamic mass for various fluids, and the corresponding mass moment of inertia has been calculated and is summarized in Table 14.

TABLE 14 . SUMMARY OF HYDRODYNAMIC  
MASS CALCULATIONS

GEOMETRIC EFFECT (G) : 11.51 in <sup>3</sup>						
DISC INERTIA (I <sub>p</sub> ) : .00680 in·lb·sec <sup>2</sup>						
DISC WEIGHT (M <sub>p</sub> ) : .644 LB						
FLUID	DENSITY		HYDRODYNAMIC MASS		MOMENT OF INERTIA	
	LB/in <sup>3</sup>	gm/cm <sup>3</sup>	LB	gm	in·lb·sec <sup>2</sup>	cm·gm·sec <sup>2</sup>
LH <sub>2</sub>	.0026	.072	.030	13.6	.00031	.3567
H <sub>2</sub> O	.0361	1.000	.420	190.3	.00443	5.0972
LF <sub>2</sub>	.0546	1.512	.630	285.4	.00664	7.6401
CCl <sub>4</sub>	.0578	1.601	.670	303.5	.00706	8.1234

The equations for angular displacement and for the change in kinetic energy, which were developed in the previous section can now be expressed in terms of total system moment of inertia:

$$\Delta W = \frac{\Delta t \cdot (p \cdot A \cdot L)}{I_p + I_H}$$

where

$I_p$  = mass moment of inertia of poppet

$I_H$  = mass moment of hydrodynamic mass

It can be seen that the change in angular velocity is influenced by total system moment of inertia. The change in kinetic energy of the poppet alone can be expressed in terms of the velocity change and in terms of the poppet moment of inertia:

$$\Delta E_p = \frac{I_p \cdot (W_f^2 - W_i^2)}{2}$$

## 7.2 Energy Losses During Deceleration

During the deceleration phase, the poppet of the Model 1356 Valve gives up some of its kinetic energy to the surrounding fluid. If a reduction in the downstream flow area, such as an orifice, is present in the flow system, the mass flow induced by the hinged poppet can be equated to the mass flow through the downstream orifice and a "projected flow area". The total flow area available is the sum of the orifice area and the projected area which decreases as the poppet approaches the valve seat. A schematic representation of the flow model is shown in Figure 47.



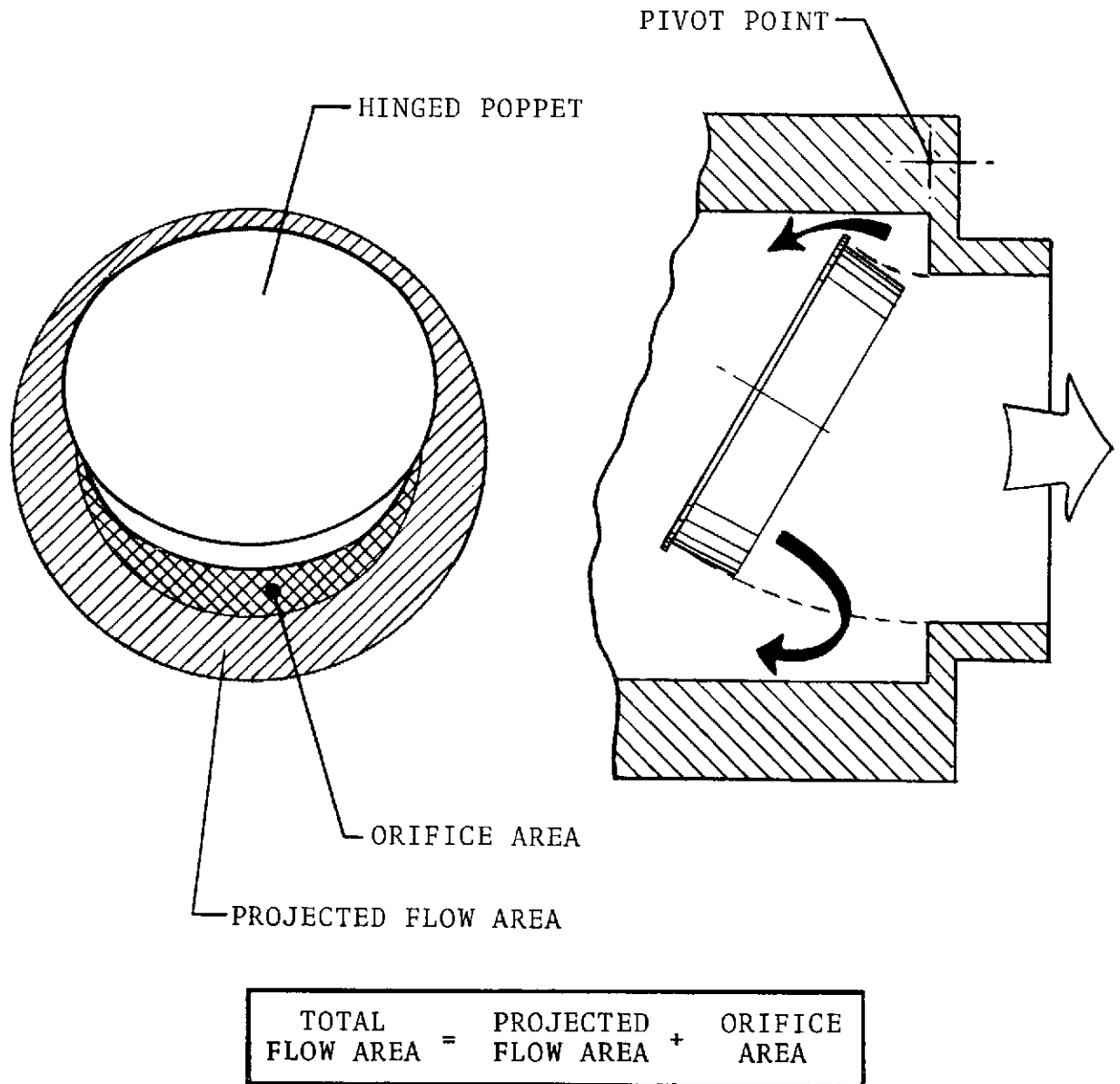


FIGURE 47. FLOW MODEL SCHEMATIC

The area projected by the poppet can be found by graphical integration at convenient intervals of angular displacement. For the special case of the Model 1356 Valve the projected area of the valve decreases between the initial poppet position and 70 degrees according to the relationship:

$$A_p = (-.0892)\theta + 6.2 \text{ (from } 8^\circ - 70^\circ)$$

where

$A_p$  = projected flow area (in<sup>2</sup>)

$\theta$  = angular displacement (degrees)

The total flow area is therefore

$$A_t = A_p + A_o$$

where

$A_t$  = total flow area

$A_o$  = orifice area

$A_p$  = instantaneous projected area

In the interval from 70° - 90° of poppet angular displacement the total flow area is very nearly constant and equal to the downstream orifice area.

With these considerations in mind the equations for energy losses due to orifice restrictions can be derived.

The weight flow through the total flow area is given by:

$$\dot{w}_2 = A_t \cdot \gamma \cdot \sqrt{\frac{2 \cdot g \cdot \Delta P}{\gamma}} \quad (1)$$

where

$\dot{w}_2$  = weight flow (lb/sec)

$A_t$  = total flow area (in<sup>2</sup>)

$\gamma$  = fluid density (lb/in<sup>3</sup>)

$g$  = gravitational acceleration (in/sec<sup>2</sup>)

$\Delta P$  = pressure drop across orifice (lb/in<sup>2</sup>)

The weight flow induced by the moving poppet is given by:

$$w_1 = A_1 \cdot \gamma \cdot \bar{R} \cdot W \quad (2)$$

where

$A_1$  = poppet area perpendicular to flow

$\bar{R}$  = distance from pivot to C.G. of poppet

$W$  = angular velocity

Solving equations 1 and 2 for  $\Delta P$  yields:

$$\Delta P = \frac{(A_1 \cdot \gamma \cdot \bar{R} \cdot W)^2}{A_t^2 \cdot 2 \cdot g \cdot \gamma} \quad (3)$$

The force (D) acting on the moving poppet and decelerating it, can be expressed in terms of poppet area (A) and differential pressure ( $\Delta P$ ).

$$D = \frac{A_1 \cdot (A_1 \cdot \gamma \cdot \bar{R} \cdot W)^2}{A_t^2 \cdot 2 \cdot g \cdot \gamma} \quad (4)$$

It will be observed that when the total flow area ( $A_t$ ) approaches the area of the poppet in Equation 4 the expression for the deceleration force becomes:

$$D = \frac{A_1 \cdot \gamma \cdot \bar{R}^2 \cdot W^2}{2g} \quad (5)$$

Equation 5 is the fundamental equation for total drag when modified for angular velocity.

The kinetic energy of a rotating body is given by:

$$E = \frac{I \cdot W^2}{2}$$

The change in kinetic energy of a rotating body which decelerates is given by:

$$\Delta E = \frac{I \cdot (W_o^2 - W_f^2)}{2}$$

The relationship between initial and final kinetic energy due to deceleration is:

$$E_f = E_i - \Delta E$$

The incremental change of angular displacement in a given time increment is:

$$\theta = \frac{\Delta t \cdot (W_o^2 - W_f^2)}{2 \cdot \Delta W}$$

The change in angular velocity due to drag is:

$$\Delta W = \frac{\Delta t \cdot D \cdot \bar{R}}{I}$$

In order to calculate incrementally the change in kinetic energy of the poppet due to drag or orifice restriction when the initial energy is known, the equations developed above can be arranged as follows and solved sequentially.

$$W_f = \sqrt{\frac{2 \cdot E_i}{I}}$$

$$D = A_1 \left[ \frac{(A_1 \cdot \gamma \cdot \bar{R} \cdot W)^2}{(A_t^2 \cdot 2 \cdot g \cdot \gamma)} \right]$$

$$\Delta W = \frac{\Delta t \cdot D \cdot \bar{R}}{I}$$

$$W_o = W_f + \Delta W$$

$$\theta = \frac{\Delta t \cdot (W_o^2 - W_f^2)}{2 \cdot \Delta W}$$

$$E = \frac{I \cdot (W_o^2 - W_f^2)}{2}$$

$$E_f = E_i - \Delta E$$

### 7.3 Summary and Application

The analytical procedure presented in the preceding paragraphs makes it possible to predict the instantaneous kinetic energy of the hinged poppet from the moment of first pressure indication within the explosive actuator to the point of impact into the valve seat. The kinetic energy required to form an effective seal between poppet and valve seat can either be established by test or can be calculated. (See Appendix A.)

By comparing the kinetic energy of the poppet just prior to impact with the required kinetic energy to form a seal the operational limits of the valve can be established.

A digital computer program has been generated (See Appendix C) which was used to predict the instantaneous kinetic energy of the poppet for various valve geometrics, for various fluid densities and for various downstream orifice restrictions.

#### Effect of Fluid Density

The curves shown in Figure 48 were generated by computer and represent the theoretical or predicted kinetic energy content of the hinged poppet of the Model 1356 Valve with JPL Cart-ridge P/N 10028049. The curves have been generated for three fluids, LH<sub>2</sub>, H<sub>2</sub>O, and LF<sub>2</sub>. The densities of these three fluids represent the maximum operational limits of the Model 1356 Valve. In order to show the theoretical variation in kinetic energy content of the poppet two curves have been generated for each fluid, by varying the following valve parameters:

1. Cartridge Pressure

This is the pressure which is generated by the cartridge when fired into a fixed volume of  $10 \text{ cm}^3$ . This variation was taken as +10%.

2. Initial Volume

This is the volume which exists within the valve actuator before the actuator piston moves. This parameter was also varied by +10%.

3. Downstream Restriction

The variation of outlet area which would occur as a result of a +0.005 in. (.013 cm) change in outlet diameter was taken as limit condition.

4. Mass Moment of Inertia

The mass moment of inertia of the hinged poppet was varied. A change in weight of +1.5% was taken as limit condition.

A review of Figure 48 shows quite obviously that the kinetic energy content of the poppet is highest when the valve is actuated while flowing liquids of very low density, such as  $\text{LH}_2$ , and is marginal when used with fluids of high density such as  $\text{LF}_2$ .

The theoretical energy content of the hinged poppet agrees reasonably well with the measured energy content during valve actuation tests. In Appendix A it has been shown that the energy content is directly proportional to the pressure required to lift the poppet from the seat after the valve has been actuated. For example, a back pressure of 250 PSIG ( $172.41 \text{ N/cm}^2$ ) corresponds to an energy content of 250 in·lb ( $172.41 \text{ N} \cdot \text{cm}$ ). The predicted energy content and the required back pressure for various fluid densities is shown in Table 15 below.

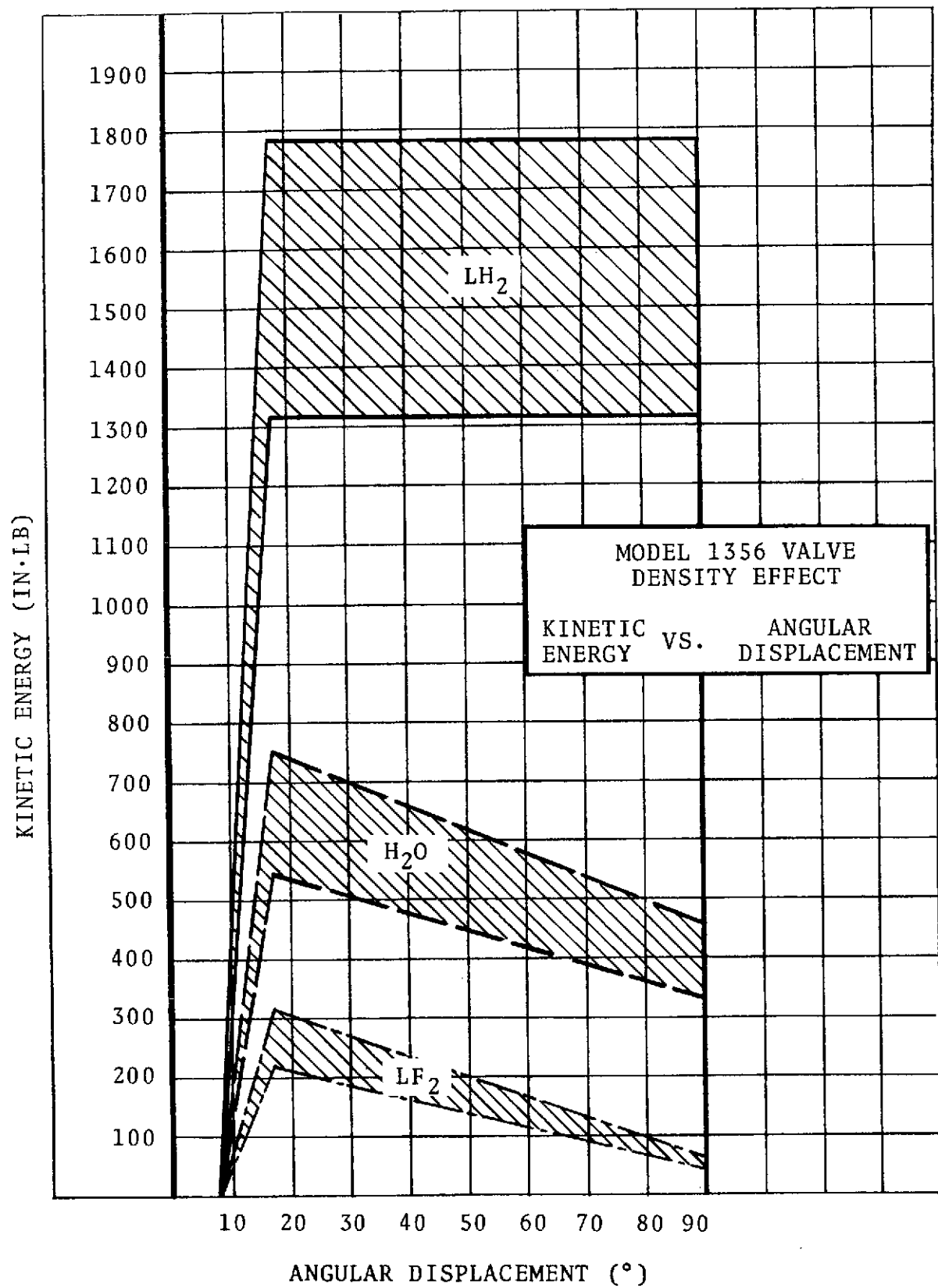


FIGURE 48. THEORETICAL EFFECT OF FLUID DENSITY

TABLE 15. EFFECT OF FLUID DENSITY

TEST MEDIUM	KINETIC ENERGY DESIGN		BACK PRESSURE ACTUAL		NUMBER OF TESTS
	IN·LB	N·CM	PSI	N/CM <sup>2</sup>	
LH <sub>2</sub>	1781-1312	20125-14826	700-1280	483-883	4
H <sub>2</sub> O	332- 468	3752-5288	350- 500	241-345	4
CCl <sub>4</sub>	38- 25	429-282	0	0	5
LF <sub>2</sub>	40- 60	452-678	0	0	1
NOTE: For the Model 1356 poppet and seat geometry the back pressure required to lift the poppet from the seat is equivalent to the kinetic energy content of the poppet.					

In tests conducted with CCl<sub>4</sub> and LF<sub>2</sub> the Model 1356 Valve failed to close. Therefore no back pressure data is available for these fluids. The predicted values of poppet kinetic energy are less than 65 in·lb (754 N·cm) which indicates that the valve is indeed marginal while flowing these high density fluids.

#### Effect of Poppet Weight and Actuator Stroke

The computer program described above has been used to analyze the effects of varying the poppet moment of inertia and the effect of varying the actuator stroke length. It will be remembered that during the initial development effort tests were conducted with valves having poppets made of aluminum alloy. These initial valve tests were unsuccessful since the poppet failed to wedge itself into the outlet-seat.

The curves presented in Figure 49 have been generated for the purpose of showing the effect of varying the moment of inertia of the poppet and the effect of changing the stroke length.



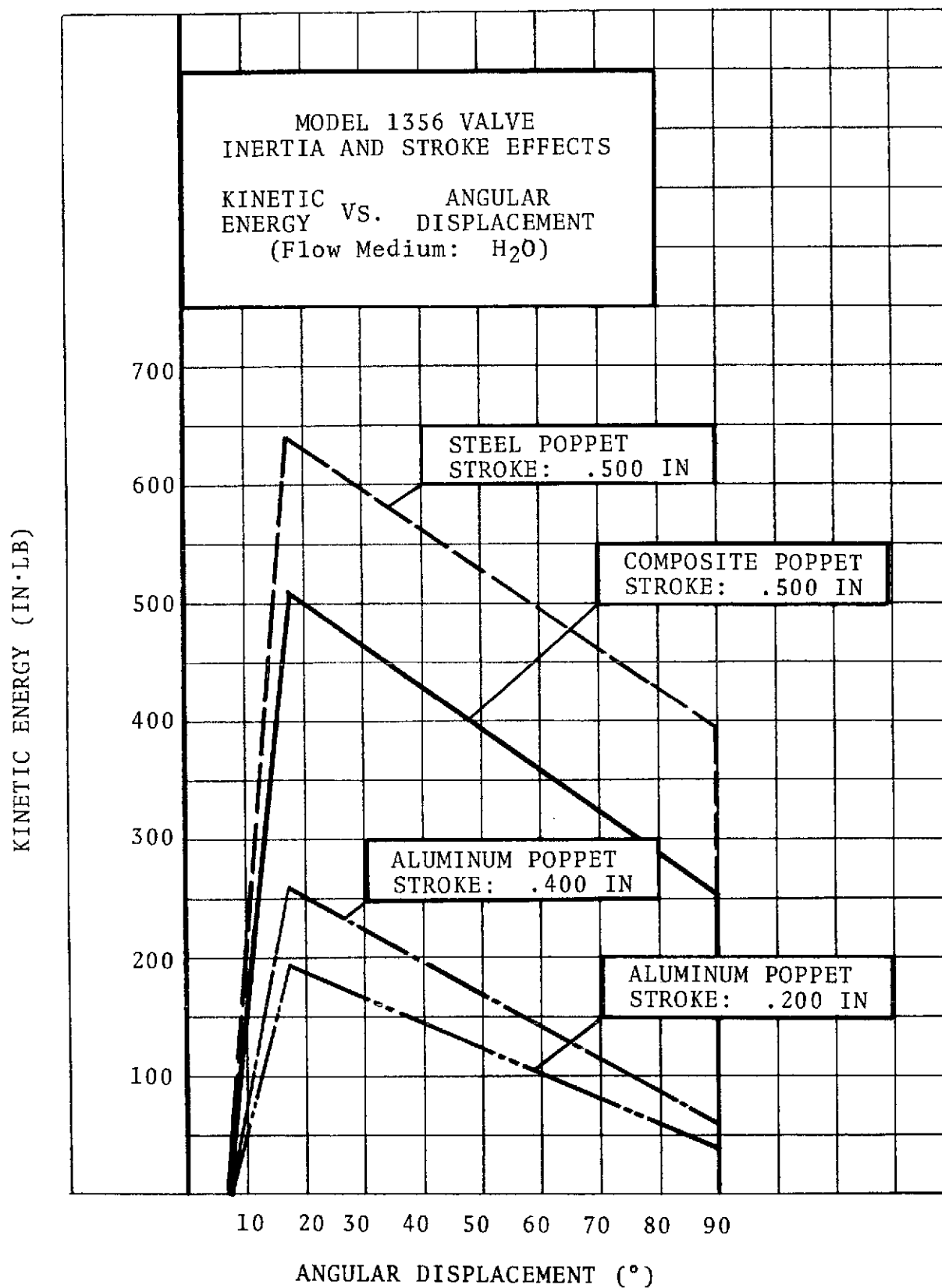


FIGURE 49. THEORETICAL EFFECT  
OF POPPET WEIGHT

The predicted levels of kinetic energy and the measured back pressures are summarized in Table 16 below, for tests conducted with H<sub>2</sub>O during the initial development effort. It can be seen that the predicted results agree reasonably well with the actually measured values for back pressure.

TABLE 16. EFFECT OF POPPET WEIGHT AND ACTUATOR STROKE

NUMBER OF TESTS	D E S I G N						A C T U A L	
	KINETIC ENERGY		STROKE		MOMENT OF INERTIA		BACK PRESSURE	
	IN·LB	N·CM	IN	CM	IN·LB·SEC <sup>2</sup>	CM·GM·SEC <sup>2</sup>	PSI	N/CM <sup>2</sup>
1	44	497	.200	.508	.00270	3.1107	0	0
1	60	678	.400	1.016	.00270	3.1107	3	2
1	254	2870	.500	1.270	.00559	6.4403	350	241
1	393	4441	.500	1.270	.00811	9.3437	425	293
1	393	4441	.500	1.270	.00811	9.3437	500	345
NOTE: For the Model 1356 Valve the back pressure to lift the poppet from the seat is directly proportional to the kinetic energy of the poppet immediately prior to impact.								

### Effect of Line Restrictions

During the initial development effort two instances of valve failure had occurred which were attributed to restrictions in the downstream line. In both instances the poppet failed to wedge itself into the valve seat with sufficient force to withstand an unseating pressure of 250 psig (172.41 N/cm<sup>2</sup>). As a result of these failures a special orifice test valve was manufactured and a series of tests conducted which had the purpose of establishing experimentally what effect a restriction in line size would have on the locking force. Figure 50 represents the theoretical energy content of the poppet when the valve is actuated with a restriction in line size present in the test system. It can be seen that for the Model 1356 a downstream orifice of 1.25 in (3.18 cm) in diameter has the effect of reducing the energy content of the poppet to zero. The predicted values of kinetic energy and

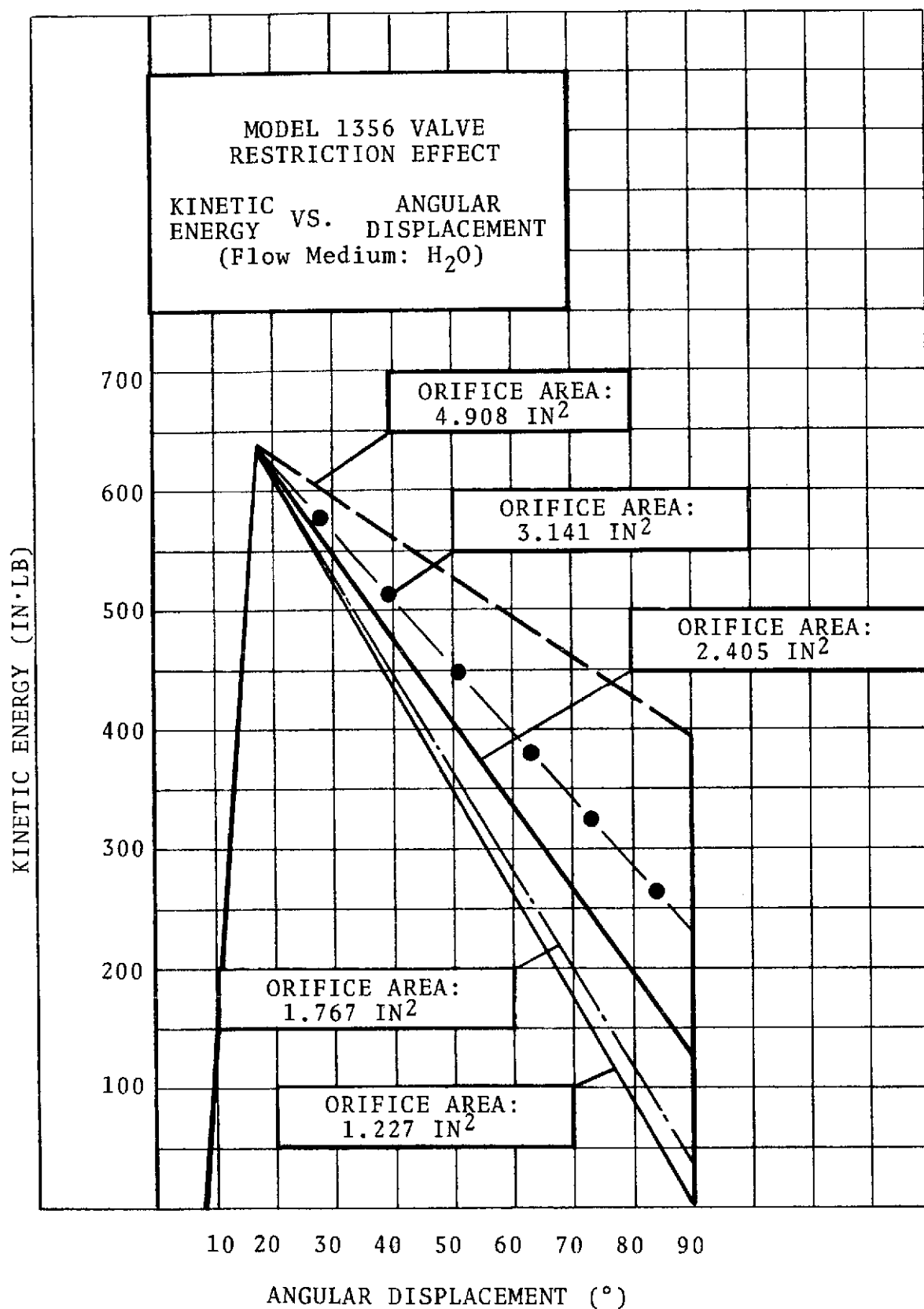


FIGURE 50. THEORETICAL EFFECT OF  
LINE RESTRICTION

the actually measured values of unseating pressure are compared in Table 17 below.

TABLE 17. EFFECT OF LINE RESTRICTION

NUMBER OF TESTS	D E S I G N				A C T U A L	
	KINETIC ENERGY		ORIFICE AREA		BACK PRESSURE	
	IN·LB	N·CM	IN <sup>2</sup>	CM <sup>2</sup>	PSIG	N/CM <sup>2</sup>
1	4	45	1.227	7.916	50	34
1	40	452	1.767	11.400	100	69
1	127	1435	2.405	15.516	245	169
1	228	2576	3.141	20.265	---	---
1	393	4441	4.908	31.665	425	293
1	393	4441	4.908	31.665	500	345
NOTE: For the Model 1356 Valve the back pressure to lift the poppet from the seat is directly proportional to the kinetic energy of the poppet immediately prior to impact.						

#### 7.4 Discussion of Results

The normal variation in valve geometry and in cartridge output results in a variation in kinetic energy of the hinged poppet. This variation is highest when the kinetic energy of the poppet is large. When the valve is actuated while flowing LH<sub>2</sub> the calculated variation in kinetic energy is 469 in·lb (5300 N·cm). When the valve is actuated while flowing LF<sub>2</sub> the calculated variation is 19 in·lb (115 N·cm).

The theoretical energy levels agree reasonably well with the actual energy levels as measured indirectly by the pressure required to unseat the poppet after valve actuation. The accuracy of the analytical method should be evaluated in view of the fact that valve and cartridge performances are subject to normal tolerance variation. It is believed that the analytical model will yield valid results for initial design calculations as related to explosively actuated swing check valves.

## 8.0 DUAL CARTRIDGE VALVE DESIGN

The Model 1356 Valve proved to be incapable of closing off the flow of high density fluids such as  $\text{LF}_2$  and  $\text{CCl}_4$ . Minor modifications made to the valve design during the development effort failed to produce a sufficiently high increase in energy transfer to the hinged poppet to effect successful valve closure. However, the basic valve concept was considered to be satisfactory in light of the performance with low density fluids such as  $\text{H}_2\text{O}$  and  $\text{LH}_2$ . The sealing capacity of the valve in those fluids was extremely good and since the actuation test in  $\text{LF}_2$  proved that the valve was compatible with that fluid an effort was made to redesign the valve by retaining the basic concept and to increase the energy output of the explosive actuator.

There are several methods by which an increase in energy output of the explosive actuator can be achieved:

Increase in cartridge output charge

Increase in length of actuator piston stroke

Increase in actuator piston diameter

The design analysis revealed that it would be necessary to incorporate all three methods into the new high density valve design.

### 8.1 Analysis

The design of the high density was governed by two guidelines:

1. Retention of the basic valve concept in order to make maximum use of the experience gained during the development and verification phases.
2. Utilization of the analytical method, i.e., the computer program, developed and used during the failure verification effort.

By retaining the basic valve concept, the design of the high density valve could be focused entirely on modification of the explosive actuator.

A significant increase in energy output of the explosive actuator can be accomplished by either selecting a cartridge with a higher output charge or by the use of dual cartridges. Because of the extensive testing which had been conducted with the JPL Cartridge P/N 10028049 the latter method was

selected as the more practical approach.

Dual cartridges, connected in parallel and actuated simultaneously have been used extensively in ordnance devices and the approach is generally regarded as reliable. In order to compensate for the higher propellant gas output of two cartridges and at the same time maintain a safe pressure level within the explosive actuator, the initial volume, i.e., the volume between actuator piston and cartridge closure disc prior to valve actuation, was increased from .089 in<sup>3</sup> (1.46 cm<sup>3</sup>) to .150 in<sup>3</sup> (2.46 cm<sup>3</sup>). The diameter of the actuator piston was increased from .625 in (1.59 cm) to 1.00 in (2.54 cm) and the stroke of the actuator piston was increased from .500 in (1.27 cm) to 1.00 in (2.54 cm).

A comparison of the input data for the computer program and the kinetic energy of the hinged poppet prior to impact for various fluids is shown in the table below for the Model 1356 Valve and for the Dual Cartridge Design.

Table 18. COMPARISON OF INPUT DATA  
AND FINAL KINETIC ENERGY

	UNITS	MODEL 1356 VALVE	DUAL CARTRIDGE VALVE DESIGN
Valve Release Pressure	(PSI)	7000	12000
Cartridge Pressure in .61 IN <sup>3</sup> Volume	(PSI)	5761	17000
Valve Initial Pre-Actuation Volume	(IN <sup>3</sup> )	.089	.150
Actuator Piston Area	(IN <sup>2</sup> )	.3067	.785
Actuator Piston Stroke	(IN)	.500	1.000
Poppet Kinetic Energy in LF <sub>2</sub>	(IN·LB)	50	168
Poppet Kinetic Energy in H <sub>2</sub> O	(IN·LB)	393	1964
Poppet Kinetic Energy in LH <sub>2</sub>	(IN·LB)	1532	7550
NOTE: Valve release pressure is the pressure at which the frangible section of the separation screen separates.			

The curves shown in Figure 51 have been generated for the Dual Cartridge Valve Design and represent the instantaneous kinetic energy level of the hinged poppet.

## 8.2 Design Description

The high density valve design which is shown in Figure 52 is identical to the design of the Model 1356 Valve in all respects except in the design of the explosive actuator. The actuator consists of the cartridge adaptor and bellows assembly, the actuator piston, a closure plug, and the two cartridges. The separation screw and the separation piston have been combined and replaced by a frangible piston. This component is guided during the power stroke by the valve actuator housing. The lower section of the actuator housing is screwed into the valve housing, thereby containing the sealing flange of the frangible piston. When the cartridges are fired the frangible piston separates at the stress riser groove.

In general, all major design features of the Model 1356 Valve have been retained. The materials selected for the actuator components are identical to those of the Model 1356 Valve. Therefore the assembly methods and contamination control procedures generated for the Model 1356 Valve require only minor modifications and can easily be adapted to the new high density valve design.

## 8.3 Development Tests

Although no development tests were conducted with the high density valve design, a tentative development program was generated. The development of this design could be accomplished by manufacturing a reuseable valve and subjecting it to the following tests.

1. Open System Test - Operating Fluid:  $H_2O$   
The purpose of this test is to verify the structural integrity of the explosive actuator.
2. Open System Test - Operating Fluid:  $CCl_4$   
The purpose of this test is to verify that the valve will function in a dense fluid and can withstand the design requirement backpressure.
3. Closed System Test - Operating Fluid:  $CCl_4$   
By installing the valve in a closed system and pressurizing the flow medium to 250 psig (172 N/cm<sup>2</sup>) the effect of system pressure on valve operation can be established.

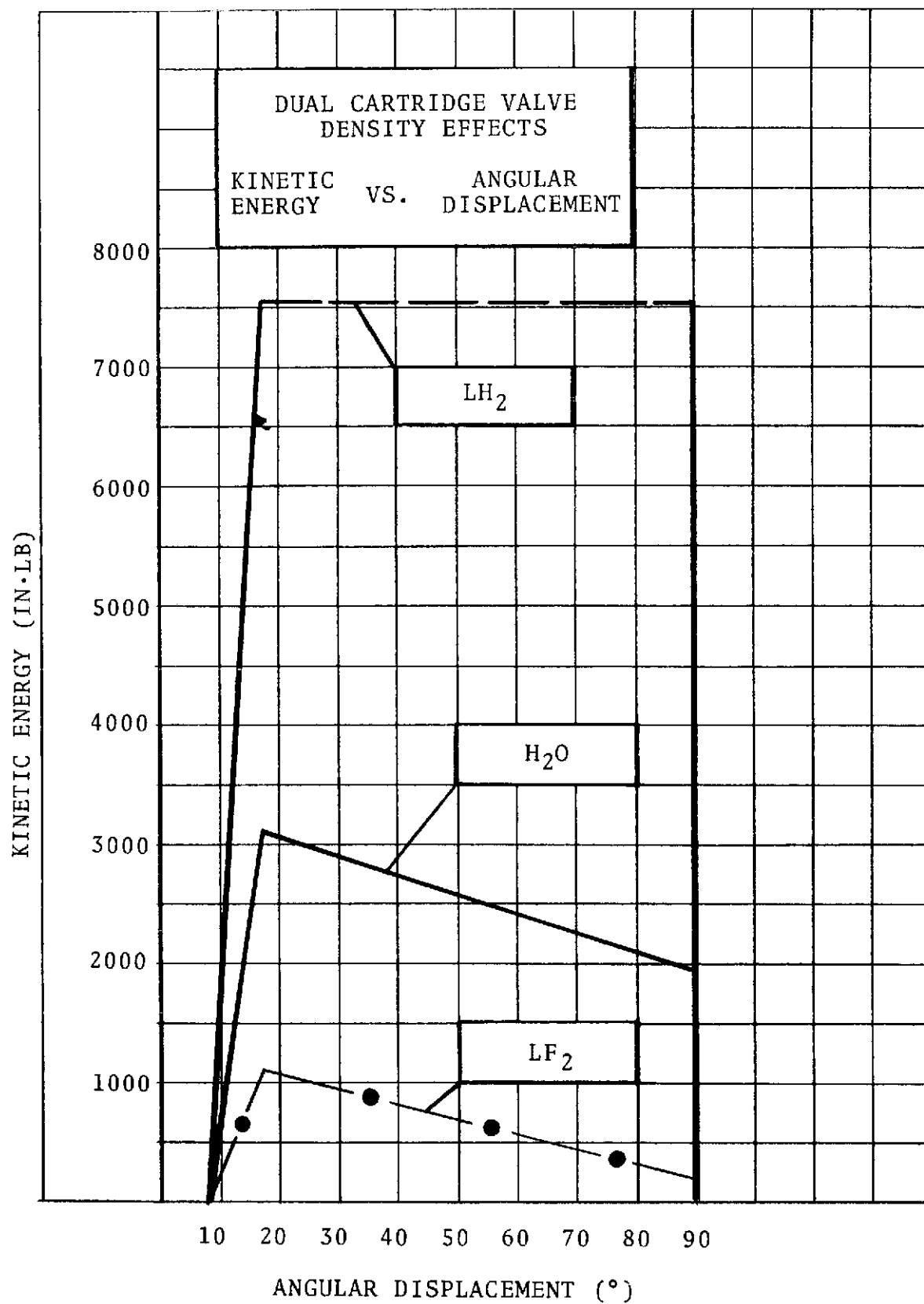


FIGURE 51. DUAL CARTRIDGE ENERGY DISTRIBUTION



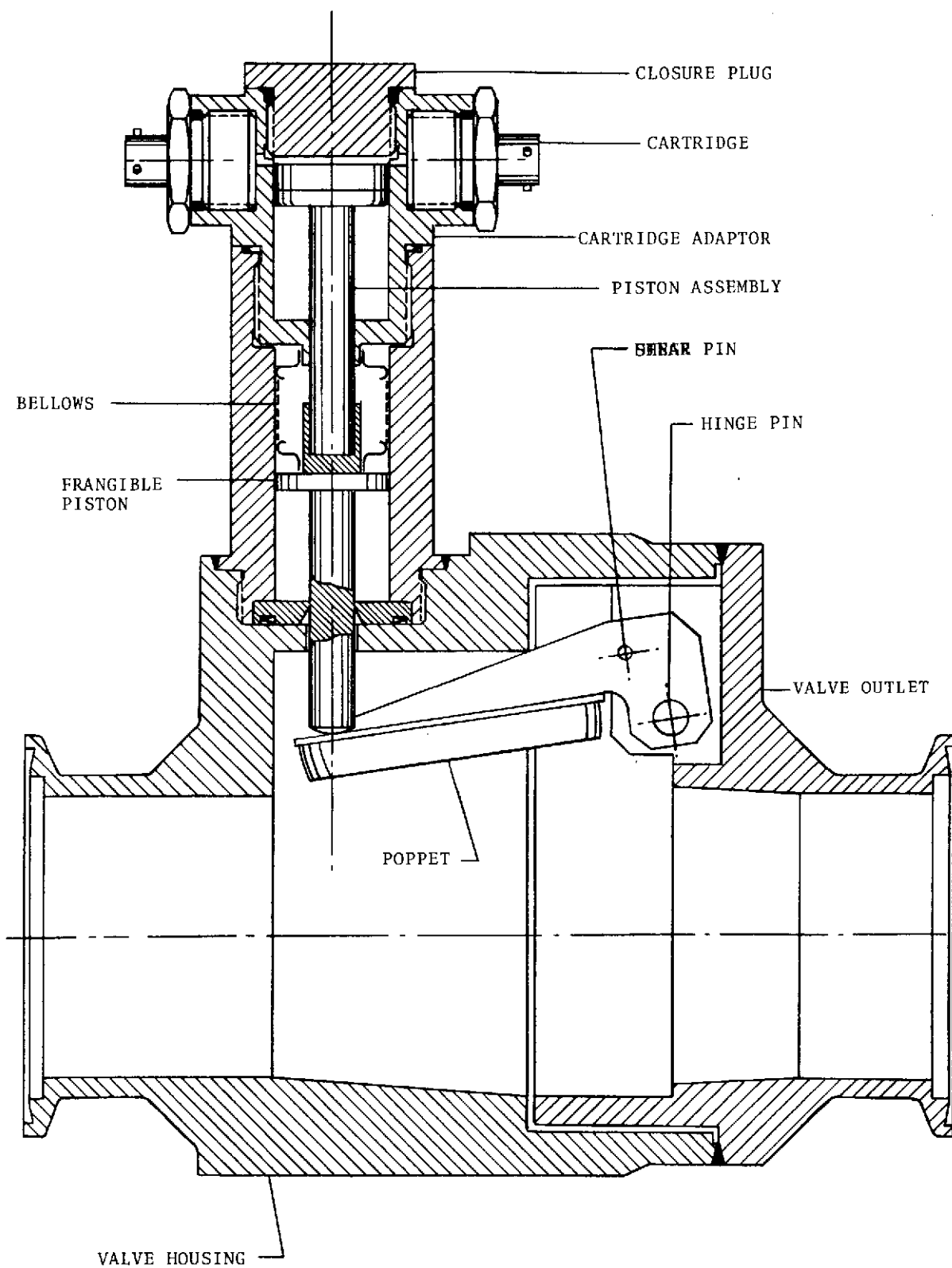


FIGURE 52. DUAL CARTRIDGE VALVE DESIGN

4. Flow Test - Operating Fluid:  $\text{CCl}_4$   
This test simulates a full flow  $\text{LF}_2$  test.  
By installing the valve in a flow system and  
flowing 60 GPM of  $\text{CCl}_4$  the flow characteristics  
of the valve can be established.

The tests listed above will establish that the Dual Cartridge Valve Design is indeed capable of closing in high density fluids.

## 9.0 CONCLUSIONS

The design and development program described in this report resulted in a 2-1/2 inch normally open, explosively actuated valve which is capable of shutting off the flow of fluids with densities of less than 62.5 lb/ft<sup>3</sup> (1 gm/cm<sup>3</sup>). The measured leak rates were better than  $1 \times 10^{-8}$  scc/sec of gaseous helium. The cartridge selected for this program proved to be reliable when actuated at ambient and liquid hydrogen temperatures.

Failure of the valve to close while flowing high density fluids, such as LF<sub>2</sub> and CCl<sub>4</sub> led to an investigation of the hydrodynamic mass effect. This investigation resulted in an analytical model of the valve which closely approximates the actual energy dissipation as measured by the pressure required to unseat the poppet.

A computer program was generated which was used to design a dual cartridge valve which will be capable of functioning in high density fluids. This design, however, was not tested.

## REFERENCES

1. Endicott, D. L. and Donahue, L. H.: Development and Demonstration of Criteria for Liquid Fluorine Feed System Components. NASA CR-72543, McDonnell Douglas Astronautics Company, Huntington Beach, California, June 1969.
2. Stokes, C. S., Smith, E. W. and Murphy, W. J.: Design, Testing, Fabrication and Launch Support of a Liquid Chemical Barium Release Payload. NASA CR-112106, Germantown Laboratories, Inc., Philadelphia, Pennsylvania.

PRECEDING PAGE BLANK NOT FILMED

## BIBLIOGRAPHY

Schmidt, H. W.: Handling and Use of Fluorine and Fluorine-Oxygen Mixtures in Rocket Systems. NASA SP-3037, Lewis Research Center, 1967.

Douglas Aircraft Company: Fluorine Systems Handbook. CR72064, Santa Monica, California, July 1967.

Anon.: Cryogenic Materials Data Handbook. MIL-TDR-64-280, Air Force Materials Laboratory, Wright-Patterson Air Force Base, Dayton, Ohio, August 1964.

Keough, J. B. and Oldland, A. H.: Final Report, Investigation of Cryogenic Rupture Disc Design. NASA CR-121118, Martin Marietta Corporation, Denver, Colorado, April 1973.

Falk, A. Y.: Space Storable Performance Gas/Liquid Like-Douplet Injector Characterization. NASA CR-120935, Rocketdyne, North American Rockwell Corporation, Canoga Park, California, October 1972.

Russell, L. M., Schmidt, H. W. and Gordon, L. H.: Compatibility of Polymeric Materials with Fluorine and Fluorine Oxygen Mixtures. NASA TN D-3392, Lewis Research Center, 1966.

PRECEDING PAGE BLANK NOT FILMED

## APPENDIX A

### POPPET/SEAT ANALYSIS

## TABLE OF CONTENTS

PARAGRAPH	TITLE	PAGE
1.0	INTRODUCTION	A-3
2.0	POPPET SEAT/INTERFACE	A-3
3.0	OPTIMIZATION OF SEAT GEOMETRY	A-9
4.0	RELATIONSHIP BETWEEN BACK PRESSURE AND KINETIC ENERGY	A-12
5.0	SUMMARY	A-15
	REFERENCES	A-16

## 1.0 INTRODUCTION

The poppet of the Model 1356 valve is retained in the seat by the friction forces existing between poppet and seat. Since seating of the poppet is due to its kinetic energy at the point of impact it is important to know what seat geometry allows for minimum energy requirements.

## 2.0 POPPET/SEAT INTERFACE

The contact area and the maximum stress between two rollers in compression are given (1) by the following two equations:

$$b = 2.15 \sqrt{\frac{P_1 D_1 D_2}{2 (D_1 + D_2) \left( \frac{1}{E_1} + \frac{1}{E_2} \right)}} \quad \text{EQ. 1}$$

$$P_{\max} = .59 \sqrt{\frac{P_1 E_1 E_2 (D_1 + D_2)}{(E_1 + E_2) D_1 D_2}} \quad \text{EQ. 2}$$

where

$b$  = width of contact area

$P_1$  = compressive force per unit length

$D_1$  = diameter of roller 1

$D_2$  = diameter of roller 2

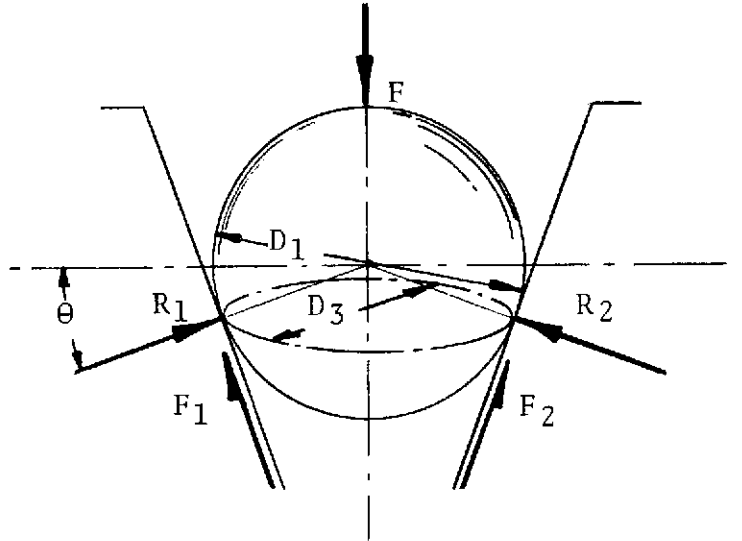
$E_1$  = modulus of elasticity of roller 1

$E_2$  = modulus of elasticity of roller 2

$P_{\max}$  = maximum contact stress between rollers

Equations 1 and 2 can be modified to describe the conditions which exist when a spherical surface contacts a conical surface as shown in the sketch below:





The force summation yields the following equation:

$$\begin{aligned}
 F &= R_1 \sin\theta + F_1 \cos\theta + F_2 \cos\theta + R_2 \sin\theta \\
 R_1 &= R_2 \\
 F_1 &= F_2 \\
 F &= 2 R_1 \sin\theta + 2 F_2 \cos\theta
 \end{aligned}$$

The friction force  $F_1$  can be expressed in terms of the normal force  $R_1$  by the expression:

$$F_1 = \eta R_1 = \tan\alpha R_1$$

where  $\eta$  is the coefficient of friction and  $\alpha$  is the angle whose tangent is equal to the coefficient of friction. It follows that:

$$\begin{aligned}
 F &= 2 R_1 \sin\theta + 2 R_1 \tan\alpha \cos\theta \\
 F &= 2 R_1 (\sin\theta + \tan\alpha \cos\theta)
 \end{aligned}$$

Solving for  $R_1$  then yields:

$$R_1 = \frac{F}{2 (\sin\theta + \tan\alpha \cos\theta)}$$

If we let  $P_1$  denote the load per unit length, in this case the circumference of the circle which represents the contact area, i.e.,  $D_3$  then:

$$P_1 = \frac{2R_1}{D_3 \pi}$$

$$P_1 = \frac{F}{\pi D_3 (\sin\theta + \tan\alpha \cos\theta)} \quad \text{EQ. 3}$$

By substituting  $D_2 = \infty$  and Equation 3 for  $P_1$ , Equations 1 and 2 now become:

$$b = 2.15 \sqrt{\frac{F D_1}{2 \pi D_3 (\sin\theta + \tan\alpha \cos\theta)} \left( \frac{1}{E_1} + \frac{1}{E_2} \right)} \quad \text{EQ. 4}$$

$$P_{\max} = .59 \sqrt{\frac{2 (E_1 E_2) F}{(E_1 + E_2) D_1 D_3 (\sin\theta + \tan\alpha \cos\theta)}} \quad \text{EQ. 5}$$

As long as the stresses induced by force  $F$  are below the yield strength of the material Hooke's law applies and we can determine the deflection of seat and poppet by:

$$\delta_1 = \frac{P_{\max} D_3}{E_1}$$

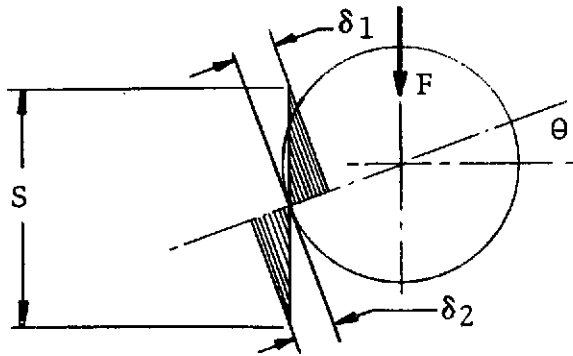
$$\delta_2 = \frac{P_{\max} D_3}{E_2}$$

The total deflection then is given by:

The total deflection then is given by:

$$\delta_t = \delta_1 + \delta_2$$

The sketch below shows the relationship between radial deflection ( $\delta$ ) and the deflection in the direction of Force F

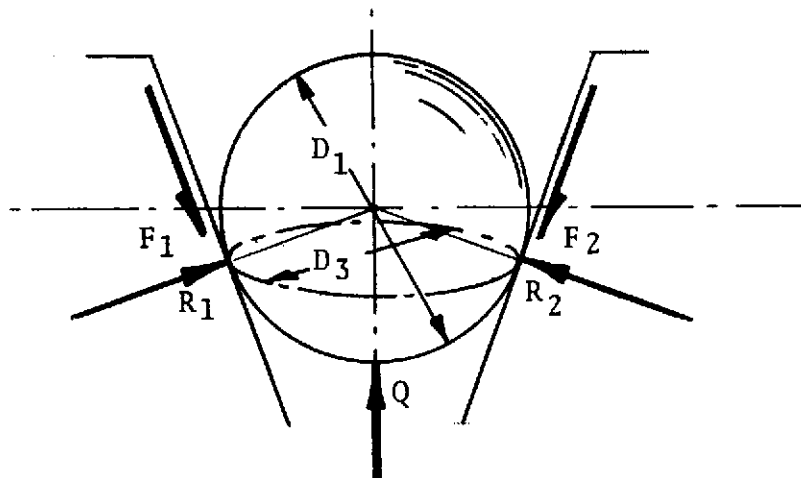


We see by inspection that

$$S = \frac{\delta_t}{\sin\theta}$$

The equations developed for maximum seat stress, contact area, and deflection can now be used to analyze the force with which the poppet is retained in the seat.

The sketch below shows the conditions which exist after a spherical surface has been forced into a conical seat. Let Q denote the force required to dislodge the sphere. The friction forces now oppose Force Q.



The force summation yields the following equation:

$$Q = (F_1 \cos \theta + F_2 \cos \theta) - (R_1 \sin \theta + R_2 \sin \theta)$$

As before:

$$F_1 = F_2$$

$$R_1 = R_2$$

$$F_1 = \tan \alpha R_2$$

Then:

$$Q = 2R_1 (\tan \alpha \cos \theta - \sin \theta)$$

Or:

$$Q = 2R_1 \cos \theta (\tan \alpha - \tan \theta)$$

And:

$$R_1 = \frac{Q}{2 \cos \theta (\tan \alpha - \tan \theta)}$$

The force Q divided by the area of the seat will yield the pressure required to dislodge the sphere ( $P_b$ ).

Thus:

$$P_b = \frac{4 Q}{\pi D_3^2}$$

The total retention force  $R_1$  can be expressed in terms of the maximum seat stress as follows:

$$R_1 = P_{\max} b D_3 \pi \quad (\text{EQ } 6)$$

Equation 5 can be solved for F to yield:

$$F = \frac{P_{\max}^2 (E_1 + E_2) D_1 D_3 (\sin\theta + \tan\alpha \cos\theta) \Pi}{(.59)^2 (2) (E_1 E_2)} \quad (\text{EQ } 7)$$

Equation 4 can be solved for F to yield:

$$F = \frac{b^2 D_3^2 (\sin\theta + \tan\alpha \cos\theta) \Pi}{(2.15)^2 D_1 \left( \frac{1}{E_1} + \frac{1}{E_2} \right)} \quad (\text{EQ } 8)$$

Equating the right sides of Equations 7 and 8 and solving for  $P_{\max}$  will yield:

$$P_{\max} = \frac{b E_1 E_2}{(1.82) D_1 (E_1 + E_2)} \quad (\text{EQ } 9)$$

Substituting Equation 6 into Equation 9 will yield:

$$P_{\max} = \sqrt{\frac{R_1 E_1 E_2 (.1748)}{D_1 D_3 (E_1 + E_2)}} \quad (\text{EQ } 10)$$

Equation 10 describes maximum seat stress in terms of maximum retention force.

From the definition of energy the work required to deform the seat and poppet is given by:

$$U = \frac{S \cdot F}{2}$$

where

S = deflection

F = force acting through distance S

### 3.0 OPTIMIZATION OF SEAT GEOMETRY

By fixing the back pressure which the poppet must withstand and the seating diameter of the poppet it is possible to calculate the minimum kinetic energy which the poppet must contain for various coefficients of friction and for various taper angles of the conical seat.

The following procedure can be followed to calculate this:

#### GIVEN:

Seat Diameter	=	$D_3$
Modulus of Elasticity of Poppet	=	$E_1$
Modulus of Elasticity of Seat	=	$E_2$
Required Back Pressure	=	$P_b$
Coefficient of Friction (Variable)	=	$\tan \alpha$
Taper Angle (Variable)	=	$\theta$

#### FIND:

Energy	=	$U$
--------	---	-----

#### CALCULATE:

$$D_1 = \frac{D_3}{\cos \theta}$$

$$Q = \frac{P_b D_3^2 \pi}{4}$$

$$R' = \frac{Q}{2 \cos \theta (\tan \alpha - \tan \theta)}$$

$$P_{\max} = \sqrt{\frac{R'^1 E_1 E_2 (.1748)}{D_1 D_3 (E_1 + E_2)}}$$

$$F = \frac{P_{\max}^2 (E_1 + E_2) D_1 D_3 (\sin\theta + \tan\alpha \cos\theta) \Pi}{(.59)^2 (2) (E_1 E_2)}$$

$$\delta_1 = \frac{P_{\max} D_3}{E_1}$$

$$\delta_2 = \frac{P_{\max} D_3}{E_2}$$

$$\delta_t = \delta_1 + \delta_2$$

$$S = \frac{\delta_t}{\sin\theta}$$

$$U = \frac{S F}{2}$$

By calculating U for various values of  $\theta$  and  $\tan\alpha$  the curves shown on Figure A-1 can be generated.

The curves in Figure A-1 have been generated for the specific case where:

$$E_s = 2.652 \text{ in}$$

$$E_1 = 10300000 \text{ psi}$$

$$E_2 = 10300000 \text{ psi}$$

$$P_b = 250 \text{ psi}$$

Considering the curves in Figure A-1, the following observations can be made:

1. The minimum energy required to withstand a backpressure of 250 psi is extremely sensitive to the coefficient of friction.
2. A minimum energy point exists which varies with the coefficient of friction.

3. A taper angle of  $3^\circ$  is optimum for the range of  $\eta = .122$  to  $\eta = .363$ .

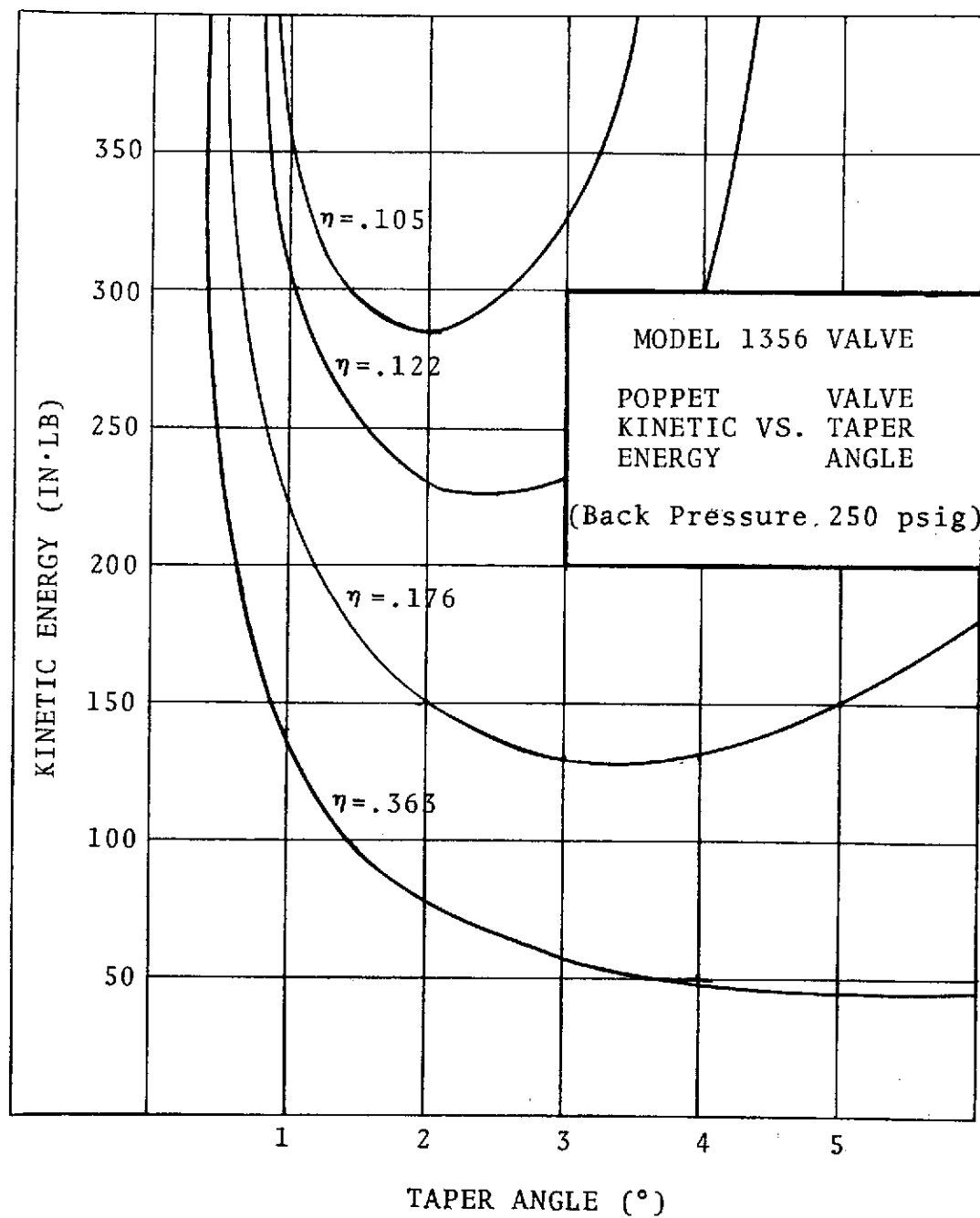


FIGURE A-1. KINETIC ENERGY REQUIREMENTS



#### 4.0 RELATIONSHIP BETWEEN BACK PRESSURE AND KINETIC ENERGY

The equations developed for the poppet/seat interface can also be used to investigate the relationship between backpressure and kinetic energy of the poppet.

By varying the force  $F$  in Equation 4 it is possible to calculate the energy input and the backpressure required to dislodge the poppet. At this point it is convenient to fix the taper angle  $\theta$  at  $3^\circ$  since it has already been established to be optimum for a wide range of friction coefficients.

The following procedure can be adopted to establish the relationship between backpressure and kinetic energy:

##### Given:

Seat Diameter	=	$D_3$
Modulus of Elasticity of Poppet	=	$E_1$
Modulus of Elasticity of Seat	=	$E_2$
Taper Angle	=	$\theta$
Coefficient of Friction (Variable)	=	$\tan \alpha$
Force (Variable)	=	$F$

##### Find:

Energy	=	$U$
--------	---	-----

##### Calculate:

$$D_1 = \frac{D_3}{\cos \theta}$$

$$b = 2.15 \sqrt{\frac{F D_1}{2 \pi D_3 (\sin \theta + \tan \alpha \cos \theta)}} \left( \frac{1}{E_1} + \frac{1}{E_2} \right)$$

$$P_{\max} = .59 \sqrt{\frac{2 (E_1 E_2) F}{(E_1 + E_2) D_1 \pi D_3 (\sin \theta + \tan \alpha \cos \theta)}}$$

$$\delta_1 = \frac{P_{\max} D_3}{E_1}$$

$$\delta_2 = \frac{P_{\max} D_3}{E_2}$$

$$\delta_t = \delta_1 + \delta_2$$

$$S = \frac{\delta_t}{\sin \theta}$$

$$U = \frac{(S)(F)}{2}$$

$$R_1 = P_{\max} b \Pi D_3$$

$$Q = 2R_1 \cos \theta (\tan \alpha - \tan \theta)$$

$$P_b = \frac{Q^4}{D_3^2 \Pi}$$

By calculating U and  $P_b$  for various values of  $\tan$  the curves shown on Figure 2 can be generated for the specific case where:

$$D_3 = 2.652 \text{ IN}$$

$$E_1 = 10300000 \text{ PSI}$$

$$E_2 = 10300000 \text{ PSI}$$

$$\theta = 3^\circ$$

Considering the curves in Figure A-2 the following observations can be made:

1. The back-pressure which the poppet can withstand after it has been forced into the valve seat with a given amount of kinetic energy is very strongly influenced by the friction coefficient between poppet and seat.
2. There exist wide discrepancies between values of friction coefficients obtained from different sources for the same material combinations and test conditions. Such discrepancies may be due to differences in experimental techniques or such factors as temperature, sliding velocity, surface finish, actual contact area, and load.
3. Tests were conducted with an aluminum poppet being forced into an aluminum seat with a known amount of kinetic energy. This data is shown graphically in Figure A-2 and indicates that the actual friction coefficient is approximately .267.
4. No tests were conducted under lubricated conditions. However, it can be safely assumed that the friction coefficient under lubricated conditions is lower than .267.
5. For the range of .105 to .122 for the friction coefficient the ratio of back-pressure versus kinetic energy of the poppet is very nearly unity.

## 5.0 SUMMARY

The poppet/seat analysis revealed two major influences on the quality of seal which can be obtained between poppet and valve seat.

There existed an optimum taper angle of approximately 3 degrees which the valve seat must possess for optimum utilization of poppet kinetic energy. Also, for a given amount of kinetic energy the back-pressure which the poppet can withstand after valve actuation is profoundly influenced by the friction coefficient. For the Model 1356 Valve this friction coefficient is between .105 and .122. In this range the ratio between back-pressure and kinetic energy of the poppet immediately prior to impact is very nearly unity.

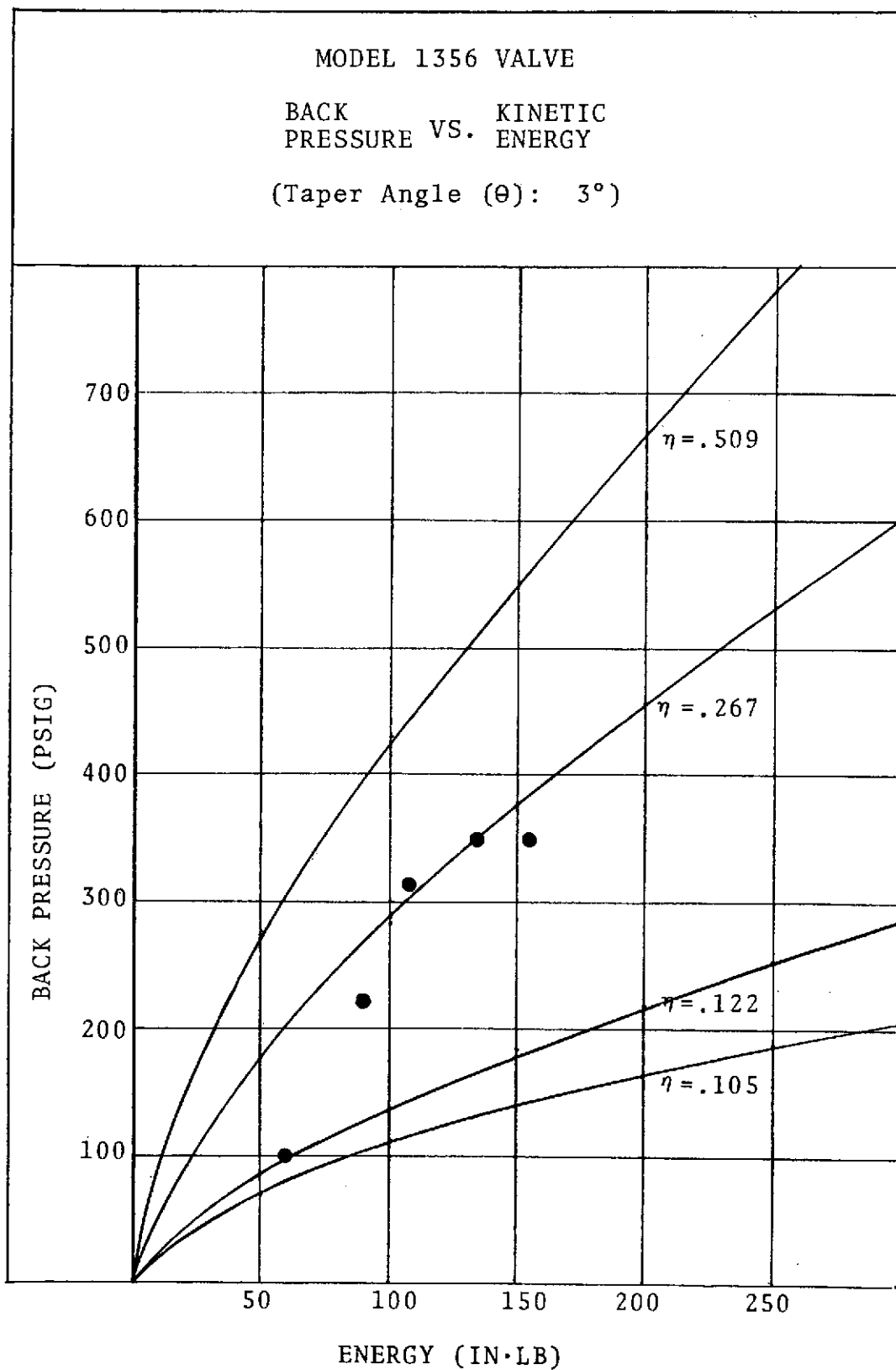


FIGURE A-2. BACK PRESSURE CAPABILITY

## REFERENCES

- A1    Faupel, J. H.: Engineering Design.    John Wiley & Sons,  
Inc., New York, 1964

APPENDIX B

VIRTUAL MASS ANALYSIS

## TABLE OF CONTENTS

	Page
1.0 INTRODUCTION	B-3
2.0 SPHERE MOVING THROUGH UNBOUNDED FLUID	B-3
3.0 DISC MOVING THROUGH UNBOUNDED FLUID	B-5
4.0 SPHERE MOVING PERPENDICULAR TO WALL	B-5
5.0 SPHERE IN UNBOUNDED FLUID MOVING PARALLEL TO TWO INFINITE WALLS	B-6
6.0 SPHERE MOVING PARALLEL TO TWO WALLS TOWARDS A THIRD WALL WHICH IS PERPENDICULAR TO THE DIRECTION OF MOTION	B-7
7.0 CIRCULAR DISC MOVING PARALLEL TO TWO WALLS TOWARD A THIRD WALL	B-8
8.0 TOTAL KINETIC ENERGY OF CIRCULAR DISC	B-9
9.0 SUMMARY	B-10
REFERENCES	B-11

## 1.0 INTRODUCTION

The hinged poppet of the Model 1356-1 Valve is essentially a flat disc moving between two parallel walls towards a third wall which is perpendicular to the direction of movement. During the acceleration phase of poppet movement, the explosive actuator accelerates not only the mass of the poppet itself but also the "hydrodynamic mass" of the fluid in front of the disc.

It can be shown that when a body which is submerged in a liquid is acted upon by a force  $F$  the body will experience an acceleration of magnitude:

$$a = \frac{F}{(M+M_1)}$$

The term  $M$  represents the mass of the body.

The term  $M_1$  represents the "hydrodynamic mass" of the fluid in front of the body.

The term  $(M+M_1)$  is the "virtual mass" of the body..

The virtual mass of a body moving through a fluid will change depending on the boundary conditions of the fluid. In this section the expression for the virtual mass of a flat disc moving parallel to two walls towards a third wall which is perpendicular to the direction of motion will be derived. The method of derivation is by analogy to a sphere moving through a fluid.

## 2.0 SPHERE MOVING THROUGH UNBOUNDED FLUID

The kinetic energy of the hydrodynamic mass of the fluid in front of a sphere which moves with velocity  $U$  in a straight line through an unbounded fluid is given (Ref. 1, p. 467) by:

$$T_f = \frac{1}{3} \left( \pi \cdot \gamma \cdot a^3 \cdot U^2 \right)$$



where

$\gamma$  = density of fluid

$a$  = radius of sphere

$U$  = velocity of sphere

$T_f$  = kinetic energy of hydrodynamic mass

The above expression can be rearranged to yield:

$$T_f = \frac{1}{4} \cdot \left( \frac{4 \cdot \gamma \cdot \Pi \cdot a^3}{3} \right) U^2$$

Let:

$$M_1 = \frac{4 \cdot \gamma \cdot \Pi \cdot a^3}{3}$$

Then:

$$T_f = \frac{1}{4} \cdot M_1 \cdot U^2$$

If:

$$M_1 = 2M_2$$

Then:

$$T_f = \frac{1}{2} \cdot M_2 \cdot U^2$$

### 3.0 DISC MOVING THROUGH UNBOUNDED FLUID

Similarly the kinetic energy of the hydrodynamic mass of the fluid in front of a circular disc is given (Ref. 1, p. 477) by:

$$T_f = \frac{4}{3} \cdot (\gamma \cdot a^3 \cdot U^2)$$

where

a = radius of the disc

The above expression can be rearranged to yield:

$$T_f = \frac{1}{2} \cdot \left( \frac{8 \cdot \gamma \cdot a^3}{3} \right) \cdot U^2$$

Let:

$$M_1 = \frac{8 \cdot \gamma \cdot a^3}{3}$$

Then:

$$T_f = \frac{1}{2} \cdot M_1 \cdot U^2 \quad (\text{EQ. 2})$$

### 4.0 SPHERE MOVING PERPENDICULAR TO A WALL

The kinetic energy of the hydrodynamic mass of the fluid in front of a sphere moving towards an infinite wall with velocity U is given (Ref. 1, p. 504) by:

$$T_f = \frac{1}{4} \cdot M_1 \cdot \left( 1 + \frac{3 \cdot a^3}{8 \cdot h^3} \right) \cdot U^2$$

where

$h$  = the distance to the wall

The above expression can be rearranged to yield:

$$T_f = \frac{1}{4} \cdot M_1 \cdot U^2 + \left( \frac{3 \cdot a^3}{32 \cdot h^3} \right) \cdot M_1 \cdot U^2$$

Let:

$$M_1 = 2M_2$$

Then:

$$T_f = \frac{1}{2} \cdot M_2 \cdot U^2 + \left( \frac{3 \cdot a^3}{16 \cdot h^3} \right) \cdot M_2 \cdot U^2 \quad (\text{EQ. 3})$$

Comparing EQ. 3 with EQ. 1 it can be seen that the first term on the right side of the equation is the kinetic energy of the hydrodynamic mass of the fluid in front of a sphere moving in an unbounded fluid. The second term is the kinetic energy due to the wall effect.

#### 5.0 SPHERE IN AN UNBOUNDED FLUID MOVING PARALLEL TO TWO INFINITE WALLS

The kinetic energy of the hydrodynamic mass of the fluid in front of a sphere moving parallel to an infinite wall at a distance  $g$  from the wall is given (Ref. 1, pg. 506) by:

$$T_f = \frac{1}{4} \cdot M_1 \cdot \left( 1 + \frac{3 \cdot a^3}{16 \cdot g^3} \right) \cdot U^2$$

where

$g$  = distance to wall

The above expression can be rearranged to yield:

$$T_f = \frac{1}{4} \cdot M_1 \cdot U^2 + \left( \frac{3 \cdot a^3}{64 \cdot g^3} \right) \cdot M_1 \cdot U^2$$

Let:

$$M_1 = 2 M_2$$

Then:

$$T_f = \frac{1}{2} \cdot M_2 \cdot U^2 + \left( \frac{3 \cdot a^3}{32 \cdot g^3} \right) \cdot M_2 \cdot U^2 \quad (\text{EQ. 4})$$

Comparing EQ. 4 with EQ. 1 it can be seen that the first term on the right side of the equation is the kinetic energy of the hydrodynamic mass of the fluid in front of a sphere moving through an unbounded fluid. The second term is the kinetic energy due to the wall effect.

If the sphere moves parallel to two walls at a distance  $g$  the second term of the equation will be twice as large and therefore the total kinetic energy of the hydrodynamic mass is:

$$T_f = \frac{1}{2} \cdot M_2 \cdot U^2 + \left( \frac{3 \cdot a^3}{16 \cdot g^3} \right) \cdot M_2 \cdot U^2 \quad (\text{EQ. 5})$$

#### 6.0 SPHERE MOVING PARALLEL TO TWO WALLS TOWARDS A THIRD WALL WHICH IS PERPENDICULAR TO THE DIRECTION OF MOTION

It has been shown that the wall effect for parallel walls is:

$$T_f^1 = \left( \frac{3 \cdot a^3}{16 \cdot g^3} \right) \cdot M_2 \cdot U^2$$

The wall effect for a perpendicular wall is:

$$T_f^2 = \left( \frac{3 \cdot a^3}{16 \cdot h^3} \right) \cdot M_2 \cdot U^2$$

The kinetic energy of the total hydrodynamic mass of the fluid in front of the sphere moving parallel to two walls towards a third perpendicular wall will then be:

$$T_f = \frac{1}{2} \cdot M_2 \cdot U^2 + \left( \frac{3 \cdot a^3}{16 \cdot g^3} \right) \cdot M_2 \cdot U^2 + \left( \frac{3 \cdot a^3}{16 \cdot h^3} \right) \cdot M_2 \cdot U^2$$

If  $h = g$ , the above expression can be rearranged to yield:

$$T_f = \frac{1}{2} \cdot M_2 \cdot U^2 + \left( \frac{3 \cdot a^3}{8 \cdot h^3} \right) \cdot M_2 \cdot U^2$$

Or:

$$T_f = \frac{1}{2} \cdot M_2 \cdot \left( 1 + \frac{6 \cdot a^3}{8 \cdot h^3} \right) \cdot U^2 \quad (\text{EQ. 6})$$

#### 7.0 CIRCULAR DISC MOVING PARALLEL TO TWO WALLS TOWARD A THIRD WALL

It has been shown in paragraph 2.0 that the kinetic energy of the hydrodynamic mass in front of a sphere moving in an unbounded fluid is

$$T_f = \frac{1}{2} \cdot M_2 \cdot U^2$$

where

$$M_2 = \frac{4 \cdot \pi \cdot \gamma \cdot a^3}{6}$$

The kinetic energy of the hydrodynamic mass in front of a disc moving in an unbounded fluid is given in paragraph 3.0 as:

$$T_f = \frac{1}{2} \cdot M_1 \cdot U^2$$

WHERE:

$$M_1 = \frac{8 \cdot \gamma \cdot a^3}{3}$$

Thus by substituting the hydrodynamic mass of the fluid in front of a disc ( $M'$ ) for the hydrodynamic mass of the fluid in front of a sphere ( $M''$ ) EQ. 6 will yield:

$$T_f = \frac{1}{2} \cdot \left( \frac{8 \cdot a^3 \cdot \gamma}{3} \right) \cdot \left( 1 + \frac{6 \cdot a^3}{8 \cdot h^3} \right) \cdot U^2$$

This equation is an expression for the kinetic energy of a circular disc moving parallel to two walls towards a third wall perpendicular to the direction of motion.

If:

$$M_3 = \left( \frac{8 a^3 h^3 + 6 a^6}{3 h^3} \right) \cdot \gamma \quad (\text{EQ. 7})$$

Then:

$$T_f = \frac{1}{2} \cdot M_3 \cdot U^2 \quad (\text{EQ. 8})$$

## 8.0 TOTAL KINETIC ENERGY OF CIRCULAR DISC

The total kinetic energy of a circular disc moving through a fluid parallel to two walls and towards a third wall which is perpendicular to the direction of motion is:

$$T = T_{\text{DISC}} + T_{\text{FLUID}}$$

where

$$T = \frac{1}{2} \cdot (M + M_3) \cdot U^2$$

The term  $(M + M_3)$  is the virtual mass of the disc, where  $M$  is the mass of the disc and  $M_3$  is the hydrodynamic mass of the fluid.

## 9.0 SUMMARY

In calculating the energy which the explosive cartridge must impart to the hinged poppet, both the mass of the poppet and the hydrodynamic mass of the fluid in front of the poppet must be considered. The hydrodynamic mass is determined by the geometry of the fluid boundary and the density of the fluid. In very dense fluid a consideration of the hydrodynamic mass is therefore essential.

## REFERENCES

- B1 Milne-Thomson, L.M.: Theoretical Hydrodynamics.  
4th Edition, The MacMillan Company, New York, 1965



APPENDIX C  
COMPUTER PROGRAM

The Computer Program reproduced below is based on the dynamic analysis of the valve as presented in Section 7.0 of the main report.

```

20  PRINT "RELEASE PRESSURE (PSI)"
25  INPUT P
30  PRINT "PEAK PRESSURE FIXED VOLUME (PSIA)"
35  INPUT P1
40  PRINT "FIXED VOLUME (CIN)"
45  INPUT V1
50  PRINT "INITIAL VOLUME "
55  INPUT V2
60  PRINT "FINAL VOLUME (CIN)"
65  INPUT V3
70  PRINT "BURN TIME (SEC)"
75  INPUT T
80  PRINT "PISTON AREA (SIN)"
85  INPUT A
90  PRINT "DISTANCE PIVOT=PISTON (IN)"
95  INPUT L
100 PRINT "INITIAL POPPET ANGLE (DEG)"
105 INPUT O1
110 PRINT "POPPET MOMENT INERTIA (IN*LB*SEC^2)"
115 INPUT I
120 PRINT "VIRTUAL MASS INERTIA (IN*LB*SEC^2)"
125 INPUT I1
130 PRINT "FLUID DENSITY (LB/IN^3)"
135 INPUT G
140 PRINT "EXPANSION COEF. (K)"
145 INPUT K
150 PRINT "TOTAL STROKE (IN)"
155 INPUT S6
160 PRINT "UPSTREAM ORIFICE AREA (IN^2)"
165 INPUT H1
170 PRINT "DOWNSTREAORIFICE AREA (IN^2)"
175 INPUT H2
180 PRINT "DISTANCE PIVOT-C.G. (IN)"
185 INPUT L1
186 PRINT "N1"
187 INPUT N1
188 N2=1940*G^2
189 N3= 1150*G^2
190 W1=0
195 T3=0
200 E1=0
205 S1=0
210 G6=0
211 PRINT "
ENERGY    PRESS    TIME    STROKE    ANGLE"
215 P2=P1*V1/V2
220 T4=P*T/P2
222 T1=(.1)*T

```

```

225 T2=T1+T3
230 P3=N1*P2*T2/T
232 IF P3<P THEN 233 ELSE 235
233 T3=T2
234 GO TO 222
235 W3=T1*P3*A*L/(1+(11*N2))
240 W2=W3+W1
245 Q=T1*(W2+2-W1+2)/(2*W3)
250 E2=(1+11)*(W2+2-W1+2)/(2)
255 E3=1*(W2+2-W1+2)/2
260 E4=E1+E2
265 E5=E1+E3
270 Q2=.01745*Q1
275 Q3=Q6+Q
280 Q7=Q2+Q3
285 S=L*TAN(Q)
290 Q4=57.324*Q7
295 S2=S1+S
300 V=S*A
305 V5=V2+V
306 IF Q4>5 THEN 315 ELSE 320
315 PRINT IN IMAGE "
      XXXX.XX XXXXXXXXX XX.XXXXXXX X.XXXXX XX.XX":E5,P3,T2,S2,Q4
320 T3=T2
325 W1=W2
330 V2=V5
335 S1=S2
340 Q6=Q3
345 E1=E5
347 P4=P3
350 IF T2<T THEN 215 ELSE 395
395 P3=P4*(((V5-V)/V5)+K)
405 T1=(.1)*T
410 T2=T1+T3
415 IF S2<S6 THEN 235 ELSE 420
420 PRINT
425 PRINT "
      DECELERATION
ENERGY          TIME          AREA          ANGLE"
430 T3=T2
435 N5=Q4
440 F1=E5
445 T1=T
450 T2=T1+T3
455 M1=(2*F1/I)+.5
457 IF N5<=70 THEN 460 ELSE 475
460 H4=(-.0892)*N5+6.2
465 H3=H4+H2
470 GO TO 480
475 H3=H2
480 D=N3*(H1*((H1*G*L1*M1)+2/(H3+2*G*772.8)))
485 M3=T1*D*L1/I
490 M2=M1-M3

```

```

495 B=T1*(M1↑2-M2↑2)/(2*M3)
500 B1=57.324*B
510 F2=I*(M1↑2-M2↑2)/2
515 F5=F1-F2
520 N5=N5+B1
530 IF N5>85 THEN 545 ELSE 560
545 PRINT IN IMAGE "
    %%.%.% %%.% %%.% %%.%":F5,T2,H3,N5
560 F1=F5
565 T3=T2
570 IF N5<=90 THEN 445
    >

```

# SAMPLE RUN

>RUN  
RELEASE PRESSURE (PSI)  
? 7000  
PEAK PRESSURE FIXED VOLUME (PSIA)  
? 5761  
FIXED VOLUME (CIN)  
? .61  
INITIAL VOLUME  
? .089  
FINAL VOLUME (CIN)  
? .242  
BURN TIME (SEC)  
? .000074  
PISTON AREA (SIN)  
? .3067  
DISTANCE PIVOT=PISTON (IN)  
? 3  
INITIAL POPPET ANGLE (DEG)  
? 8  
POPPET MOMENT INERTIA (IN\*LB\*SEC<sup>2</sup>)  
? .00811  
VIRTUAL MASS INERTIA (IN\*LB\*SEC<sup>2</sup>)  
? .00443  
FLUID DENSITY (LB/IN<sup>3</sup>)  
? .0361  
EXPANSION COEF. (K)  
? 1.3  
TOTAL STROKE (IN)  
? .5  
UPSTREAM ORIFICE AREA (IN<sup>2</sup>)  
? 4.908  
DOWNSTREAM ORIFICE AREA (IN<sup>2</sup>)  
? 2.405  
DISTANCE PIVOT-C.G. (IN)  
? 1.9

N1

? .45

ENERGY	PRESS	TIME	STROKE	ANGLE
622.48	5595	.000710	.47923	17.16
628.67	5513	.000718	.48795	17.33
634.80	5433	.000725	.49671	17.49
640.87	5355	.000733	.50551	17.66

## DECELERATION ENERGY

155.39	.004514	2.405	85.34
149.99	.004588	2.405	86.16
144.87	.004662	2.405	86.97
140.00	.004736	2.405	87.77
135.38	.004810	2.405	88.55
130.99	.004884	2.405	89.32
126.81	.004958	2.405	90.07